Report No. KS-22-02 ▪ FINAL REPORT ▪ May 2022

Evaluation of Lightweight Aggregate for Internal Curing on Concrete Pavement in Kansas

Andrew Jenkins, P.E.
David A. Meggers, P.E.
Nicole Schmiedeke, M.S., E.I.T.

Kansas Department of Transportation
Bureau of Research

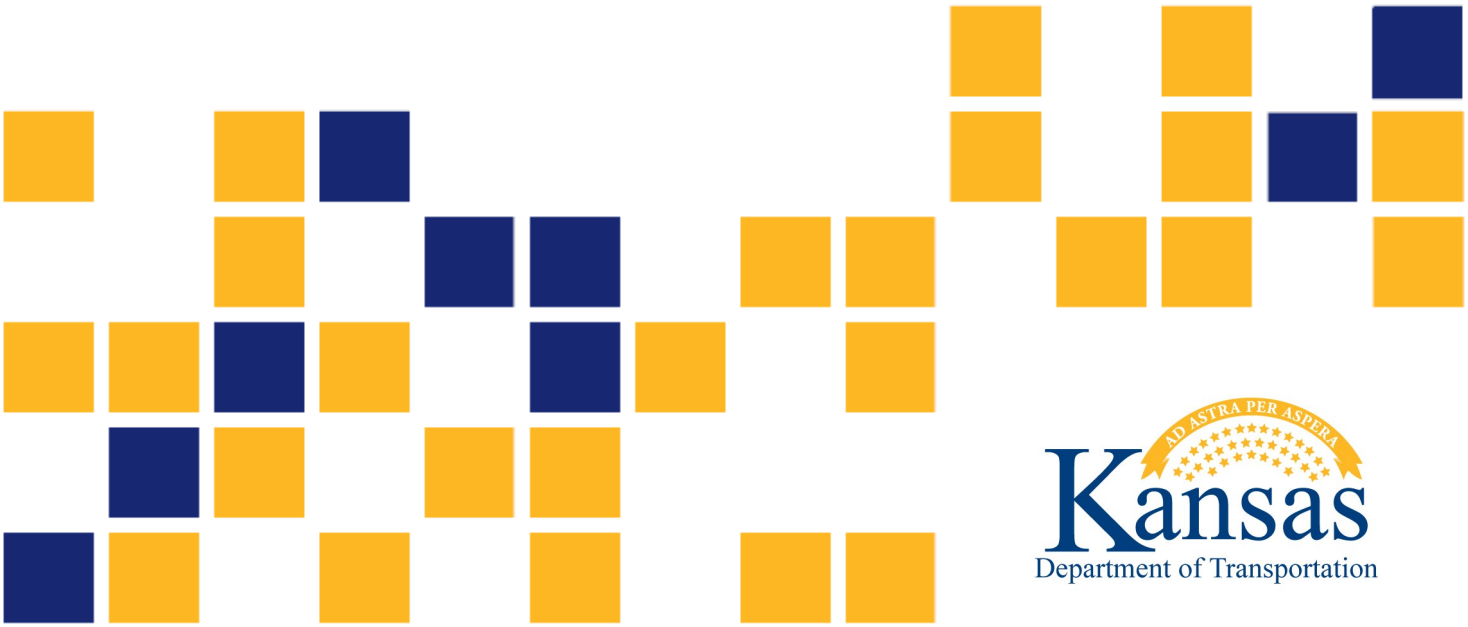

Kansas
Department of Transportation

1 Report No. KS-22-02	**2 Government Accession No.**	**3 Recipient Catalog No.**
4 Title and Subtitle Evaluation of Lightweight Aggregate for Internal Curing on Concrete Pavement in Kansas		**5 Report Date** May 2022 **6 Performing Organization Code**
7 Author(s) Andrew Jenkins, P.E. David A. Meggers, P.E. Nicole Schmiedeke, M.S., E.I.T.		**8 Performing Organization Report No.**
9 Performing Organization Name and Address Kansas Department of Transportation Bureau of Research 2300 SW Van Buren Topeka, Kansas 66611-1195		**10 Work Unit No. (TRAIS)** **11 Contract or Grant No.**
12 Sponsoring Agency Name and Address Kansas Department of Transportation Bureau of Research 2300 SW Van Buren Topeka, Kansas 66611-1195		**13 Type of Report and Period Covered** Final Report **14 Sponsoring Agency Code**

15 Supplementary Notes
For more information write to address in block 9.

16 Abstract

The purpose of this project and the Internally Cured Concrete (ICC) test section was to evaluate the benefits obtained through internal curing using pre-saturated lightweight aggregate (LWA). Two test sections were constructed on the mainline of US-54 near Iola, Kansas: a Control section and an ICC section using lightweight aggregate. Traditional laboratory testing was conducted on each test section to compare fresh and hardened concrete properties including, but not limited to, slump, temperature, air content, unit weight, strength, permeability, and freeze/thaw. Also, several strain gages and moisture sensors were embedded in each test section to monitor the actual strain and moisture content present in the concrete. In addition, a Dipstick Profiler was used on five panels to get a full panel surface profile at the highest and lowest temperatures for several days after pavement construction. Last, HIPERPAV III analysis was used to compare early age stress and cracking risk.

The plastic and hardened concrete results presented in this report indicate no significant impact of the LWA material. For the majority of the properties tested, when comparing the results from the two sections, the values fall within the multiple laboratory precision expected when testing from the same concrete batch. However, the reduction in unit weight, the slight reduction of elastic modulus, and the slight increase in tensile strength of the ICC indicate a potential improvement in overall durability and potentially increased service life. Additional research into these properties would be required to support that data.

The methods used to collect strain, moisture, and deflection data were highly successful. All methods of data collection including strain, curvature, moisture, deflection, and HIPERPAV III results infer the use of lightweight aggregate and internally cured concrete reduce the initial strain and undesirable deformations in the concrete. However, the test sections were not able to be constructed at the same time due to lack of staff, weather delays, and contractor's schedule, and therefore, were constructed 3 months apart. As a result, the significant weather differences between the placement dates have been observed to have impacted the data from the strain gages and moisture sensors. Therefore, it cannot be concluded with certainty if the use of LWA in the ICC improved the quality and durability of the concrete compared to the Control section. General condition surveys will be performed every five years of the 20-year design life, or until a major rehabilitation occurs and the original sections can no longer be surveyed.

17 Key Words Concrete curing, Concrete tests, Lightweight aggregates, Durability, Deformation curve		**18 Distribution Statement** No restrictions. This document is available to the public through the National Technical Information Service www.ntis.gov.	
19 Security Classification (of this report) Unclassified	**20 Security Classification (of this page)** Unclassified	**21 No. of pages** 142	**22 Price**

Form DOT F 1700.7 (8-72)

This page intentionally left blank.

Evaluation of Lightweight Aggregate for Internal Curing on Concrete Pavement in Kansas

Construction Report

Prepared by

Andrew Jenkins, P.E.
David A. Meggers, P.E.
Nicole Schmiedeke, M.S., E.I.T.

Kansas Department of Transportation
Bureau of Research

A Report on Research Sponsored by

THE KANSAS DEPARTMENT OF TRANSPORTATION
TOPEKA, KANSAS

May 2022

NOTICE

The authors and the state of Kansas do not endorse products or manufacturers. Trade and manufacturers names appear herein solely because they are considered essential to the object of this report.

This information is available in alternative accessible formats. To obtain an alternative format, contact the Office of Public Affairs, Kansas Department of Transportation, 700 SW Harrison, 2nd Floor – West Wing, Topeka, Kansas 66603-3745 or phone (785) 296-3585 (Voice) (TDD).

DISCLAIMER

The contents of this report reflect the views of the authors who are responsible for the facts and accuracy of the data presented herein. The contents do not necessarily reflect the views or the policies of the state of Kansas. This report does not constitute a standard, specification or regulation.

Abstract

The purpose of this project and the Internally Cured Concrete (ICC) test section was to evaluate the benefits obtained through internal curing using pre-saturated lightweight aggregate (LWA). Two test sections were constructed on the mainline of US-54 near Iola, Kansas: a Control section and an ICC section using lightweight aggregate. Traditional laboratory testing was conducted on each test section to compare fresh and hardened concrete properties including, but not limited to, slump, temperature, air content, unit weight, strength, permeability, and freeze/thaw. Also, several strain gages and moisture sensors were embedded in each test section to monitor the actual strain and moisture content present in the concrete. In addition, a Dipstick Profiler was used on five panels to get a full panel surface profile at the highest and lowest temperatures for several days after pavement construction. Last, HIPERPAV III analysis was used to compare early age stress and cracking risk.

The plastic and hardened concrete results presented in this report indicate no significant impact of the LWA material. For the majority of the properties tested, when comparing the results from the two sections, the values fall within the multiple laboratory precision expected when testing from the same concrete batch. However, the reduction in unit weight, the slight reduction of elastic modulus, and the slight increase in tensile strength of the ICC indicate a potential improvement in overall durability and potentially increased service life. Additional research into these properties would be required to support that data.

The methods used to collect strain, moisture, and deflection data were highly successful. All methods of data collection including strain, curvature, moisture, deflection, and HIPERPAV III results infer the use of lightweight aggregate and internally cured concrete reduce the initial strain and undesirable deformations in the concrete. However, the test sections were not able to be constructed at the same time due to lack of staff, weather delays, and contractor's schedule, and therefore, were constructed 3 months apart. As a result, the significant weather differences between the placement dates have been observed to have impacted the data from the strain gages and moisture sensors. Therefore, it cannot be concluded with certainty if the use of LWA in the ICC improved the quality and durability of the concrete compared to the Control section. General condition surveys will be performed every five years of the 20-year design life, or until a major rehabilitation occurs and the original sections can no longer be surveyed.

Acknowledgements

Special thanks are extended to John Ries from the Expanded Shale, Clay and Slate Institute (ESCSI) for his support of the project and the funding of equipment used. Thanks to Daron Brown formerly of Buildex (lightweight aggregate supplier) for his guidance in developing the mix design, purchasing equipment and on-site support during placement. Kansas Department of Transportation (KDOT) Research personnel Rodney Montney for his assistance in evaluating the data acquisition plans, Andrew Jenkins for his extensive planning and collecting of data, and Jennifer Distlehorst for her assistance in the field with instrumentation setup and data acquisition. Thanks are extended to KDOT Research technicians for their efforts during placement, data collection and field and sample testing. To KDOT District field personnel for their support throughout the project. To the FHWA and the Mobile Concrete Technology Center for their participation in the project as well as input regarding the HIPERPAV III analysis. Final thanks are extended to the contractor, Koss Construction, particularly Robert Kennedy and Shane Griggs.

Table of Contents

List of Tables

List of Figures

Chapter 1: Introduction

In 2012, the Kansas Department of Transportation (KDOT) made the decision to build a concrete pavement test section utilizing internal curing with pre-saturated lightweight aggregate (LWA). In 2013, project number 54-01 KA-2202-01 on US-54 near Iola, KS, was identified as a potential test location. The project is located from 826 feet west of the east city limits of Iola (M.P. 7.3) and proceeds approximately 5.25 miles east to La Harpe, KS (M.P. 12.6). The existing pavement was jointed concrete pavement with doweled joints. Existing base material was left in place and reshaped as needed.

1.1 Research Purpose

The purpose of this project and the Internally Cured Concrete (ICC) test section was to evaluate the benefits obtained through internal curing using pre-saturated LWA. In theory, the usage of LWA would improve shrinkage properties and therefore reduce pavement cracking; this was not a primary focus for this project as the new pavement would be jointed. The pavements will be evaluated to determine if there is a significant reduction in permanent panel warping. Permanent panel warping, caused by excessive moisture loss at the pavement surface during curing, can lead to poor ride quality. Excessive warping can also lead to structural failure of the pavement such as mid-panel cracking, corner breaks, and base pumping. Additional testing was performed to determine any additional benefits to concrete strength and durability.

Chapter 2: Materials, Instrumentation, and Testing

2.1 Materials

2.1.1 Concrete Materials

When using LWA for internal curing, the LWA is substituted for a small percentage (typically between 20-30% by weight) of the fine aggregate with a similar gradation as the fine aggregate. For this project, the LWA used had a slightly coarser gradation to help optimize the overall gradation and was directly substituted for the intermediate aggregate. The LWA for this project was supplied by Buildex from the New Market plant north of Kansas City, MO. The physical properties of the LWA are presented in Table 2.1. The gradation used for the LWA is presented in Table 2.2. This information can be found at Buildex.com and is listed as an ASTM C330-3/8 X 0 gradation.

Table 2.1: Lightweight Aggregate Properties

Specific Gravity	Oven Dry Loose Density, lbs/ft^3	Percent Absorption, %	Degree of Desorption, %
1.71	54	14	90

Table 2.2: Lightweight Aggregate Gradation

Sieve	Percent Retained
1/2”	0
3/8”	0
No. 4	18
No. 8	42
No. 16	62
No. 30	77
No. 50	87
No. 100	91

All materials used in the pavement were KDOT approved. Coarse aggregate was a coarse paving limestone aggregate produced by Nelson Quarries from their Allen County, KS, quarry (KDOT quarry number 4-001-01-LS) with a specific gravity of 2.56. The gradation for the coarse paving limestone aggregate is presented in Table 2.3. An intermediate mixed aggregate, crushed

limestone, from the same quarry was used during paving of the Control section pavement. The gradation for the intermediate crushed limestone is presented in Table 2.4. The fine aggregate was Cornejo & Sons basic sand, sand-gravel for mixed aggregate out of Sedgwick County, KS (KDOT producer ID 819304) with a specific gravity of 2.61. The gradation for the fine aggregate is presented in Table 2.5.

Table 2.3: Coarse Paving Aggregate Limestone Gradation

Sieve	Percent Retained
3/4”	12
1/2”	45
3/8”	65
No. 4	95
No. 8	98
No. 16	98
No. 30	98
No. 50	99
No. 100	99

Table 2.4: Intermediate Mixed Aggregate Crushed Limestone Gradation

Sieve	Percent Retained
1/2”	0
3/8”	0
No. 4	20
No. 8	95
No. 16	99
No. 30	99
No. 50	99
No. 100	100

Table 2.5: Basic Sand, Sand-Gravel for Mixed Aggregate Gradation

Sieve	Percent Retained
1/2”	0
3/8”	0
No. 4	4
No. 8	17
No. 16	45
No. 30	66
No. 50	89
No. 100	99

Type I/II cement with a specific gravity of 3.15 produced by Ash Grove Cement Co. in Chanute, KS, was used for the project. Class C Fly Ash with a specific gravity of 2.65 produced by Kansas City Power and Light (KCPL), La Cygne, KS, plant was used as a supplemental cementitious material (SCM).

Both air entraining agent (AEA) and water reducer (WR) supplied by Euclid Chemical Company were used on the project. The air entraining agent used was AEA-92S; the water reducer was WR-91. City of Gas, KS, water was used for the project.

2.1.2 Material Proportions

Two concrete mix designs were used during this project. The Control concrete mix contained the materials presented in Section 2.1 in proportions outlined in Table 2.6.

Table 2.6: Concrete Mix Design 4P131K2D; Control Design

	lbs/yd^3	%
Cement Content	540	-
6.5 % Air Content		
Type I/II Cement	405	75
SCM: Class C Fly Ash	135	25
w/c	0.41	-
CPA-4 Limestone	1515	50
IMA- Crushed Limestone	303	10
Basic SSG for MA-3	1212	40

The ICC mix design is based on the mix proportioning guidelines developed by the Expanded Shale, Clay, and Slate Institute (ESCSI). Based on ESCSI's mixing guidelines of requiring approximately 7 pounds of water to be supplied by the LWA per 100 pounds of cementitious material, using the properties outlined in Table 2.1, laboratory testing indicated approximately 2.46 ft^3 of LWA are needed per cubic yard of concrete; actual in place concrete required 3.21 ft^3 of LWA. See ESCSI's website for more information and batching calculator (escsi.org). Due to the significant difference in density between the LWA and the paving aggregates used, the volume of the LWA must be taken into consideration and the entire mix design may have to be shifted to account for this difference. For this project a slightly coarser gradation of the LWA was used so that it could be substituted for the intermediate aggregate and maintain the overall gradation and the quality of the concrete with minimal changes to the quantity of the coarse and fine aggregates. See Table 2.7 for comparison between laboratory mixes and the actual field mix.

Table 2.7: Concrete Mix ICC Design

	Laboratory Mix		Field 4P141K1E	
	lbs/yd^3	%	lbs/yd^3	%
Cement Content	540	-	542	-
6.5 % Air Content	-	-	-	-
Type I/II Cement	405	75	406	75
SCM: Class C Fly Ash	135	25	136	25
w/c	0.40	-	0.40	-
CPA-4 Limestone	1485	51	1515	53
LWA	262	9	343	12
Basic SSG for MA-3	1165	40	1000	35

2.2 Instrumentation

Two panels in both the ICC section and the Control section were instrumented (see Figure 3.1 for addition details). Weather conditions were also measured for the duration of the strain and moisture data collection period. Both test sections included five adjacent panels, including the two instrumented panels in each section, that were read for deflection during the initial curing window. Additionally, samples were cast during placement to evaluate a variety of hardened concrete

properties. The Federal Highway Administration's (FHWA) Mobile Concrete Technology Center was on site during the placement of the ICC test section; see Section 2.3.3 for more details.

2.2.1 Strain and Moisture

Geokon 4200 Series vibrating wire strain gages (Figure 2.1) were used to measure strain. The strain gages collected data for internal concrete strain and temperature. The data was used to develop strain and temperature profiles through the depth of the slabs. The strain gages were read with a Campbell Scientific CR1000 data-logger with an AVW200 vibrating wire analyzer (Figure 2.5).

Figure 2.1: Geokon 4200 Vibrating Wire Strain Gage

Decagon Devices GS3 Moisture Sensors (Figure 2.2) were used to collect pavement moisture data. The moisture sensors collected both volumetric water content and temperature. This was also used to create moisture and temperature profiles through the depth of the slab. The moisture sensors were read with the Decagon Devices Em50 data-logger (Figure 2.5).

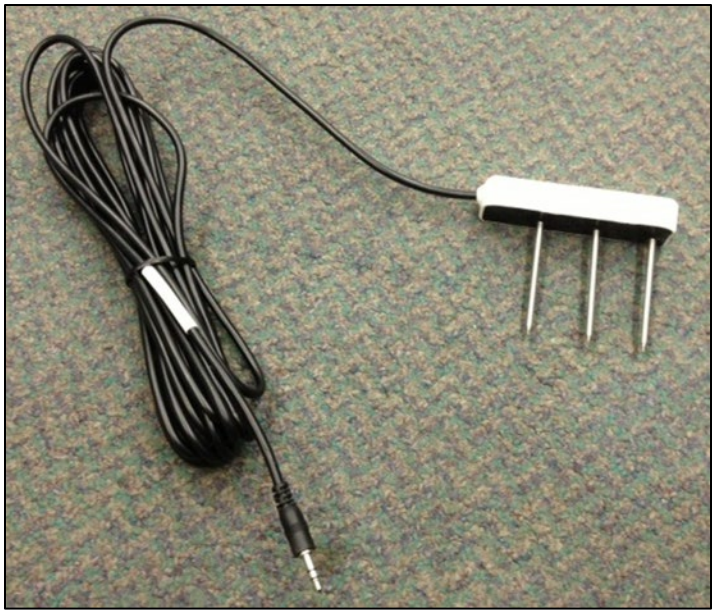

Figure 2.2: Decagon Devices GS3 Moisture Sensor

The reading frequency for both the strain gages and moisture sensors are presented in Table 2.8. The Control Section collected data from July 2014 until May 2015 (approximately 10 months), and the ICC Section collected data from May 2014 until May 2015 (approximately 12 months).

Table 2.8: Reading Frequency for Strain Gages and Moisture Sensors

Age of Section	Reading Frequency, minutes
0 - 24 hrs.	5
24 hrs. - 21 days	15
21 days+	60

2.2.2 Weather

Weather conditions were measured starting from one day prior to the ICC placement date until removal of equipment in May 2015. A Campbell Scientific Met-One Anemometer (Figure 2.3) and Rotronic HygroClip2 Temperature/Relative Humidity probe (Figure 2.4) were used to collect wind speed, ambient temperature, and relative humidity, respectively. Both sensors were read using the CR1000 data-logger (Figure 2.5).

Figure 2.3: Met-One Anemometer (outlined by black rectangle) Attached to Data Logging Equipment

Figure 2.4: Rotronic HygroClip2 Temperature/Relative Humidity Probe Inside Solar Radiation Shield (outlined by black rectangle) Attached to Data Logging Equipment

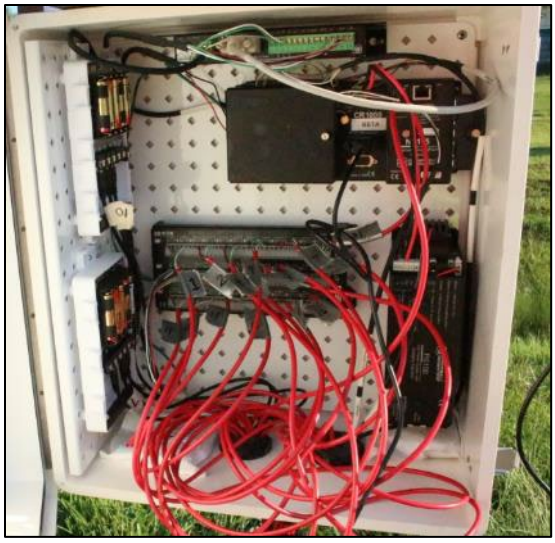

Figure 2.5: CR1000 Data-Logger (top-right) in weather-proof box. Decagon Devices Em50 Data Loggers (left side)

2.2.3 Pavement Deflections

Deflection readings were taken with a Face Dipstick (Figure 2.6). Readings were taken during the diurnal low and high temperature time blocks. It was determined prior to the placement that the low and high temperatures typically occur between 5:00 and 7:00 AM and 4:00 and 5:30 PM, respectively. Deflection readings were taken between 4:30 and 7:30 AM and 3:00 and 6:00 PM to ensure readings during the diurnal temperature ranges.

Figure 2.6: Face Dipstick

A reading pattern was developed to establish a profile that could be used to plot the deflections in 3-D space and to ensure the integrity of the readings. The reading pattern can be seen in Figure 2.7. This pattern was mapped out on all panels P1–P5. See Figure 3.1 for panel layout. Readings began on panel P1 and then proceeded to P2, P3, P4, and P5. "One pass" or one set of readings from all five panels was a single data set. The reading pattern was repeated three times; thus, each panel was read a total of three times during each three-hour time block described above. For an experienced two-person crew, each pass took approximately 50–60 minutes to complete with each panel taking an average of 10 minutes. Other information such as ambient temperature and pavement surface temperature were recorded at the start of every panel and at the conclusion of the final of three passes on panel P5.

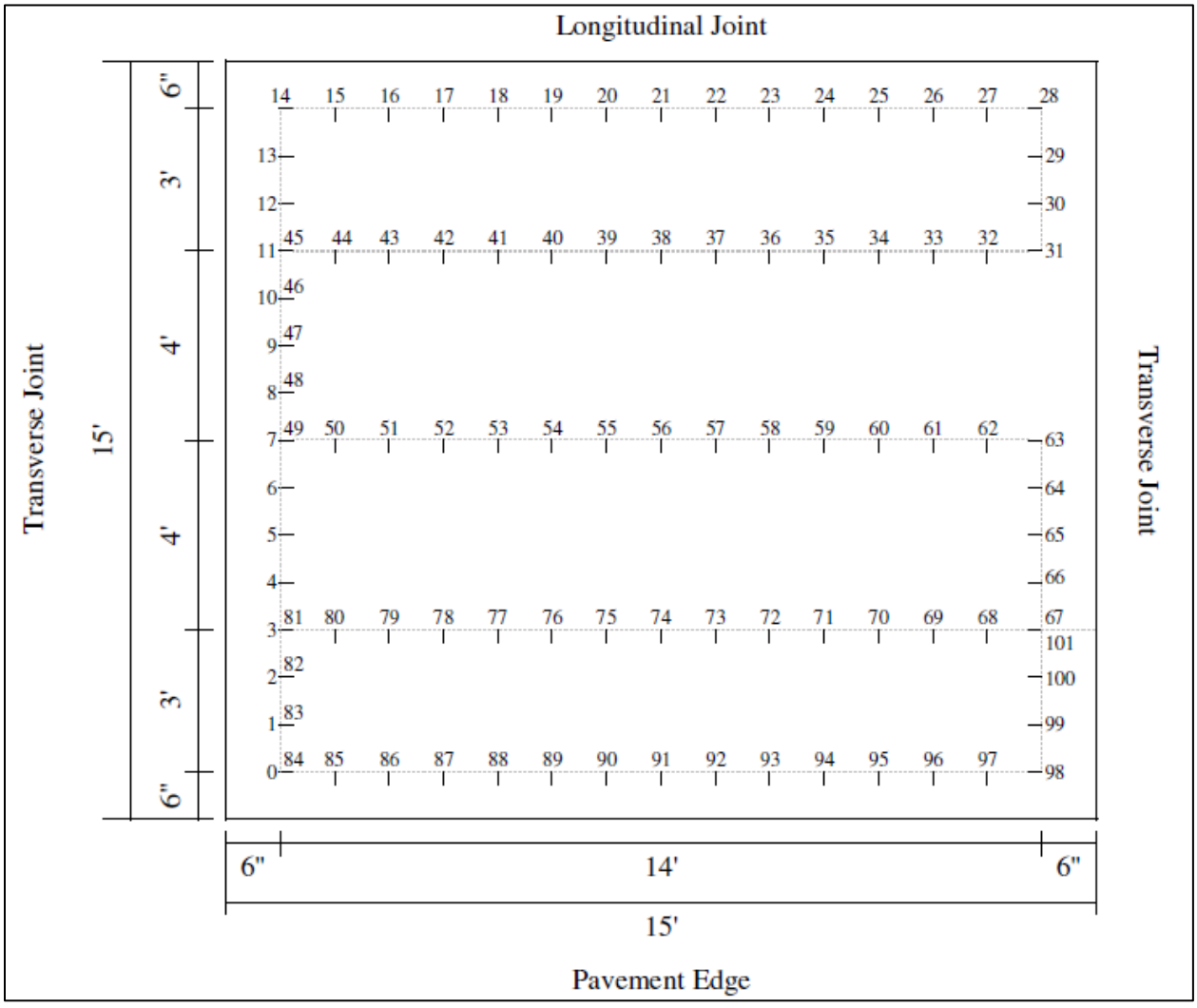

Figure 2.7: Deflection Reading Pattern for One 15-foot by 15-foot Panel (Not to Scale)

For the ICC test section, an initial reading was performed immediately prior to and immediately after joint sawing the morning of 5/3/2014 at approximately 20 hours of age. Deflections were taken during the two time blocks until a section age of seven days beginning with the afternoon readings on 5/3/2014 and concluding after the morning reading on 5/9/2014. Additional readings were taken the afternoon of 5/21/2014 and the morning of 5/22/2014, representing approximately 21 days of age.

For the Control test section, an initial reading was performed immediately prior to and immediately after joint sawing the afternoon of 7/24/2014 at approximately 8 hours of age. Deflections were taken during the two-time blocks until a section age of seven days beginning with the morning readings on 7/25/2014 and concluding after the morning reading on 7/31/2014. No additional readings were taken on the control section because the contractor began diamond grinding of the entire pavement surface. The grinding is standard KDOT procedure for urban concrete pavement construction.

2.3 Concrete Testing

2.3.1 Plastic Concrete Testing

Testing performed on plastic concrete at the time of placement for both the ICC and Control test sections consisted of the following:

- Temperature (ASTM C1064)
- Unit weight (ASTM C138)
- Slump (ASTM C143)
- Air Content, Pressure Method (ASTM C231)
- Air Void Spacing (Performed with Air Void Analyzer, KT-71, Appendix A)
- Penetration Resistance (ASTM C403)
- Casting of concrete specimens for physical property testing (ASTM C31)

2.3.2 Hardened Concrete Testing

Concrete samples were cast from both the ICC and Control sections for various hardened concrete property testing. Note that all samples underwent standard curing as specified in their respective test methods. Also note that "KTMR" test methods are Kansas specific test methods. Samples cast for laboratory testing included:

- 7-Day Elastic modulus/Poisson's Ratio (ASTM C469)
- 28-Day Compressive Strength (AASHTO T22)
- 28-Day Split Tensile Test (ASTM C496)
- 28-Day Flexural strength (center-point loading, AASHTO T177)
- 28-Day Elastic modulus/Poisson's Ratio (ASTM C469)
- 28-Day Volume of Permeable Voids (VPV) (ASTM C642)
- 28-Day Surface Resistivity (AASHTO T358)
- 28-Day Shrinkage (ASTM C157)
- 56-Day Rapid Chloride Permeability Test (RCPT) (ASTM C1202)
- Linear Traverse (ASTM C457)
- Resistance of Concrete to Rapid Freezing and Thawing (KTMR-22, Appendix B)
- Wetting and Drying Test of Sand and Sand Gravel Aggregate for Concrete (KTMR-23, Appendix C)

KTMR testing is typically performed by a KDOT laboratory; KT testing may be performed by KDOT, a consulting firm, or in some cases the contractor.

2.3.3 FHWA Mobile Concrete Laboratory Testing

The FHWA Mobile Concrete Technology Center was on site during the construction of the ICC test section. A brief FHWA report is attached in Appendix D. The FHWA report was created to supplement this report and will not be published as a stand-alone document. Note that the "control" testing performed by the FHWA was performed on the control concrete mix at the time the laboratory was on-site in May 2014 and does not correspond to the control testing performed by KDOT in July 2014.

Chapter 3: Construction

3.1 Locations

As previously stated, the test sections are located on US-54 between Iola and La Harpe, KS. The project starts at the east city limits of Iola and proceeds approximately 5.25 miles east to La Harpe. The pavement design calls for four lanes of 9-inch concrete pavement with 15-ft joint spacing. The pavement cross-section varies between 24 and 27 feet wide depending on the location. The 24-ft sections consist of two 12-ft lanes with curb and gutter in the residential portions of the project. The 27-ft sections consist of one 12-ft passing lane and one 15-ft driving lane; the driving lane itself will be striped at 12 ft with a 3-ft shoulder. The pavement is on 4 inches of granular base. Both the ICC and Control test sections were built with the 27-ft cross-section.

Approximately 400 ft of ICC pavement was constructed on May 2, 2014, on the eastbound lanes from Station 220+16 to Station 223+95, between McArthur Road and the next entrance to the west. The corresponding control section was constructed on July 24, 2014, in the westbound lanes with the instrumented panels from Station 302+25 to 303+00 starting 60 feet west of the centerline of Belton Road intersection. The 15-ft driving lane of each test section was instrumented with strain gages and moisture sensors. Two panels in both the ICC and Control test sections were instrumented. Figure 3.1 is a plan view of one test section.

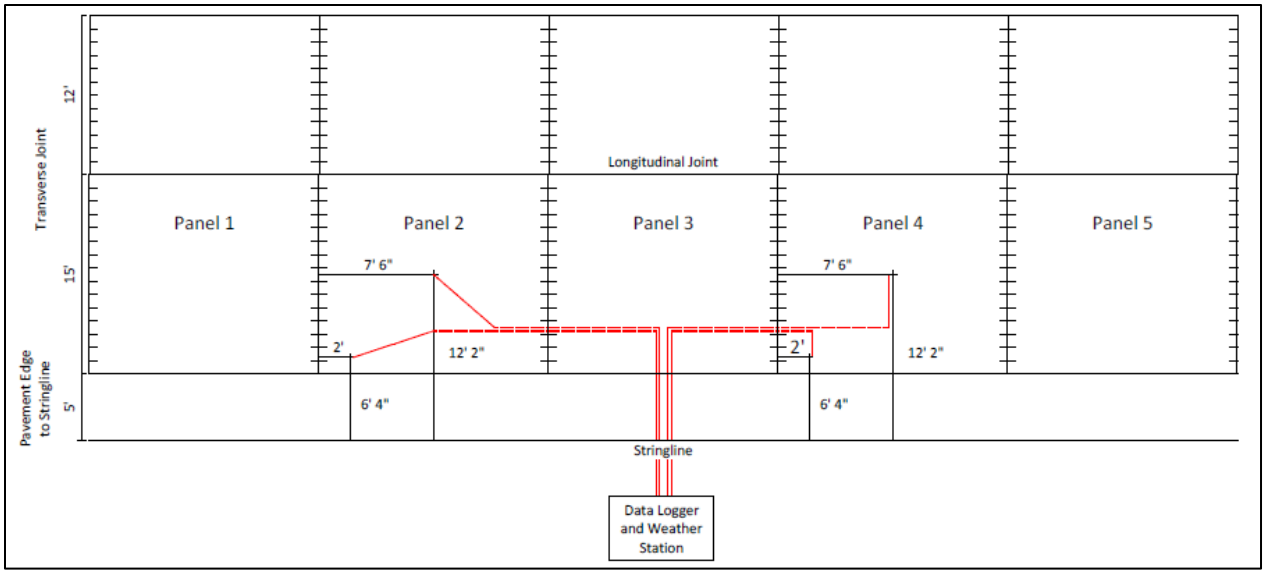

Figure 3.1: Plan View of ICC and Control Test Sections (Not to Scale)

Strain gages and moisture sensors were placed in the second and fourth panels of the test section and the data recording equipment was located at the shoulder in the center of the section. Figure 3.2 is a photo of the sensors in place.

Figure 3.2: Installed Sensors

Each instrumented panel contained five sensors in the corner of the panel, two in the longitudinal direction, two in the transverse direction, and one vertical gage. Figure 3.3 is a detail of the strain gage installation in the corner of the panel.

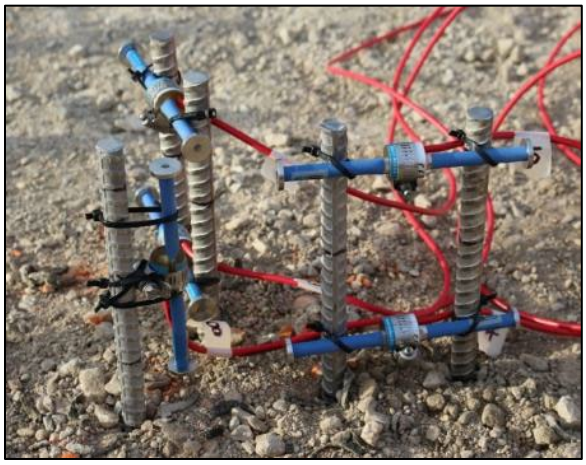

Figure 3.3: Detail of Strain Gage Installation in the Corner of the Panel

Three strain gages and three moisture sensors were placed in the center of each instrumented panel with the moisture sensors stacked vertically through the depth of the pavement. See Figure 3.4. Moisture sensors and strain gages were placed at three levels to determine the moisture gradient and strain gradient through the pavement section.

Figure 3.4: Moisture Sensors and Strain Gages in Center of Panel

Figure 3.5 is a detailed plan view of a single instrumented panel, showing the location of the corner gages and center gages with respect to the pavement edge and vibrator tracks.

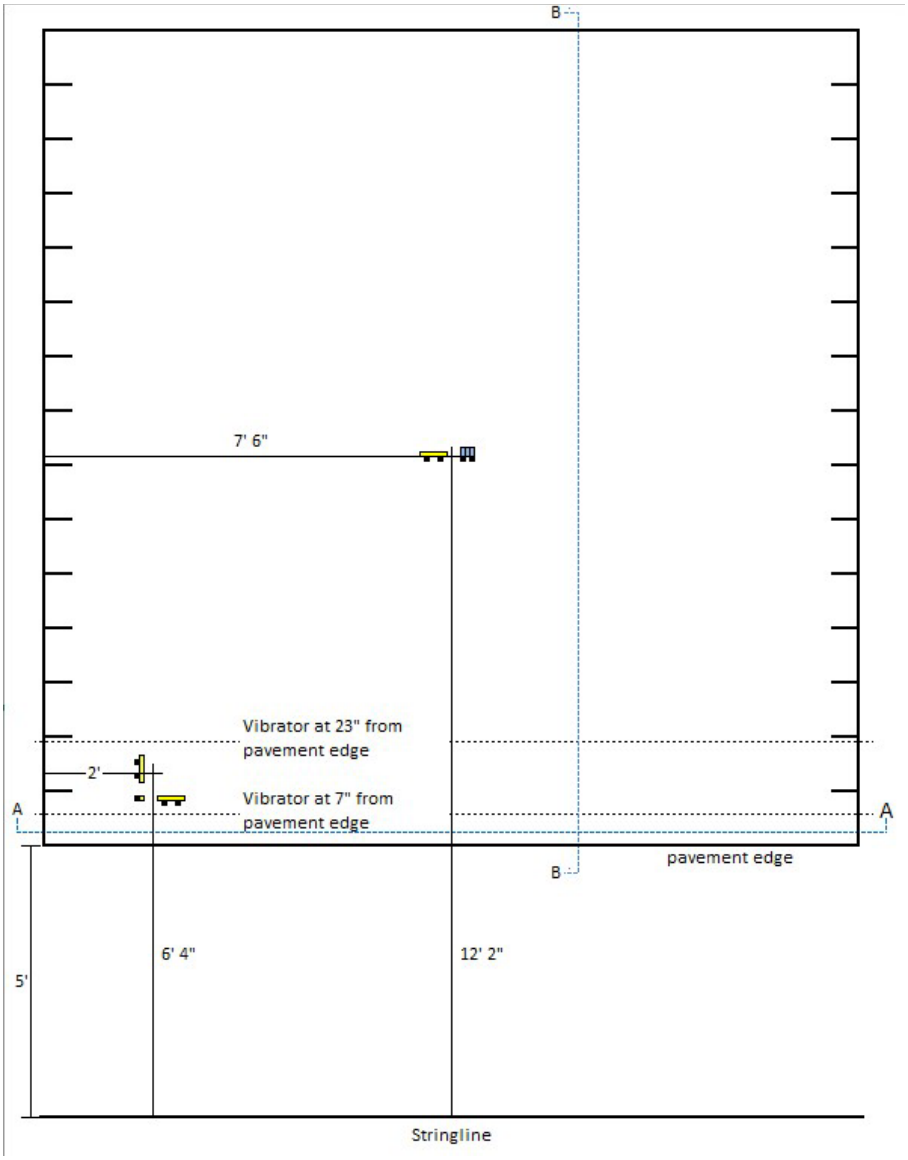

Figure 3.5: Plan View of Single Instrumented Panel with Gage Location (Not to Scale)

Figure 3.6 is a detail of the orientation of the sensors through the depth of the pavement. The corner sensor orientation can be seen on the left and the center sensor orientation can be seen on the right.

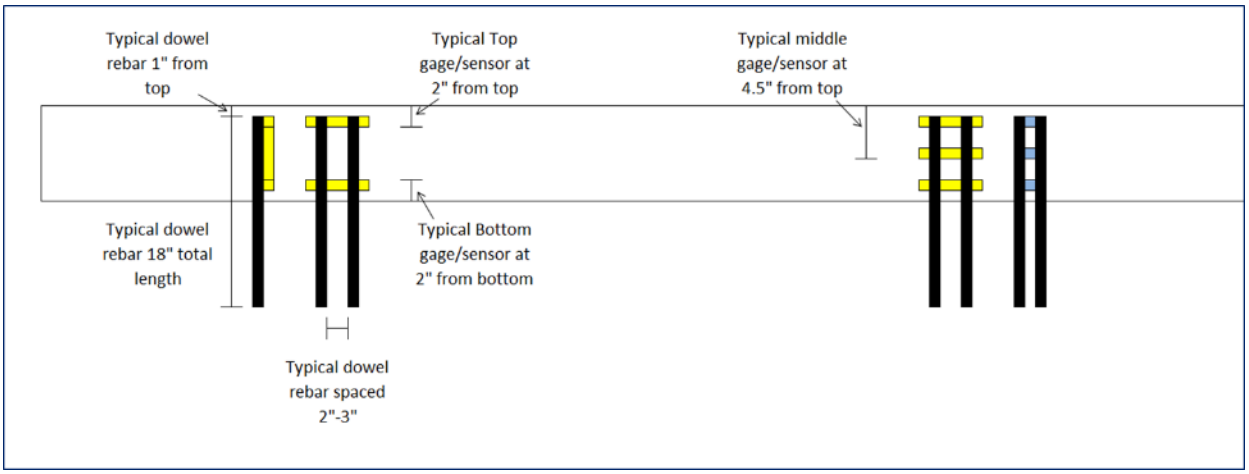

Figure 3.6: Partial Cross-Section View of Instrumented Panel Showing Gage Location Through Depth of Panel (Not to Scale)

Note in Figure 3.1 that five 15-ft panels (P1–P5) are outlined. Deflection readings were taken on the five panels as described in 2.2.3. In the ICC test section, panel P1 begins at Station 222+12 and Panel P5 ends at Station 222+87, 165 feet west of the centerline of the McArthur Road intersection. In the Control test section, Panel P1 begins at Station 303+00 and Panel P5 ends at Station 302+25, 60 feet west of the centerline of the Belton Road intersection.

Table 3.1 lists the strain gages used in the project and their respective locations as installed on the project. The strain gage numbers presented in the table will correspond to the graphs displayed in Chapter 4 regarding strain gages.

Table 3.1: Strain Gage Numbering and Locations

Test Section	Strain Gage Label	Location			Height Above Base	X Distance	Y Distance
ICC-P2	1	Center	Longitudinal	Bottom	2"	7.5'	7.5'
ICC-P2	2	Center	Longitudinal	Middle	4.5"	7.5'	7.5'
ICC-P2	3	Center	Longitudinal	Top	7"	7.5'	7.5'
ICC-P2	4	Corner	Longitudinal	Bottom	2"	1'	0.5'
ICC-P2	5	Corner	Longitudinal	Top	7"	1'	0.5'
ICC-P2	6	Corner	Transverse	Bottom	2"	0.5'	1'
ICC-P2	7	Corner	Transverse	Top	7"	0.5'	1'
ICC-P2	8	Corner	Vertical		4.5"	0.5'	0.5'
ICC-P4	9	Center	Longitudinal	Bottom	2"	7.5'	7.5'
ICC-P4	10	Center	Longitudinal	Middle	4.5"	7.5'	7.5'
ICC-P4	11	Center	Longitudinal	Top	7"	7.5'	7.5'
ICC-P4	12	Corner	Longitudinal	Bottom	2"	1'	0.5'
ICC-P4	13	Corner	Longitudinal	Top	7"	1'	0.5'
ICC-P4	14	Corner	Transverse	Bottom	2"	0.5'	1'
ICC-P4	15	Corner	Transverse	Top	7"	0.5'	1'
ICC-P4	16	Corner	Vertical		4.5"	0.5'	0.5'
Control-P2	1	Center	Longitudinal	Bottom	2"	7.5'	7.5'
Control-P2	2	Center	Longitudinal	Middle	4.5"	7.5'	7.5'
Control-P2	3	Center	Longitudinal	Top	7"	7.5'	7.5'
Control-P2	4	Corner	Longitudinal	Bottom	2"	1'	0.5'
Control-P2	5	Corner	Longitudinal	Top	7"	1'	0.5'
Control-P2	6	Corner	Transverse	Bottom	2"	0.5'	1'
Control-P2	7	Corner	Transverse	Top	7"	0.5'	1'
Control-P2	8	Corner	Vertical		4.5"	0.5'	0.5'
Control-P4	9	Center	Longitudinal	Bottom	2"	7.5'	7.5'
Control-P4	10	Center	Longitudinal	Middle	4.5"	7.5'	7.5'
Control-P4	11	Center	Longitudinal	Top	7"	7.5'	7.5'
Control-P4	12	Corner	Longitudinal	Bottom	2"	1'	0.5'
Control-P4	13	Corner	Longitudinal	Top	7"	1'	0.5'
Control-P4	14	Corner	Transverse	Bottom	2"	0.5'	1'
Control-P4	15	Corner	Transverse	Top	7"	0.5'	1'
Control-P4	16	Corner	Vertical		4.5"	0.5'	0.5'

3.2 Placement

As stated, the ICC test section was placed on May 2, 2014. The control test section was placed on July 24, 2014. Logistic issues with testing equipment and staff were the initial reason for the test sections not being constructed at the same time. Additionally, the contractor's schedule pushed the construction of the control section further into the summer than originally anticipated.

The ambient conditions during construction of the ICC and Control test sections are presented in Table 3.2. Ambient conditions during joint sawing of the ICC and Control test sections are presented in Table 3.3.

Table 3.2: Ambient Conditions During Construction

	ICC Section	Control Section
Placement Date/Time	5/2/14 9:11 AM	7/24/14 9:58 AM
Ambient Temperature	60.3°F	78.0°F
Relative Humidity	46.2%	63.2%
Wind Speed	2.1 mph	5.2 mph
Base Temperature	52.0°F	N/A

Table 3.3: Ambient Conditions During Joint Sawing of ICC Section

	ICC Section	Control Section
Date/Time of Sawing	5/3/14 5:00 AM	7/24/14 6:00 PM
Date/Time Sawing P1-P5 Joints	5/3/14 5:20 to 6:30 AM[1]	7/24/14 6:30 to 6:40 PM[2]
Age of Section at Sawing	20 hours	8.5 hours
Ambient Temperature	47.7°F	86.9°F
Relative Humidity	62.9%	51.8%
Wind Speed	1.8 mph (average)	4.0 mph (average)

Figure 3.7 through Figure 3.10 illustrate typical placement of concrete around the sensors during construction. In Figure 3.7, concrete is being placed over the sensors previous to vibrating with a hand vibrator to ensure consolidation around the sensor array. In Figure 3.8, concrete is being placed against the sensors and between the sensors in the array. In Figure 3.9 and Figure

[1] The transverse joints for the entire ICC test section were cut prior to the longitudinal joint being cut resulting in a time window during which all of the joints for P1-P2 were cut.
[2] The transverse joints for the entire Control test section were cut prior to the longitudinal joint being cut resulting in a time window during which all of the joints for P1-P2 were cut.

3.10, sensors and connecting wires were placed such that the vibrators or augers of the paving machine would not cause damage. Figure 3.11 shows poor application of white pigmented curing compound on the ICC test section. Curing compound was reapplied to the section approximately one hour after the initial application.

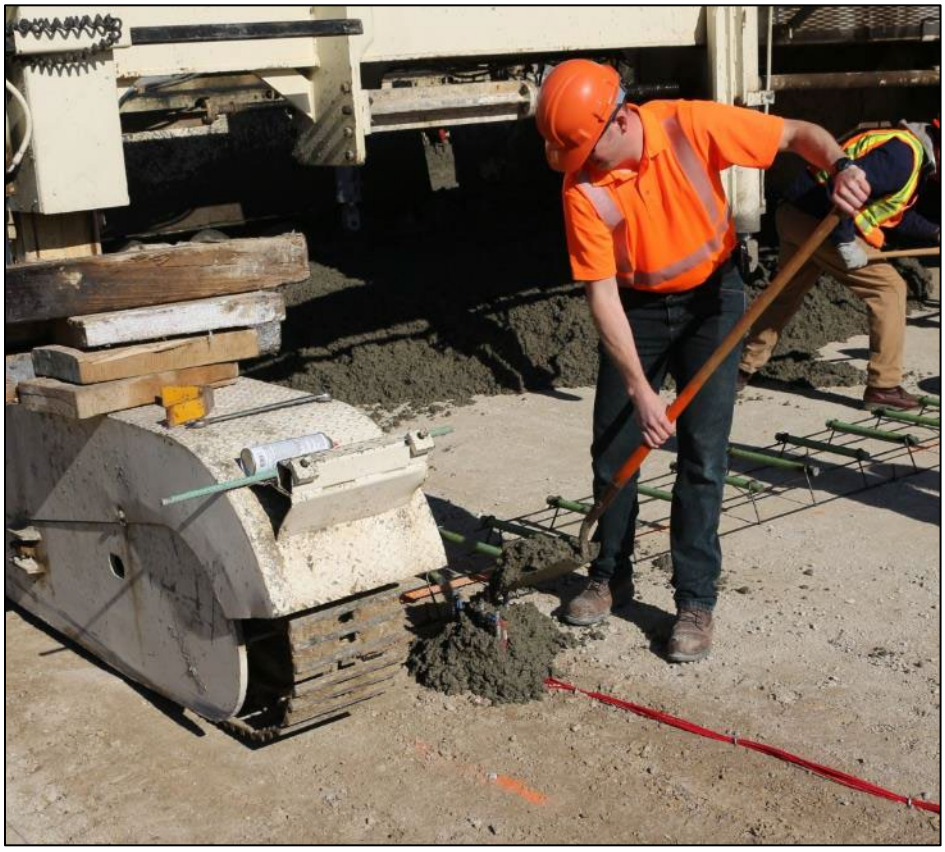

Figure 3.7: Placing Concrete Around Sensors

Figure 3.8: Packing Concrete Around Sensors to Ensure Proper Compaction

Figure 3.9: Concrete Laydown Machine Approaching Sensors

Figure 3.10: Sensors Between Laydown Machine and Finish Paver

Figure 3.11: Initial Application of White Pigmented Curing Compound

Chapter 4: Results

4.1 Plastic Concrete Test Results

Plastic concrete test results for the ICC and Control test sections are presented in Table 4.1.

Table 4.1: Plastic Concrete Test Results

	ICC Section	Control Section
Date and Time of Sampling	5/2/2014 9:38 AM	7/24/2014 9:58 AM
Concrete Temperature	59.5°F	84.5°F
Unit Weight	133.52 lb/ft^3	140.47 lb/ft^3
Slump	2.25 in	2.25 in
Air Content	7.8%	6.7%
AVA Spacing Factor	0.013 in	0.013 in
AVA Specific Surface	399 in^2/in^3	499 in^2/in^3

Results for ASTM C403, Penetration Resistance, for both sections are presented in Table 4.2. According to ASTM C403, initial set is defined as 500 psi and final set as 4000 psi. The penetration resistance was graphed with respect to elapsed time for the ICC and Control test sections in Figure 4.1 and Figure 4.2, respectively.

Table 4.2: ASTM C403 Penetration Resistance Test Results

	ICC Section	Control Section
Date and Time of Sampling	5/2/2014 9:38 AM	7/24/2014 10:30 AM
Initial Set (500 psi)	530 min. (8.8 hrs.)	386 min. (6.4 hrs.)
Final Set (4000 psi)	780 min. (13 hrs.)	489 min. (8.2 hrs.)

There was a considerable temperature difference in both the concrete temperature and the ambient temperature for the placement of the two instrumented test sections. Ambient temperature differed by 180° F and concrete temperatures differed by 250° F. The control section having both higher concrete and ambient temperatures due to the July placement considerably reduced both initial and final set times.

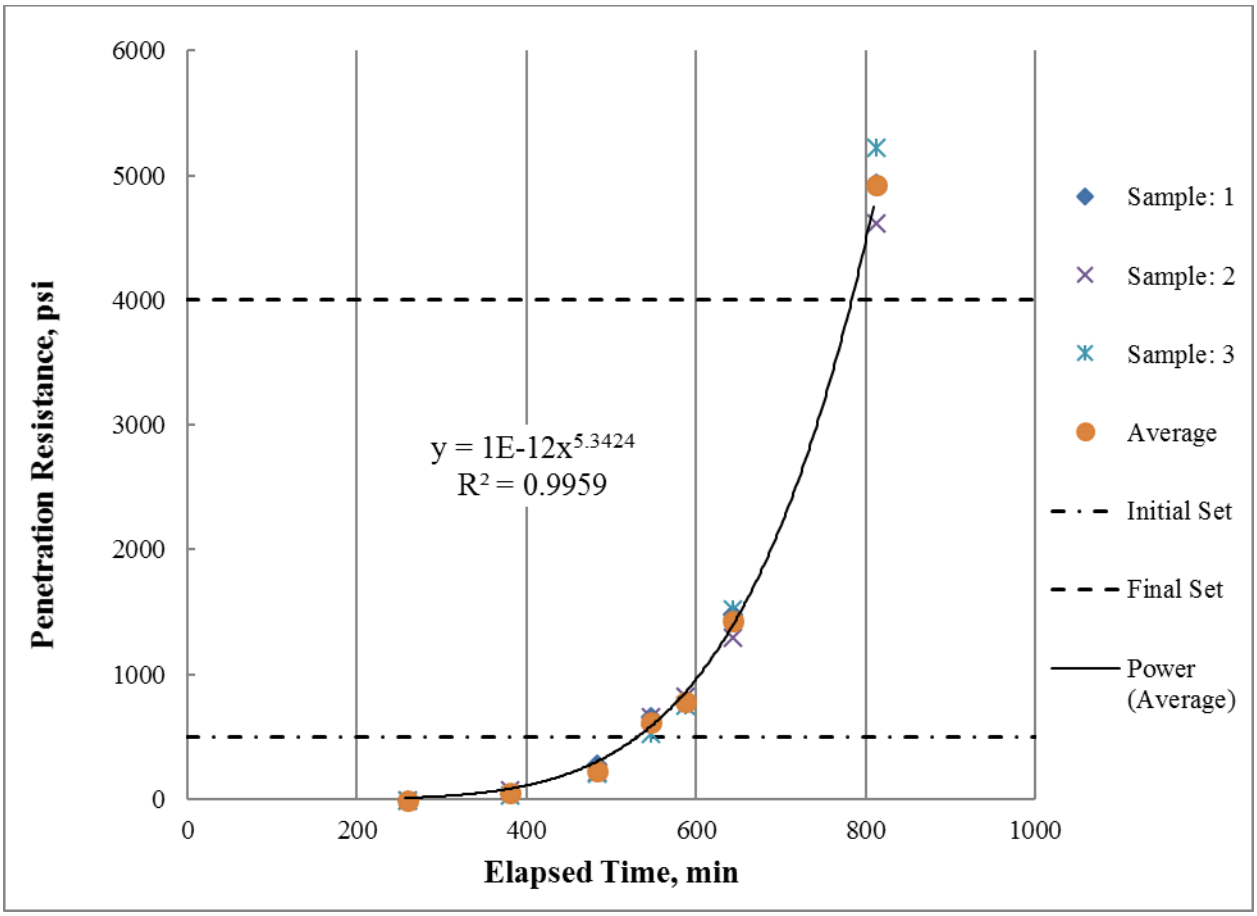

Figure 4.1: ASTM C403 Penetration Resistance Test Results for ICC Test Section

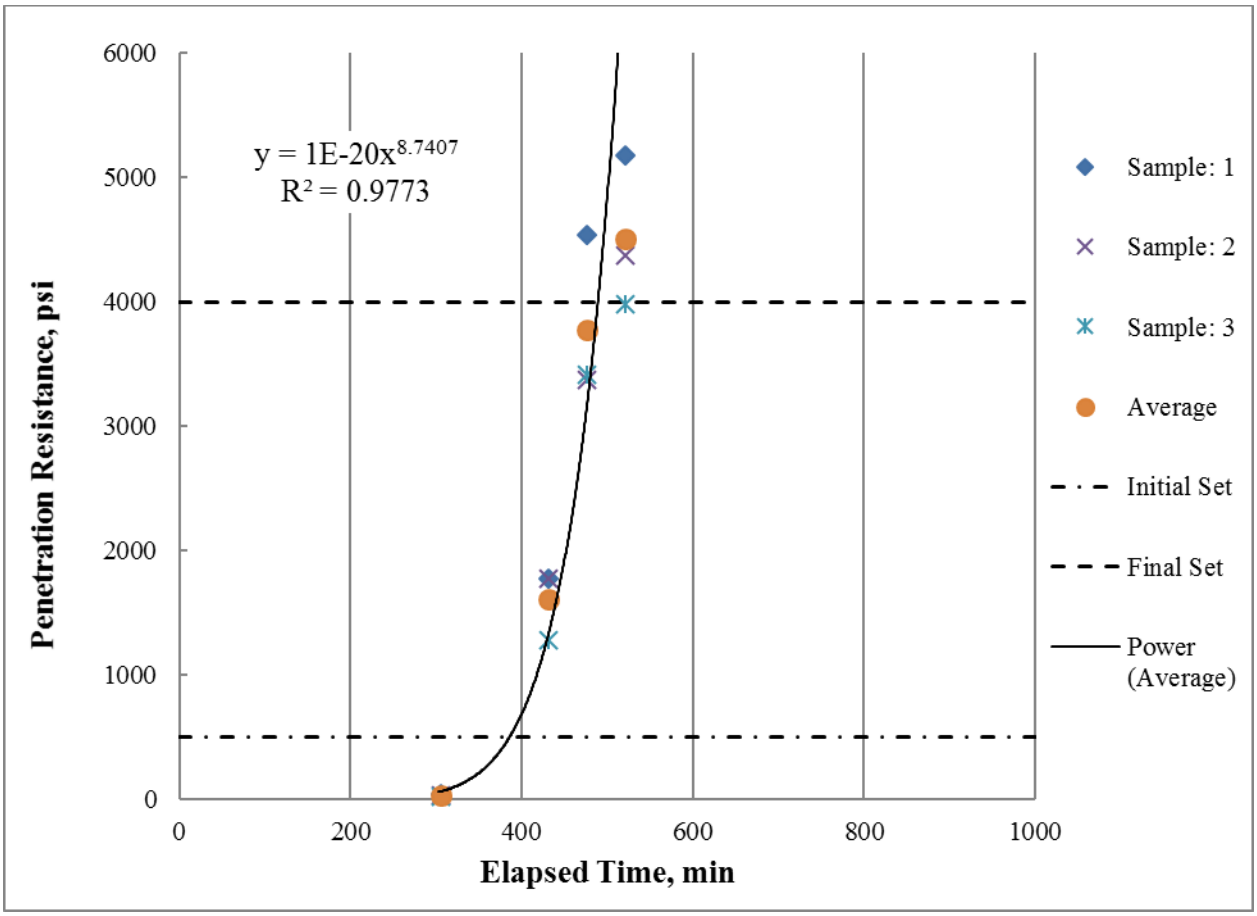

Figure 4.2: ASTM C403 Penetration Resistance Test Results for Control Test Section

4.2 Hardened Concrete Test Results

Hardened concrete test results for both test sections are presented in Table 4.3. Note that initial coefficient of thermal expansion testing was performed by the FHWA. Determining the coefficient of thermal expansion by using the strain gage data collected did indicate a significant difference between the two test sections and over the period of time the data was collected (see Figure 4.13, Figure 4.14, Table 4.8, and Table 4.9).

Reviewing the initial test data between the ICC and the control sections indicated very little difference, the lightweight aggregate did not appear to affect the basic properties of the concrete by a significant amount. Both sections, however, had poorer concrete permeability values than was expected. Both sections did pass the specified Rapid Chloride Permeability, but the numbers were higher than expected. Neither section passed the Volume of Permeable Voids specified requirement and the Surface Resistivity values (not specified) were very low (below present requirements).

Testing for Volume of Permeable Voids and Rapid Chloride Permeability in 2020 indicated the permeability of the concrete continued to improve over time as expected.

Table 4.3: Hardened Concrete Results

	ICC Section	Control Section
7-Day Elastic Modulus (E)	2890 ksi	3350 ksi
28-Day Elastic Modulus (E)	3500 ksi	3630 ksi
28-Day Poisson's Ratio (μ)	0.21	0.19
28-Day Compressive Strength (f'c)	4940 psi	5290 psi
28-Day Flexural Strength (center-point loading)	740 psi	760 psi
28-Day Tensile Strength	490 psi	470 psi
28-Day Volume of Permeable Voids	14.1%	13.9%
28-Day Surface Resistivity Measurement	6.0 kΩ-cm	7.4 kΩ-cm
56-Day Rapid Chloride Permeability	2540 C	2440 C
28-Day Shrinkage	0.030%	0.035%
Linear Traverse Spacing Factor	0.0044 in	0.0034 in
Linear Traverse Specific Surface	693 in^2/in^3	837 in^2/in^3
Coefficient of Thermal Expansion (α) (performed by FHWA)	7.50 με/˚C	7.50 με/˚C
October 9, 2020, Rapid Chloride Permeability	145 C	415 C
October 10, 2020, Volume of Permeable Voids	12.5%	13.2%

4.3 Strain

Strain gages were used to evaluate several aspects in the project including time of zero stress, cracking of saw joints, the strain and temperature relationship, the stress profile through the depth of the slab, slab curvature, and coefficient of thermal expansion. For the following figures showing actual strain, a positive strain value indicates tensile forces and negative strain values represent compressive forces. A panel is considered flat when the actual strain of the top and bottom gages are equal values.

It should be noted that due to the significantly different ambient and concrete temperatures at time of placement, time of zero stress occurs significantly earlier for the control section than the ICC section. The significance of this difference is the strain profile cast into the section. The strains present in the panel at time of zero stress are permanently cast into the section. In the ICC section, the surface of the panel was much cooler than the bottom, resulting in temperature related

shrinkage at the top (relative to the bottom) to be permanently cast into the panels. Given the high temperatures during placement of the control section, the opposite occurred; a permanent expansion of the surface (again relative to the bottom) was developed. While either scenario is neither detrimental nor beneficial by itself, it makes comparing the two test sections somewhat difficult.

When evaluating strain, the first step is to determine the time of final set in each panel. This step is required to calculate the actual strain based on the raw strain data gathered from the strain gages. The time of zero stress was found by analyzing individual strain gages for when the strain started to cycle linearly with temperature. A detailed description of strain gage calculations and finding the time of zero stress can be found in Appendix E. Table 4.4 presents the time of placement, time of zero stress, age at zero stress, and ambient temperature at the time of zero stress.

Table 4.4: Time of Zero Stress

Section	Time of Placement	Time of Zero Stress	Age at Zero Stress, h:m	Temp. at Time of Zero Stress, ^{0}F
ICC Section	9:39 AM 5/2/14	3:10 AM 5/3/2014	17:32	47.3
Control Section	10:30 AM 7/24/14	7:15 PM 2/24/14	8:45	86.9

It is notable that the age of the test section at the time of zero stress based on strain gage analysis nearly coincide with saw cutting times for both test sections. The ICC section was saw cut between 5:20 AM and 6:30 AM and the Control section was saw cut at approximately 6:35 PM (Table 3.3).

The evidence of saw cutting can be seen in Figure 4.3 for the ICC section and Figure 4.4 for the Control section. In both graphs, a jump in strain during the time of joint sawing can be seen followed by some erratic strain data that can be attributed to the concrete cracking through the depth of the panel joints. Longitudinal strain for the corner of ICC Panel 2 (Strain Gage 4 and Strain Gage 5) and the corner of ICC Panel 4 (Strain Gage 12 and Strain Gage 13) are plotted at the time of sawing. Based on Figure 4.3, the ICC panels appears to have cracked completely through at the time of sawing on 5/3/14 at approximately 5:30 AM with minimal erratic data

following. This is likely due to the cooler weather conditions causing the lightweight concrete section to contract and crack through its depth quickly.

Figure 4.4 shows the longitudinal strain for the corner of Control Panel 2 and Control Panel 4. Strain Gage 4 and Strain Gage 5 for Panel 2 and Strain Gage 12 and Strain Gage 13 for Panel 4. The data indicates that the cracking started at the time of sawing on 7/24/14 at approximately 6:30 PM, but the erratic strain data following shows the panels took roughly 8 hours to crack completely through; visual observation confirmed this. This is most likely a result of the higher ambient temperatures and higher concrete temperatures preventing the paving from contracting sufficiently to allow for rapid full depth cracking. Once the pavement cracked through full depth, the data displays a sinusoidal pattern exhibiting individual panel behavior.

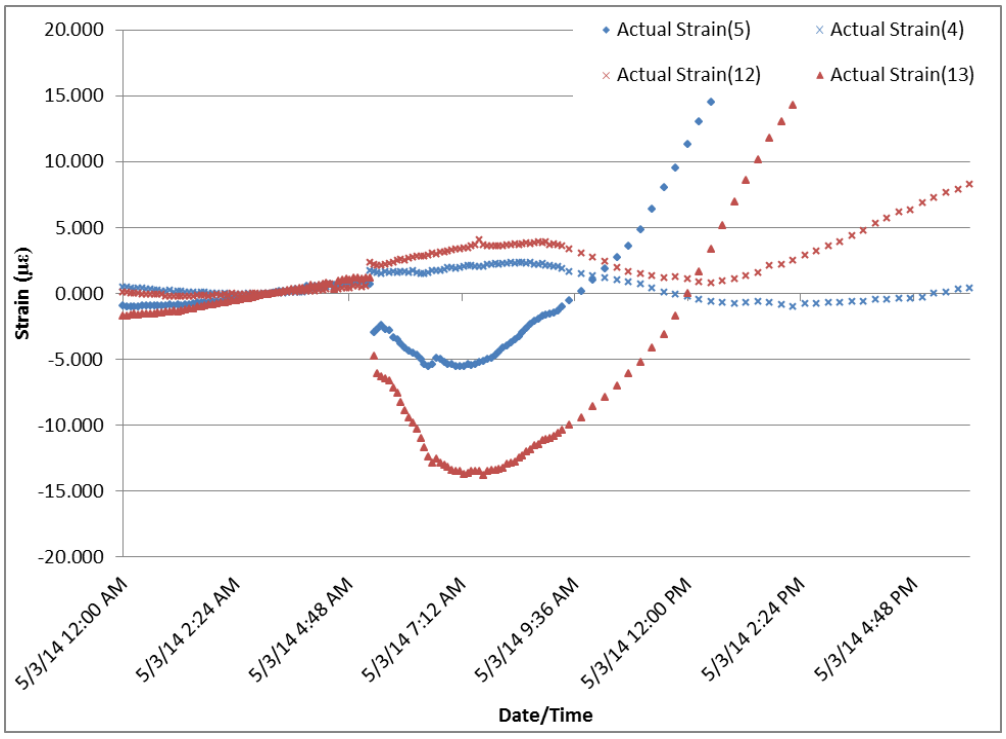

Figure 4.3: ICC Section Actual Strain, Evidence of Saw Cutting Operation

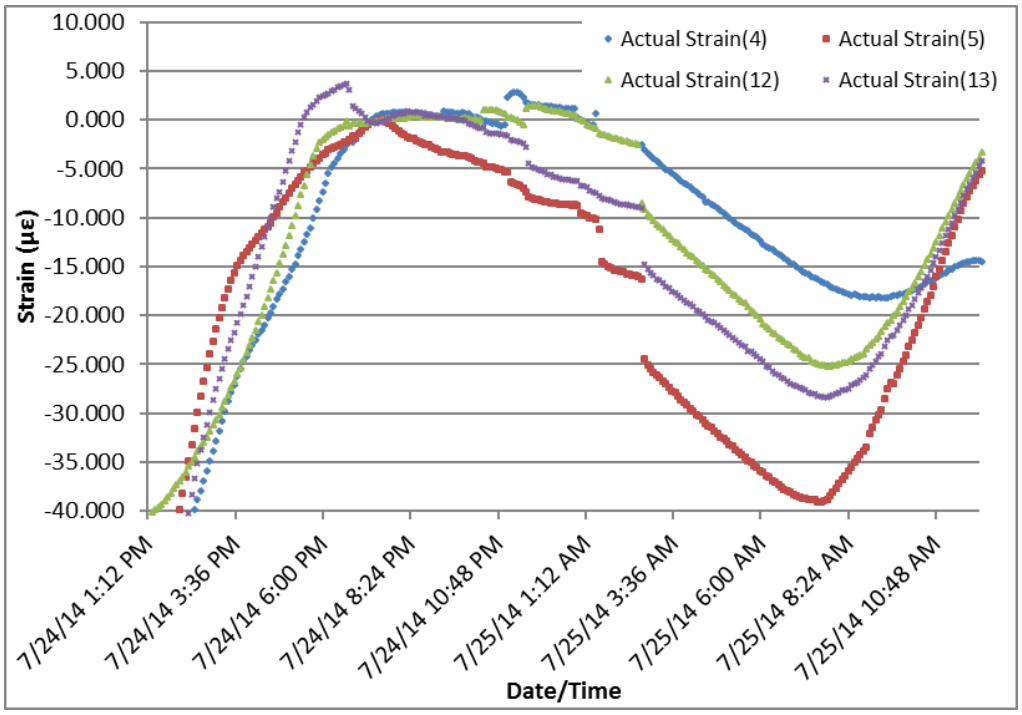

Figure 4.4: Control Section Actual Strain, Evidence of Saw Cutting Operation

Figure 4.5 and Figure 4.6 display the typical longitudinal strain and ambient temperature relationship through the depth of the panel for the ICC and Control sections, respectively, for the first two weeks after each section was constructed. For both sections, strain cycles daily with ambient temperature, which is known as pavement curling. The gages in Figure 4.5 are in the center of Panel 2. Gage 1 is at the bottom of the pavement section, Gage 2 at the middle of the section, and Gage 3 at the top of the section. The data also includes ambient temperature.

The figure also shows the top gage (Actual Strain 3) experiences more extreme strain cycles than the bottom gage (Actual Strain 1). This behavior is due to the response of the panel to the radiant heat of the sun. Conversely, the bottom gage response is less due to the subgrade heat sync and the cooler concrete at the bottom and does not experience as extreme changes in temperature inducing strain. This behavior is typical for both the ICC and Control sections throughout the testing period.

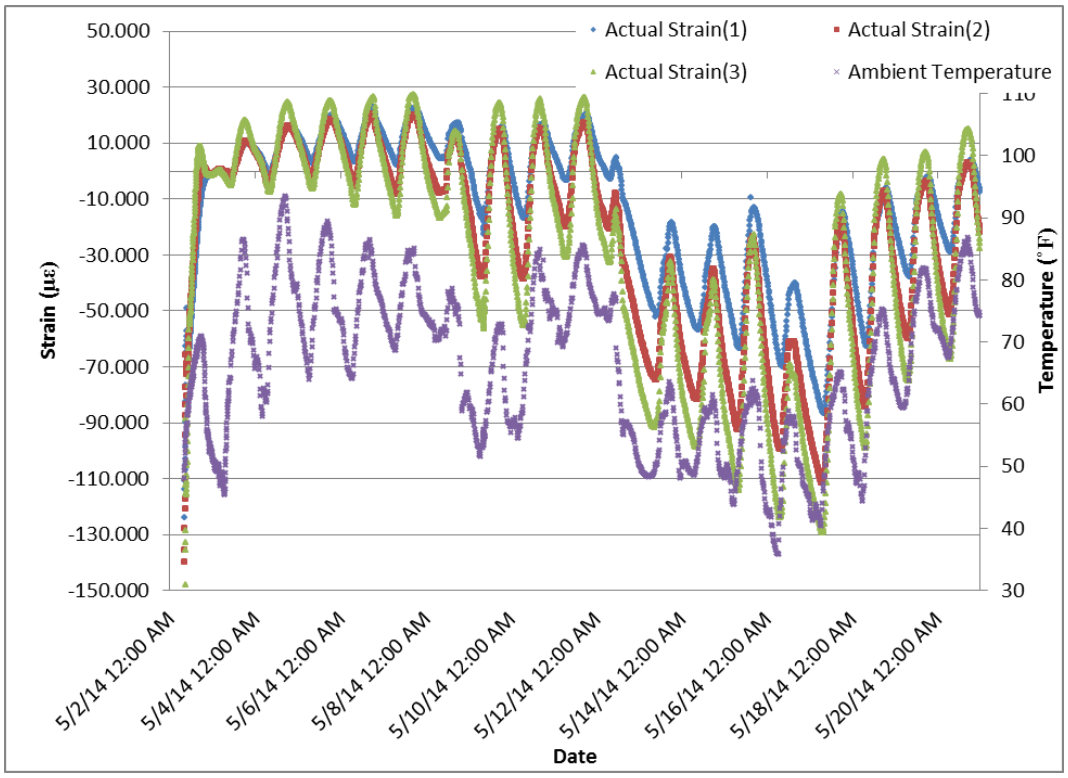

Figure 4.5: ICC Section Panel 2 Actual Strain and Ambient Temperature

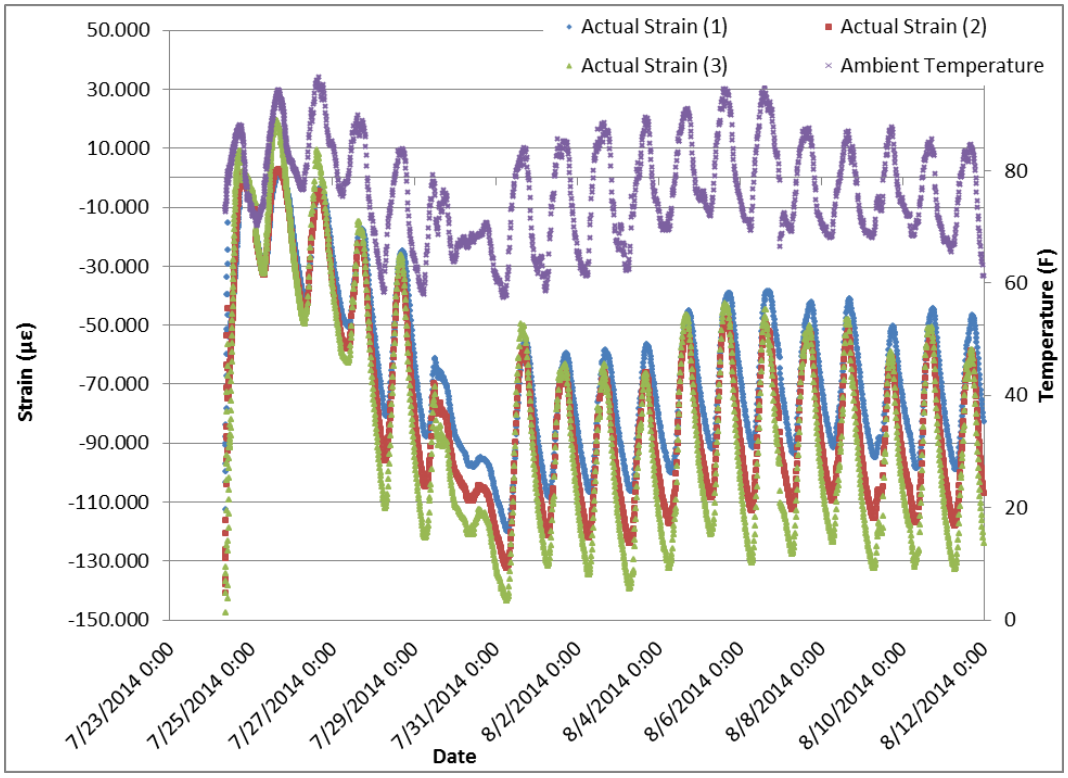

Figure 4.6: Control Section Panel 2 Actual Strain and Ambient Temperature

Closer examination of the data for the first 24 hours after placement for both the ICC Section 2 and the Control Section 2 indicate a significant difference in the response in strain to the concrete temperatures. Figure 4.7 and Figure 4.8 show the early response to concrete temperatures of both concrete mixes. To simplify the graphs the strain is the average of Strain Gage 1, Strain Gage 2, and Strain Gage 3 in ICC Panel 2 for the ICC strains and Strain Gage 1, Strain Gage 2, and Strain Gage 3 in Control Panel 2; these strain gages are stacked vertically in the middle of the panel as noted in Table 3.1. ICC Section 2 average strain rose from approximately -80 με at placement to an initial peak of 1.06 με and remained relatively constant dropping slightly to -2.88 με over a time period of 14:00 hrs. After placement, Control Section 2 average strain rose from approximately -90 με to initial peak of 3.1 με then dropped significantly to -32.5 με over a period of 13:00 hours. See Table 4.5 for a summary of concrete temperature and strain responses over time.

Table 4.5: Early Strain Response Summary, ICC and Control Sections First 24 hrs.

	ICC, Placed 5/2/2014, 9:11 AM				Control, Placed 7/24/2014, 9:58 AM			
	Max	Min	Change	Δ Time,	Max	Min	Change	Δ Time
Date	5/2	5/3			7/24	7/25		
Ambient Temperature, ^{0}C	21.5	7.5	14.0	12:55	31.0	21.2	9.8	9:45
Concrete Temperature, ^{0}C	20.9	17.4	3.5	14:00	40.4	32.2	8.2	13:35
Average Strain, με	1.06	-2.88	3.94	15:45	3.1	-32.5	35.6	13:00

Initial and final set did not appear to significantly affect the response of the average strain to the concrete temperatures. Using the initial and final set data in Chapter 3 the ICC section initial set would have occurred at approximately 6:30 pm and final set would have occurred at approximately 10:40 pm on May 2nd. The Control section initial set would have occurred at approximately 5:00 pm and final set at 6:45 pm on July 24th.

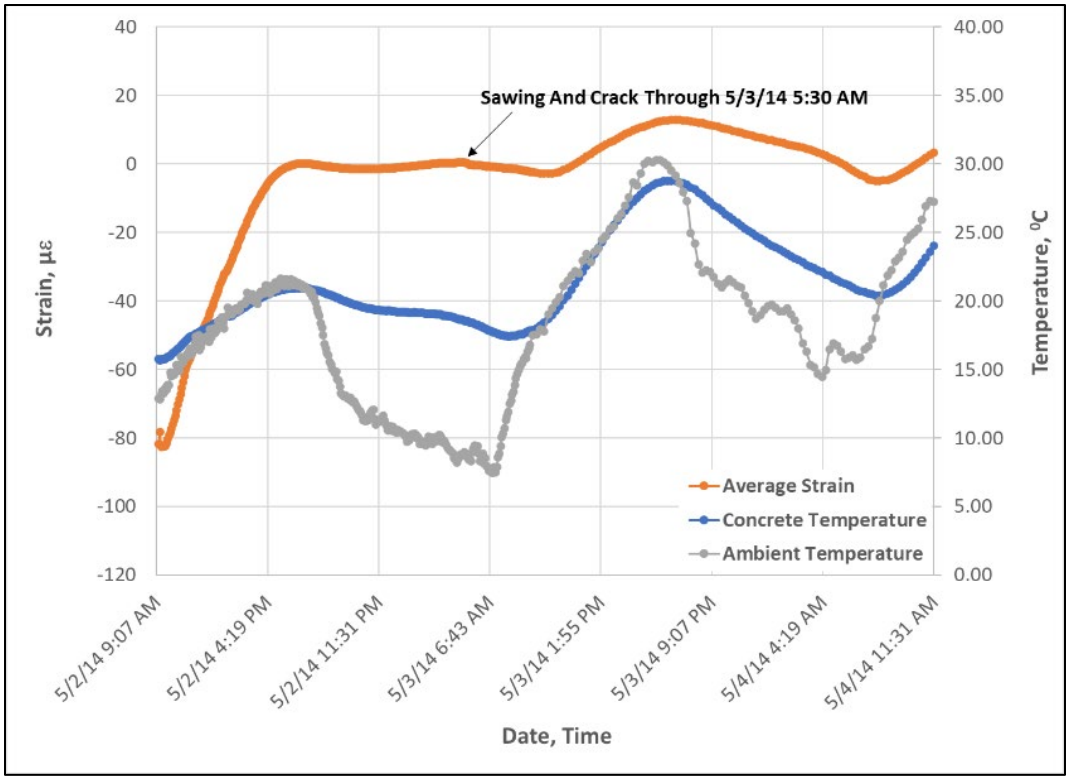

Figure 4.7: ICC Panel 2, Strain, Concrete and Ambient Temperature, 48 hrs.

Continuing into the second 24 hours after placement the strains of ICC Section 2 again showed a lower response to the change in concrete temperature than Control Section 2 (see Figures 4.7 and 4.8).

ICC Section 2 average strain rose to a second peak of 12.8 με and then dropped to -4.9 με over a time period of 13:15 hrs. After placement, Control Section 2 strain rose to a second peak of 7.2 με and then dropped significantly to -46.0 με over a period of 15:45 hours. See Table 4.6 for a summary of concrete temperature and strain responses and time.

Table 4.6: Early Strain Response Summary, ICC and Control Sections Second 24 hrs.

	ICC, Placed 5/2/2014, 9:11 AM				Control, Placed 7/24/2014, 9:58 AM			
	Max	Min	Change	Δ Time,	Max	Min	Change	Δ Time
Date	5/3	5/6			7/25	7/26		
Ambient Temperature, ⁰C	30.3	14.5	15.8	10:45	34.3	24.4	9.9	13:05
Concrete Temperature, ⁰C	28.8	20.4	8.4	13:45	43.0	32.9	7.1	14:30
Average Strain, με	12.8	-4.9	17.7	13:15	7.2	-46.0	53.2	15:45

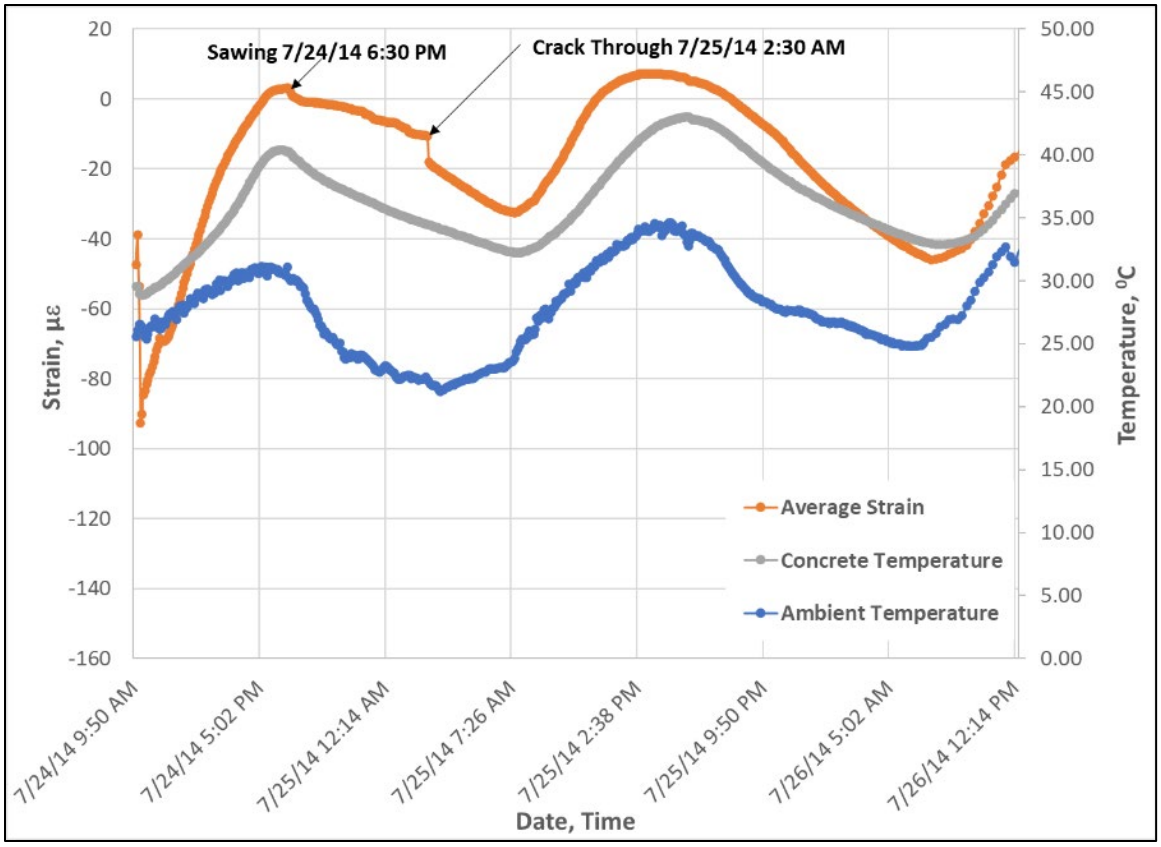

Figure 4.8: Control Panel 2, Strain Concrete and Ambient Temperature, 48 hrs.

Evaluating the Δε/ΔTime for both the ICC and Control Sections and evaluating the Δε/ΔTime/Change in Concrete Temperature the ICC Section has a much lower ratio than the Control Section (see Table 4.7).

Table 4.7: Strain-Time Factor for ICC and Control Panels.

	ICC	Control	Factor	ICC	Control	Factor
	First 24 Hours			Second 24 hours		
	Δε/ΔTime	Δε/ΔTime		Δε/ΔTime/ΔTemp	Δε/ΔTime/ΔTemp	
First 24 hours	0.250	2.738	10.9	0.071	0.334	4.7
Second 24 hours	1.336	3.378	2.5	0.159	0.476	3.0

After the initial 48 hours the ICC and the Control sections both tend to closely follow the ambient temperature changes which drive the concrete temperature changes causing strain cycles in the paving panels. The less severe strain cycles in the ICC concrete would have reduced

movement and thus reduce shock causing micro cracking when the concrete is young and tender and has lower tensile strength. The reduction in micro cracking would potentially reduce long term cracking. This would not be as critical in a jointed and doweled pavement structure but could be important for a bridge structure.

Figures 4.9 and Figure 4.10 display the average actual longitudinal strain observed in the center of Panel 2 and Panel 4, the average strain due to changes in temperature, the average strain due to "other" factors, and the ambient temperature for the ICC and Control sections, respectively. Actual strain and strain due to temperature were calculated using the equations found in Appendix E.

It was assumed that strain due to other factors was the difference between the actual strain and the strain due to temperature. Some of the "other" factors that affect the strain may include, but are not limited to, loss of moisture, humidity, shrinkage, and potentially creep.

Based on Figure 4.9, it is evident that the strain due to temperature for the ICC section coincides with the ambient temperature. The temperature strain initially causes expansion of the concrete during the warmer season as indicated by the positive strain values, and then causes compression of the concrete during the colder weather. The strain due to other factors drops significantly within the first few weeks after construction and appears to fluctuate daily until the temperature drops for the winter. This behavior is presumably strain due to early shrinkage and moisture loss over time in the lightweight aggregate mix whereas the fluctuations may be due to changes in humidity or environmental conditions. During the cooler season from September 2014 to March 2015, the strain due to other factors remains fairly constant without cycling. This is likely due to smaller temperature swings and lower humidity. As temperatures rise, the strain due to other factors continues to slowly drop. This could be due to long-term shrinkage or creep of the concrete.

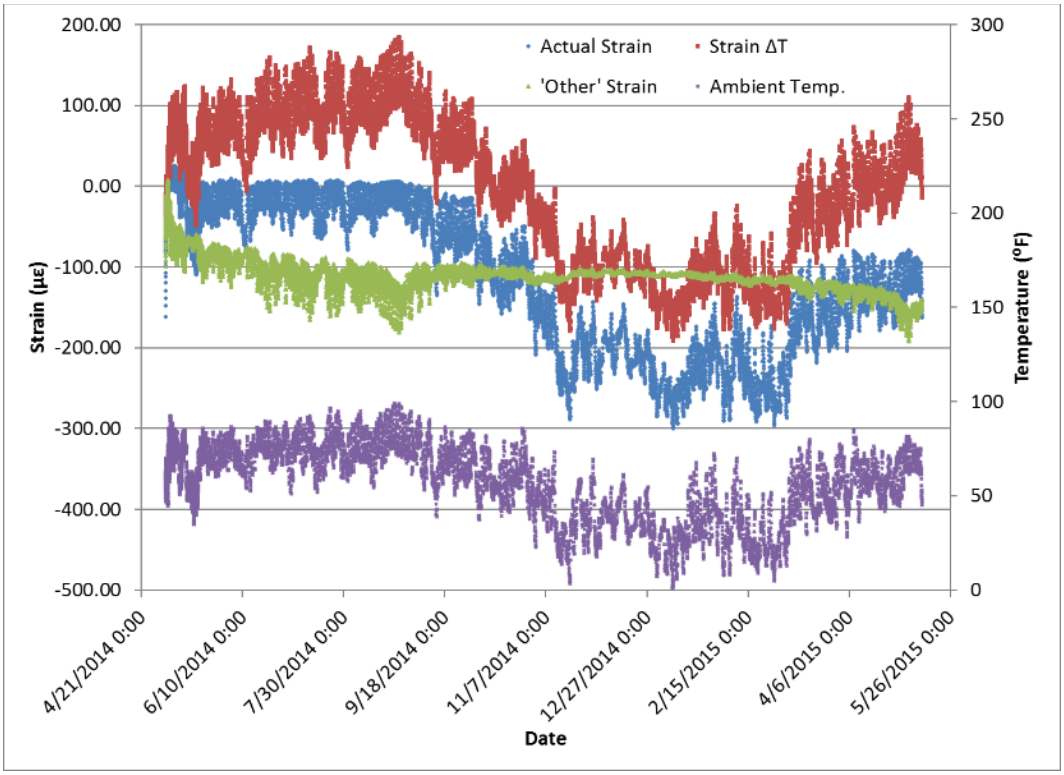

Figure 4.9: ICC Section Average Panel Actual Strain, Temp. Strain, and Strain due to 'Other' factors

Figure 4.10 depicts different strain behavior for the Control section in comparison to the ICC section. The strain due to temperature for the Control section coincides with the ambient temperature, but only results in compressive forces within the concrete as indicated by negative strain values. The strain due to temperature is the main component of the actual strain for the Control section, whereas there is little strain due to other factors that contributes to the actual strain. Regardless, the Control section still initially experiences a small drop in strain due to loss of moisture, as well as minimal early shrinkage. In addition, the Control section experiences near constant strain due to other factors during the cold weather from September 2014 to March 2015 as a result of lower temperatures and lower humidity. Last, as temperatures rise through May 2015, the strain due to other factors continues to drop slowly which is presumably due to long-term shrinkage or creep of the concrete.

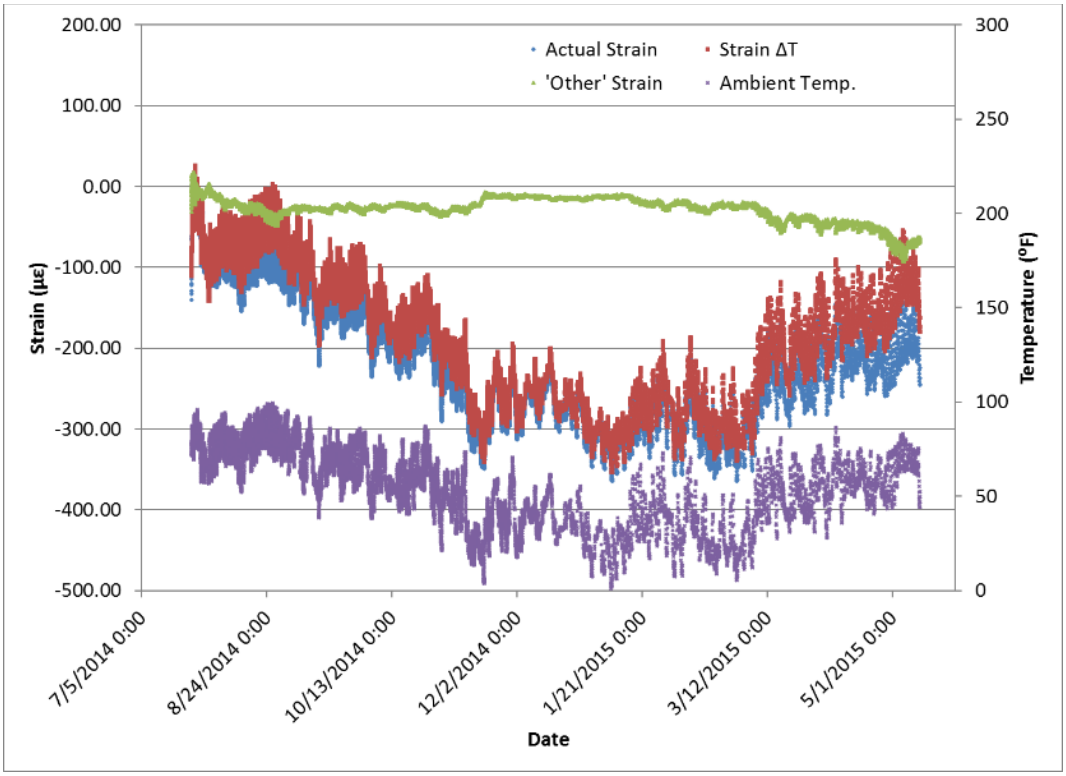

Figure 4.10: Control Section Average Panel Actual Strain, Temp. Strain, and Strain due to 'Other' factors

Figure 4.9 and Figure 4.10 displays the ambient temperature and the actual strain values for the average of the six strain gages positioned at the top, middle, and bottom in the center of Panels 2 and Panel 4 for both the ICC and Control sections. When each test section was initially constructed, both sections experienced a rapid shift in strain within the first week of construction due to loss of moisture during the curing process, and potential longitudinal movement of the panels as the paving structure ages and stabilizes. After the initial shift in strain, the ICC section cycled back to zero strain between May 2014 and September 2014 where the average daily strain during that time frame was approximately -25 με, indicating compression. The Control section never cycled back to zero strain after the initial shift, and the average daily strain through August 2014 was compression of approximately -90 με. During the winter season as temperatures decline between October 2014 and March 2015, both sections exhibit a significant shift in strain values, indicating compression (thermal shrinkage). As temperatures rise between March and May 2015, both sections experience a shift in strain indicating expansion. However, throughout the year of monitoring strain, the ICC section consistently experiences approximately 50-75 με more positive

(lower compression) than the Control Section. The reduction in strain could be attributed to either lower modulus of elasticity, internal curing performing as theorized using the LWA in the ICC section, or a result of favorable curing conditions for constructing the ICC section and less favorable curing conditions for the Control section. It is uncertain as to what resulted in the reduced shift in strain for the ICC section, but it is likely a combination of lower modulus of elasticity, internal curing, and favorable curing conditions. This data indicates that the joints were working as designed.

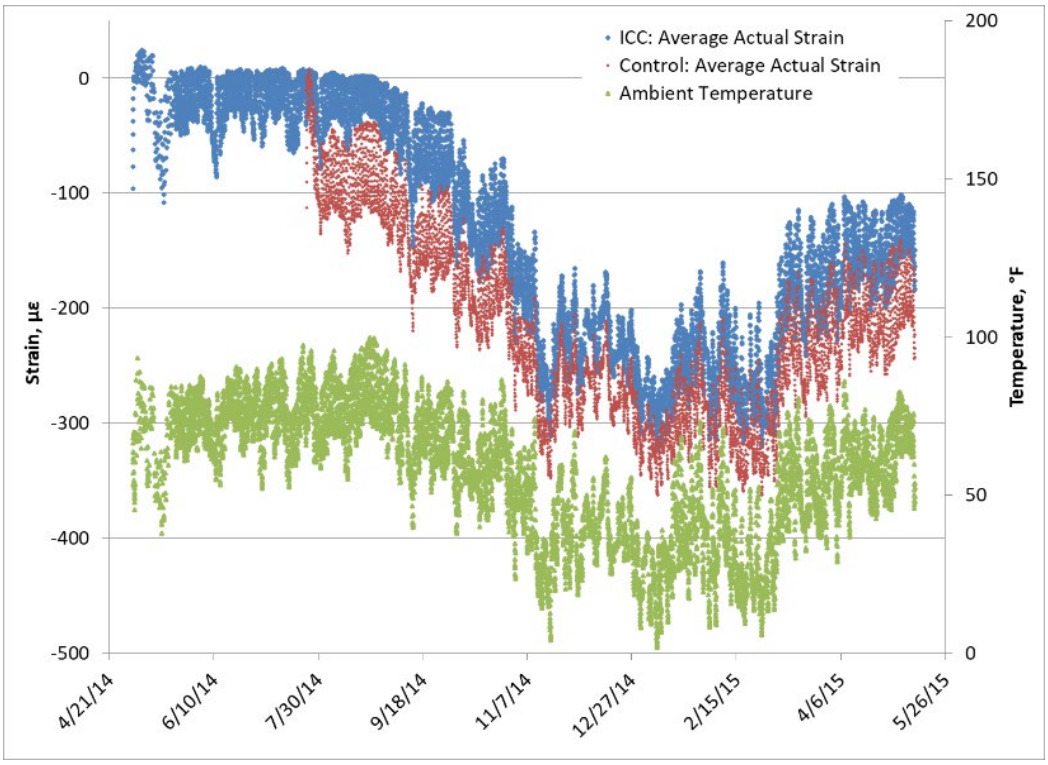

Figure 4.11: Average Actual Strain for Both ICC and Control Sections Compared to Ambient Temperature

Figure 4.12 displays the average center panel curvature for both the ICC and Control sections from the day of construction to the day the data acquisitioning equipment was removed. The curvature calculation is presented in Appendix E. A negative curvature value indicates the top of the panel is in compression whereas the bottom is in tension resulting in a bowl-like deformation. A positive curvature value has the opposite effect resulting in a hill-like deformation. Curvature is defined by the strain deformation between the top and bottom strain gages. Based on the figure,

during the first five months after construction, the ICC section experiences extreme changes in curvature implying the pavement remains capable of responding to daily temperature changes. During this time frame, the ICC section curvature averages at approximately -0.12 per inch. After that, the ICC section curvature stabilizes at approximately -0.01 per inch until the data acquisition equipment is removed. On the other hand, the Control section only experienced extreme changes in curvature for the first two days after construction and stabilized to approximately -0.04 per inch for the remainder of data collection.

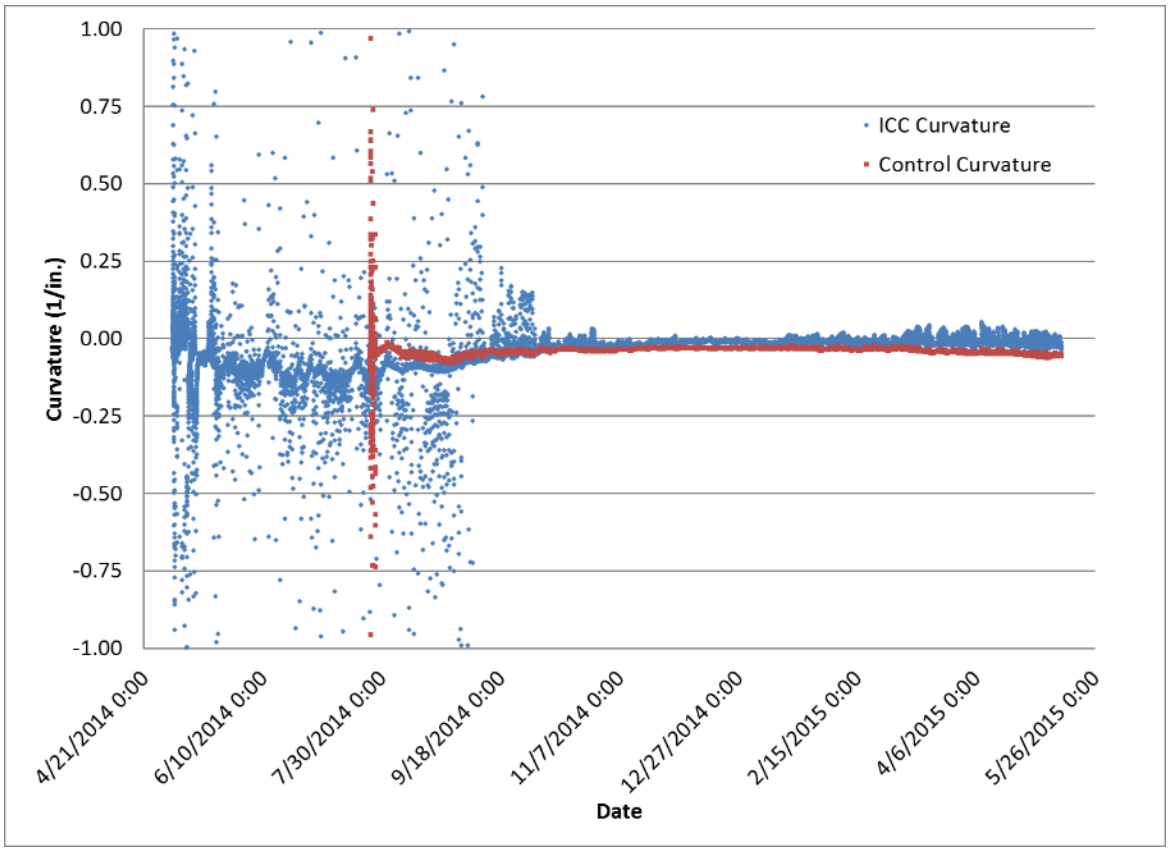

Figure 4.12: Average Panel Curvature

4.4 Coefficient of Thermal Expansion

The coefficient of thermal expansion (CTE) of concrete is a relationship between the change in actual strain and change in temperature. Figure 4.13 and Figure 4.14 display the typical temperature and strain relationship obtained from the strain gages embedded in the ICC and Control sections, respectively. Due to the restraint by the adjacent slab and the friction of the

subgrade on the instrumented panels the CTE for both locations is quite different from the unrestrained value of 7.50 με/ºC determined by the FHWA laboratory testing. Both test sections were constructed on the same base. The ICC section displayed in Figure 4.13 indicated a continual shift in the coefficient of thermal expansion. Values ranged from 4.29 με/ºC to 10.68 με/ºC. Values were higher during the summer months, dropped during the winter, and began to increase in the spring.

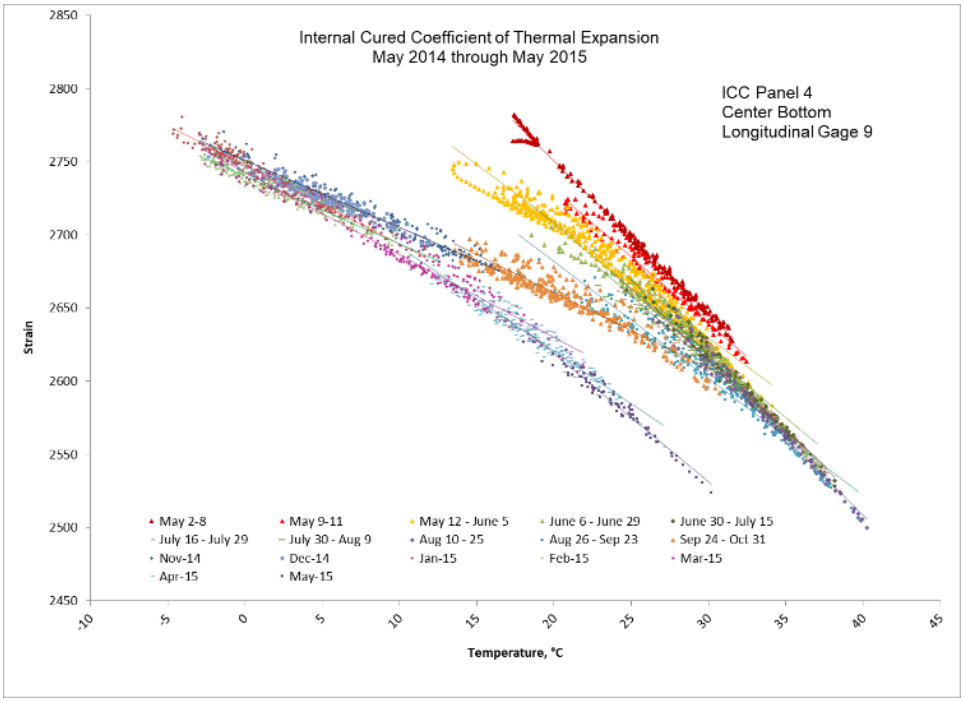

Figure 4.13: ICC Section Variation in Coefficient of Thermal Expansion

The CTE for the Control section was also determined. Values ranged from 4.83 με/ºC to 9.97 με/ºC. The control CTE did not indicate the extensive shift or the response to the winter months that the ICC section did. See Figure 4.14 for the Control section CTE.

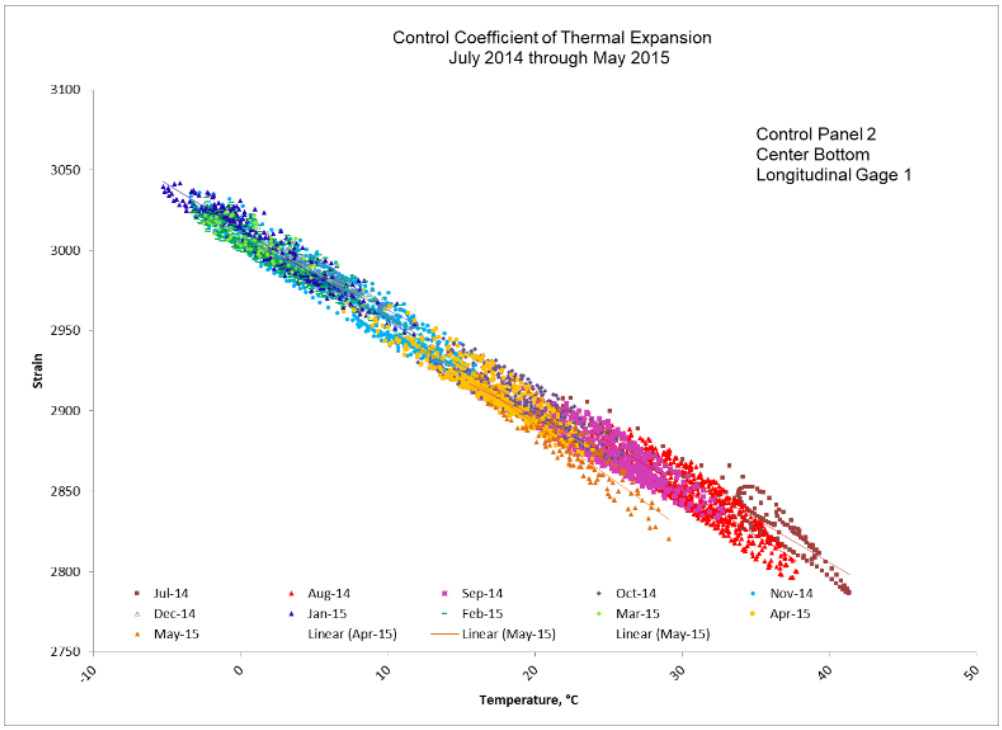

Figure 4.14: Control Section Shift in Coefficient of Thermal Expansion

The CTE was calculated for Panel 2 and Panel 4 in each test section. The CTE was determined at the corner of the panels and in the center of the panels. Table 4.8 is a short summary of the CTE for the corners of Panel 4 in the ICC section and Panel 2 in the Control Section. Table 4.9 is a short summary of the CTE for the centers of Panel 4 for the ICC section and Panel 2 for the Control section.

Table 4.8: Determined CTE for ICC and Control Corner Gages

Summary of Coefficient of Thermal (CTE) Expansion Shift			
Internal Cure Section (May 2014)		Control Section (July 2014)	
Panel 4 Corner Bottom Gage 12		Panel 2 Corner Bottom Gage 4	
Time Period	Average CTE, με/ºC	Time Period	Average CTE, με/ºC
Initial Readings	10.68		
May-June	8.63	Initial Readings	5.85
July	10.35	July	5.85
August	10.52	August	6.56
September	7.56	September	5.10
October-November	4.29	October-November	5.03
Dec 2014-Feb 2015	4.34	Dec 2014-Feb 2015	4.83
March	4.78	March	6.36
April	5.41	April	8.33
May 2015	8.02	May 2015	9.97
FHWA Test	7.50		

Table 4.9: Determined CTE for ICC and Control Center Gages

Summary of Coefficient of Thermal (CTE) Expansion Shift			
Internal Cure Section (May 2014)		Control Section (July 2014)	
Panel 4 Center Bottom Gage 9		Panel 2 Center Bottom Gage 1	
Time Period	Average CTE, με/ºC	Time Period	Average CTE, με/ºC
Initial Readings	10.43		
May-June	8.61	Initial Readings	5.44
July	9.86	July	5.44
August	9.78	August	5.84
September	7.97	September	4.56
October–November	4.88	October–November	5.07
Dec 2014–Feb 2015	4.74	Dec 2014–Feb 2015	5.09
March	5.66	March	4.61
April	7.15	April	5.43
May 2015	8.72	May 2015	6.53

From the previous graphs and tables, it can be seen the ICC section, other than the cold weather months, responded to the change in temperature at a higher level than the Control section.

4.5 Moisture

As described in Chapter 3, three moisture sensors were placed in the center of Panel 2 and Panel 4 of both the ICC and Control sections vertically through the depth (see Figure 3.4 and Figure 3.6). Sensors were labeled “Bottom, Center, and Top.” The ICC section Panel 2 sensors were labelled 1, 2, and 3 and Panel 4 sensors were labeled 4, 5, and 6, respectively. The Control

section Panel 2 sensors were labelled 10, 11, and 12 and Panel 4 sensors were labeled 7, 8, and 9, respectively. In the following figures the Concrete Temperature is the average of the recorded sensor temperatures.

Figure 4.15 and Figure 4.16 track the Volumetric Water Content (VWC) of ICC Section Panel 2 and Panel 4 for 1 month after placement. Figure 4.17 and Figure 4.18 track the VWC of Control Section Panel 2 and Panel 4 for 1 month after placement. Two sensors, the bottom sensor (1) in ICC Panel 2 and the top sensor (6) in ICC Panel 4 appear to be in error as they were consistently reading significantly higher moisture content than the companion sensors in the two panels. The Volumetric Water Content offset for both sensors was approximately the same at 0.03 m^3/m^3.

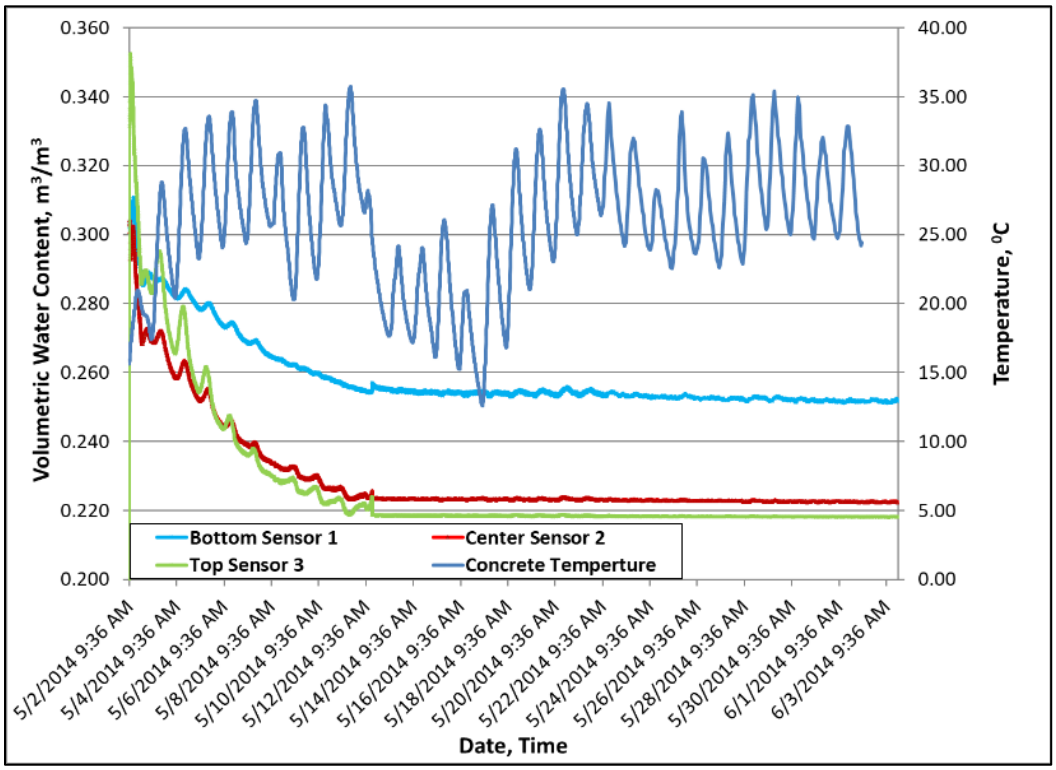

Figure 4.15: ICC Section Panel 2 Total Water Content, 1 Month

Initially, it was thought that the wires were labeled incorrectly and that the "Top" sensor was in place as the bottom sensor. However, through in-place wiring photos of the set-up and the construction process, and more importantly verifying the moisture sensor temperature readings

against those from the strain gages, it was determined that the sensors were labeled correctly. It was also noted at this time that several of the moisture sensors received an incorrect calibration from the manufacturer. A file was obtained from the manufacturer that enabled correction of the data on the affected sensors (note that all data presented in this report has been corrected). The correction adjusted the magnitude of the water content reading and was needed on all three sensors (4, 5, and 6) in ICC Panel 4. The raw data was also submitted to the manufacturer for review. Unfortunately, the manufacturer was unable to identify a specific issue or a correction for the data.

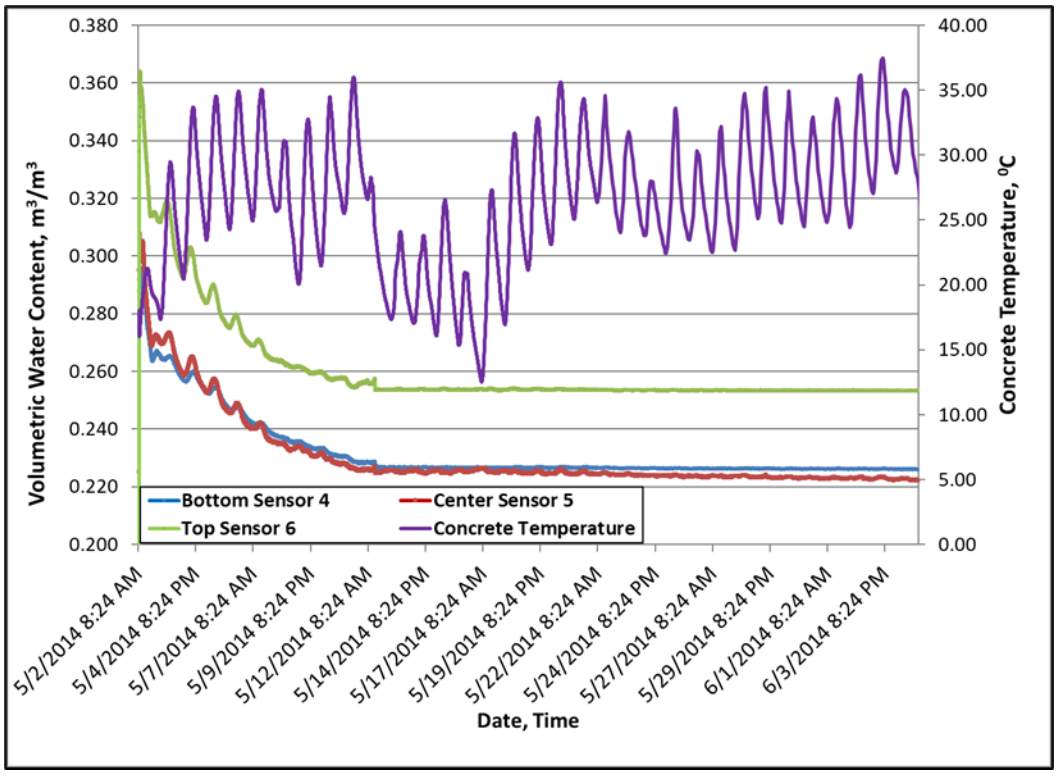

Figure 4.16: ICC Section Panel 4 Total Water Content, 1 Month

It should also be noted that the data indicates the center (2) and top (3) gages in Panel 2 of the ICC section and the top (6) and bottom (4) gages in Panel 4 of the ICC section stopped working at approximately 10 days after placement. The one remaining gage in each of the ICC panels are also questionable due to the minimal response recorded. The data indicates the top (12) and center (11) gages of Panel 2 of the Control section also stopped working at approximately 7 days after placement. The only test section with working moisture sensors throughout the long-term data

collection were those in Panel 4 of the Control section. The data indicates that the moisture side of two of the data acquisition units may have failed while the temperature reading and recording continued. Temperatures were compared to the strain gage temperatures and weather station temperatures and verified. A separate data acquisition unit was used for each of the four panels.

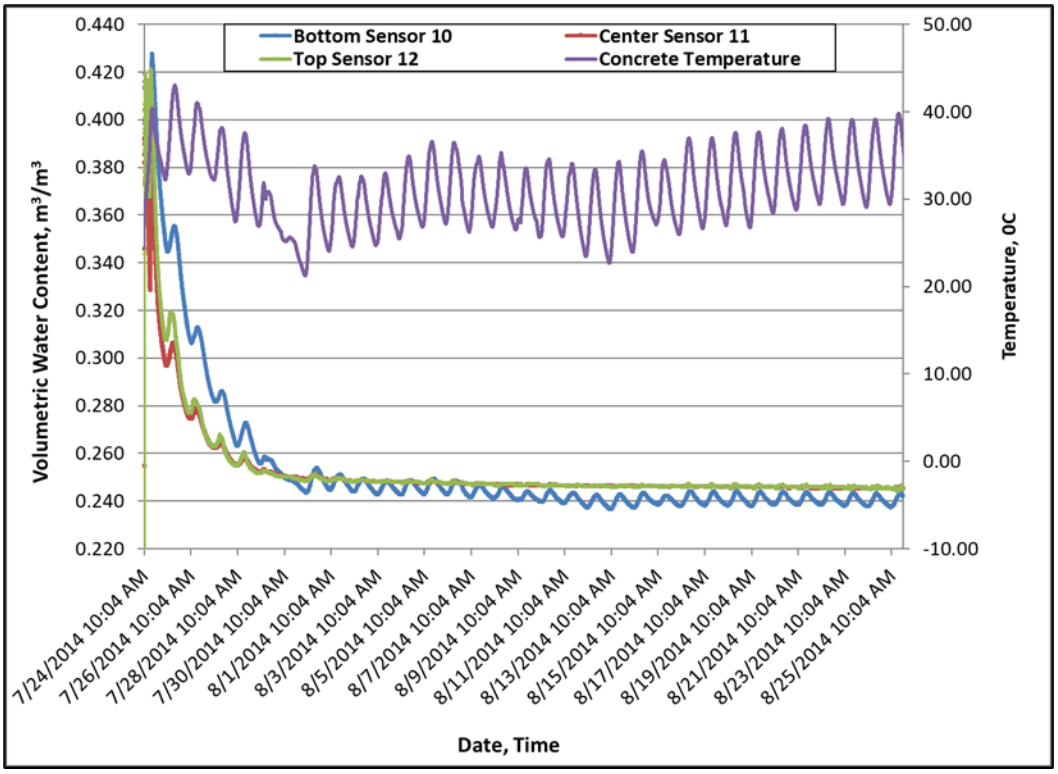

Figure 4.17: Control Section Panel 2 Total Water Content, 1 Month

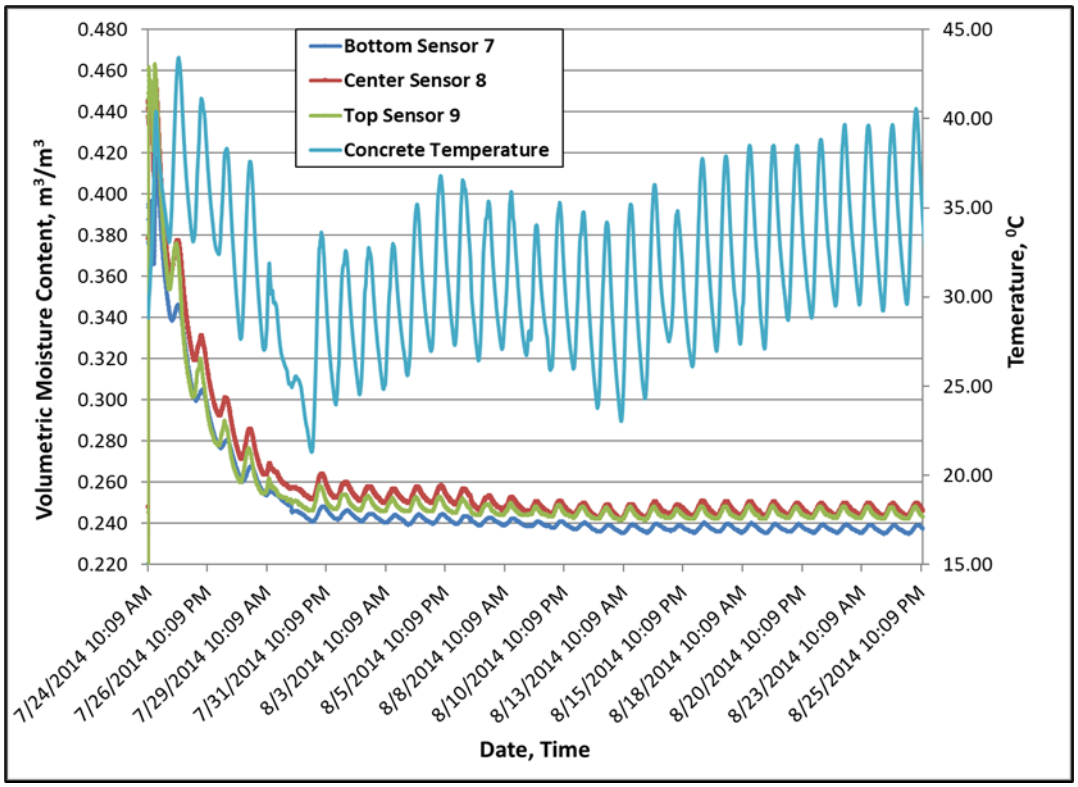

Figure 4.18: Control Section Panel 4 Total Water Content, 1 Month

Comparing the remaining long term (1 month) VWC data and the 10-day data of the four panels it can be seen that the VWC for the ICC panels reached a steady state at approximately 10 days after placement while the Control panels reached a steady state at approximately 7 days after concrete placement. This can be seen more clearly in the 10-day data (Figures 4.19, Figure 4.20, Figure 4.21, and Figure 4.22). Additionally, it should be noted that the VWC varies with Concrete temperature long term, but this variation is greatly reduced in both sections after steady state is reached.

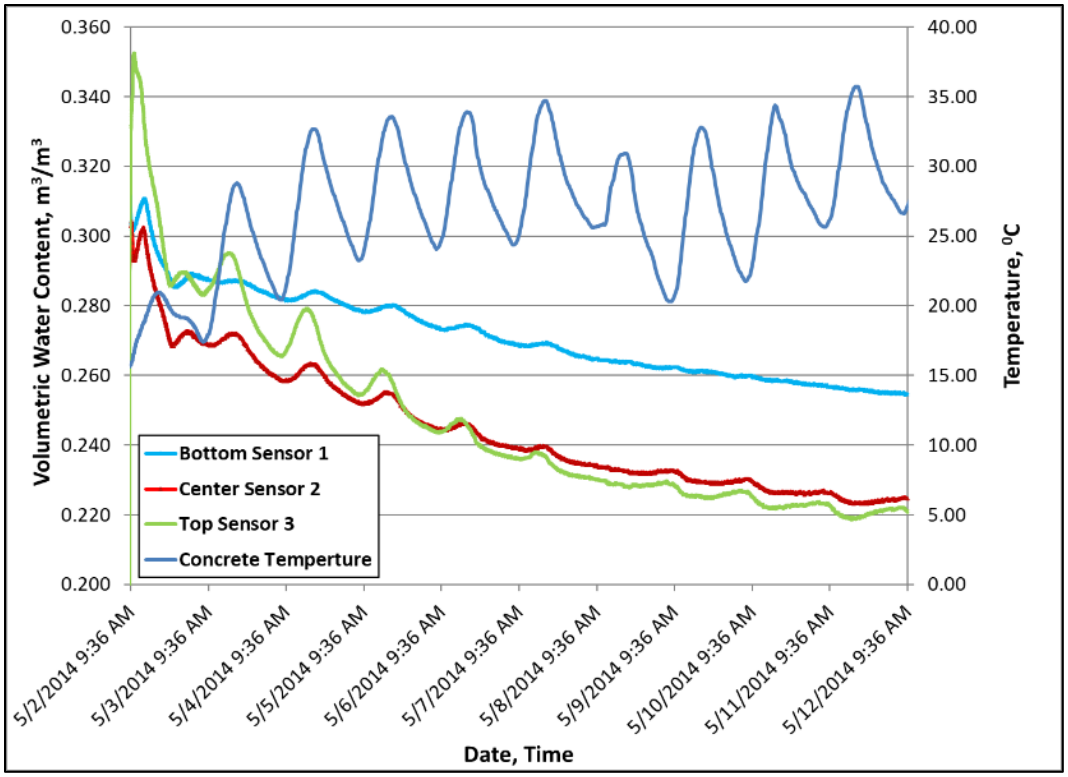

Figure 4.19: ICC Section Panel 2 Total Water Content, 10 Days

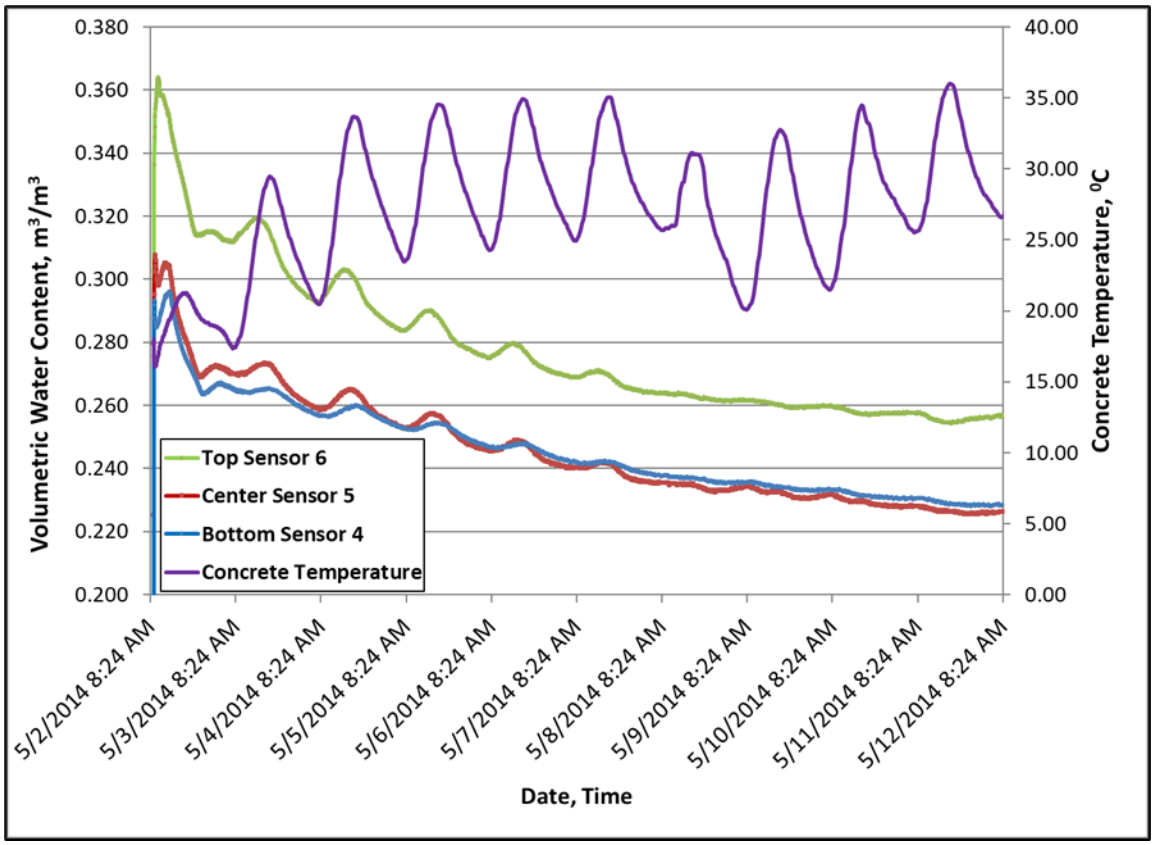

Figure 4.20: ICC Section Panel 4 Total Water Content, 10 Days

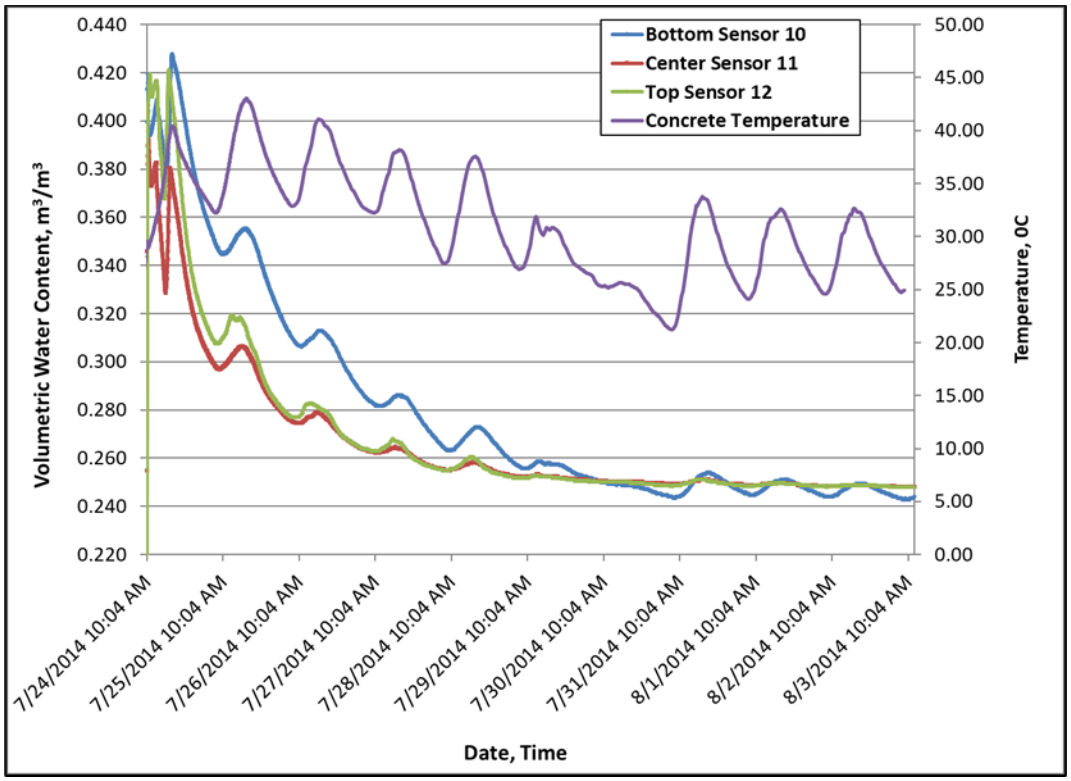

Figure 4.21: Control Section Panel 2 Total Water Content, 10 Days

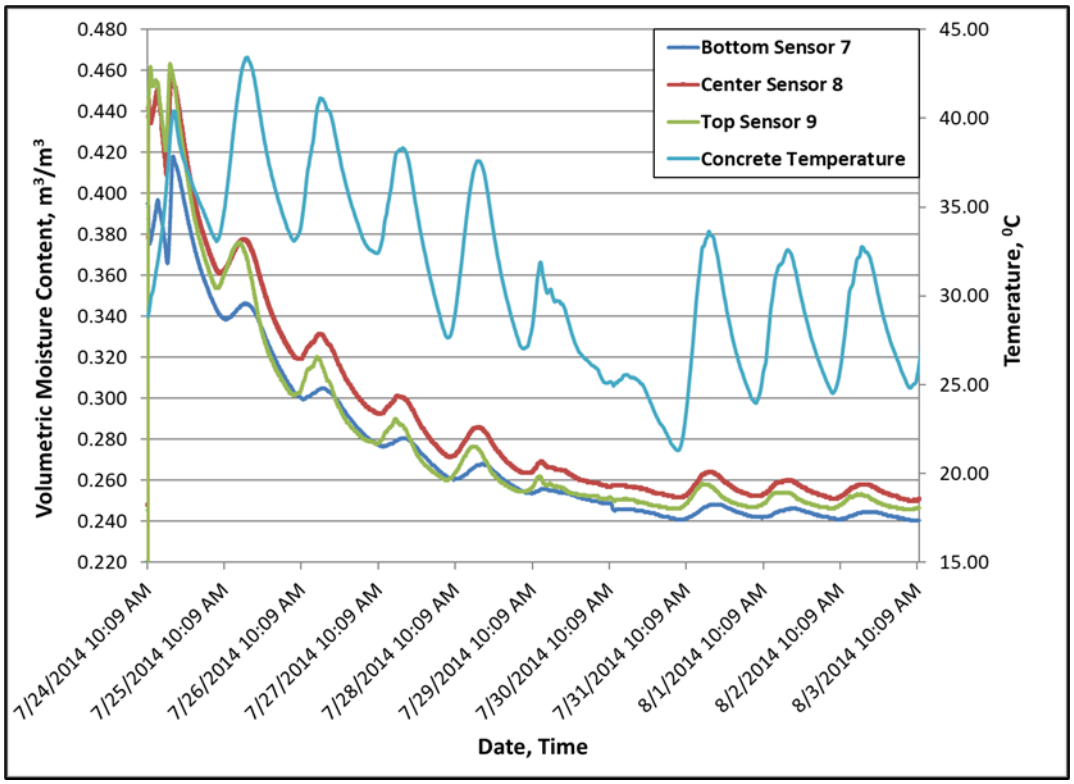

Figure 4.22: Control Section Panel 4 Total Water Content, 10 Days

The 10-day data figures also show that both test sections had early spikes in VWC. These spikes are more easily seen in the 48-hour data (Figure 4.23, Figure 4.24, Figure 4.25, and Figure 4.26). The figures also indicate that the previously described unexplained offsets for the two moisture sensors did not start until roughly 12 hours after placement of the concrete. The Control section indicated no offsets of the moisture sensor data.

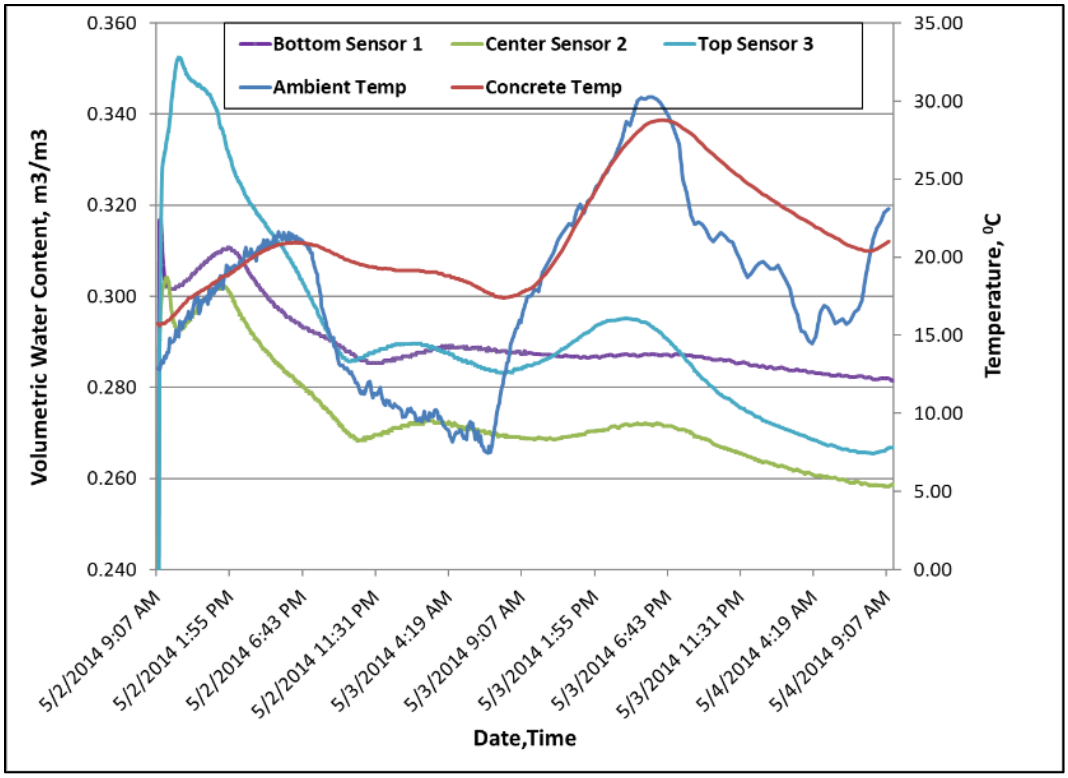

Figure 4.23: ICC Section Panel 2 Total Water Content, 48 Hrs

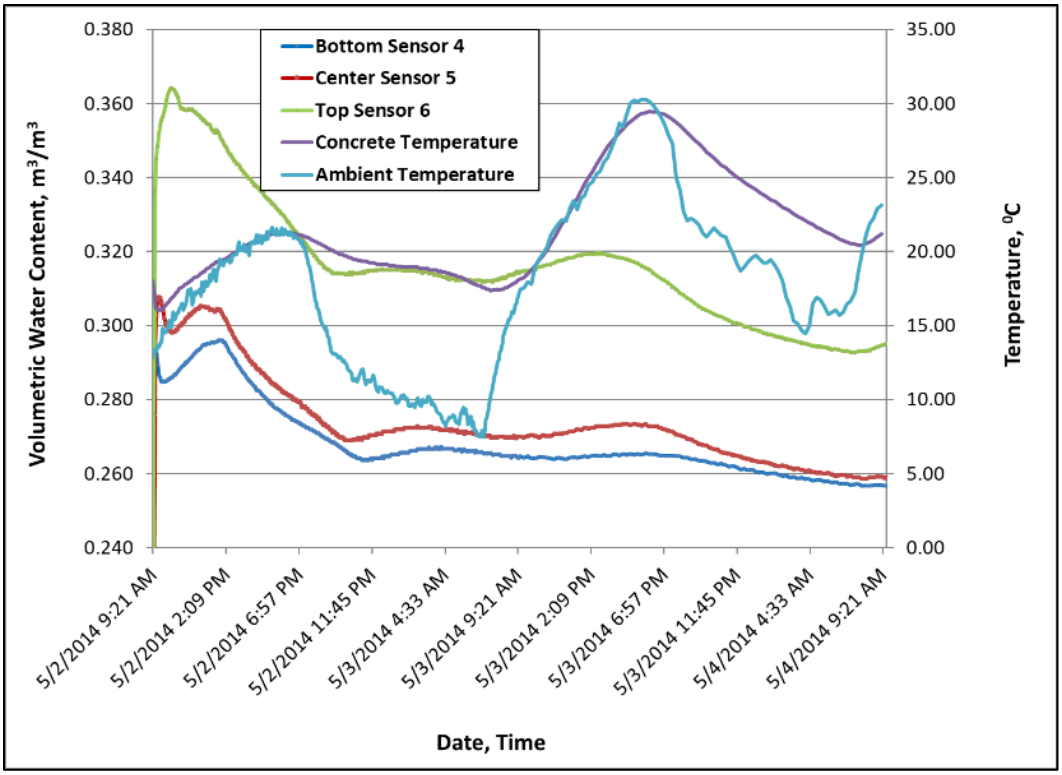

Figure 4.24: ICC Section Panel 4 Total Water Content, 48 Hrs

The initial spike in moisture occurs with the top sensors as bleed water migrates to the surface of the panels during the early curing process, this occurs in all four test panels. It should be noted that the ICC panels had a much lower initial moisture peak than the Control panels. The top sensors in the ICC panels indicate a slow drop in moisture over the next 12 hours as the concrete temperature rose. The center and bottom sensors indicated an initial peak followed closely be a slight drop in moisture and a second peak during this same time frame. During the initial 12 hours the Control section sensors indicated three peaks in moisture with slight drops between the peaks. As the concrete temperature began to fall all sensors indicated a drop in moisture content. After this initial response the moisture began to rise and fall in response to the concrete temperature. The lower moisture content indications in the ICC section may be due to the expanded aggregate's ability to absorb water thus reducing the amount of free water in the paste in the early stages of hydration. Little more can be determined from the available data with the apparent failure of the data acquisition systems.

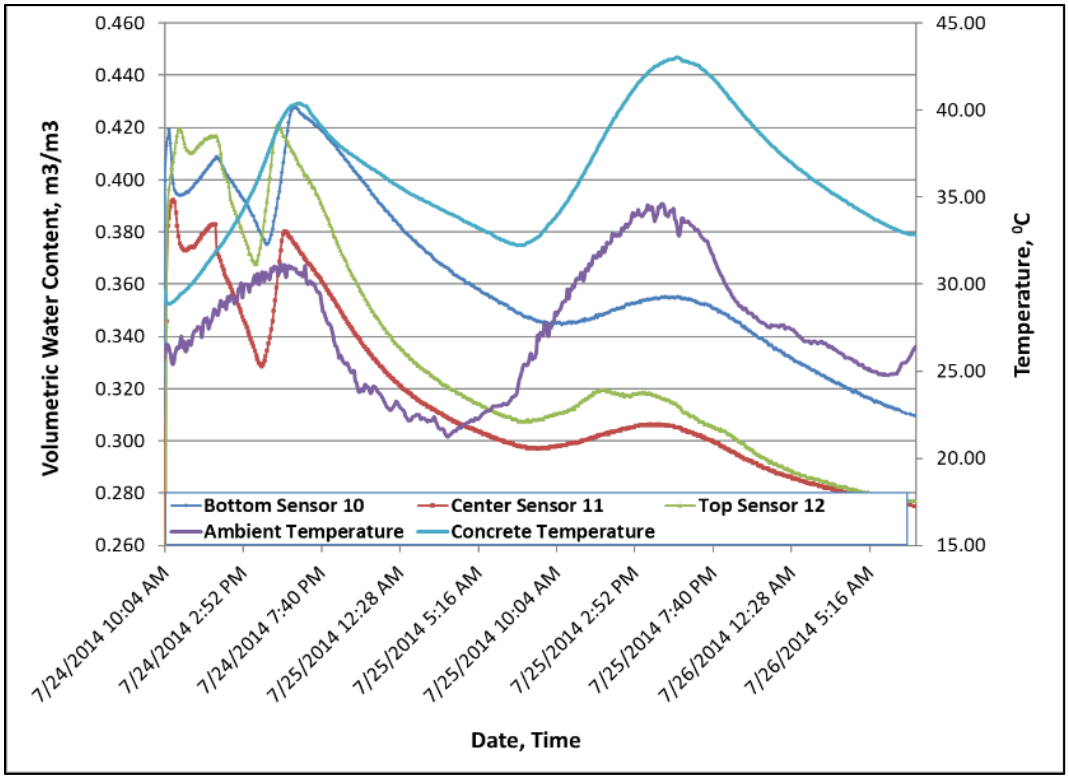

Figure 4.25: Control Section Panel 2 Total Water Content, 48 Hrs.

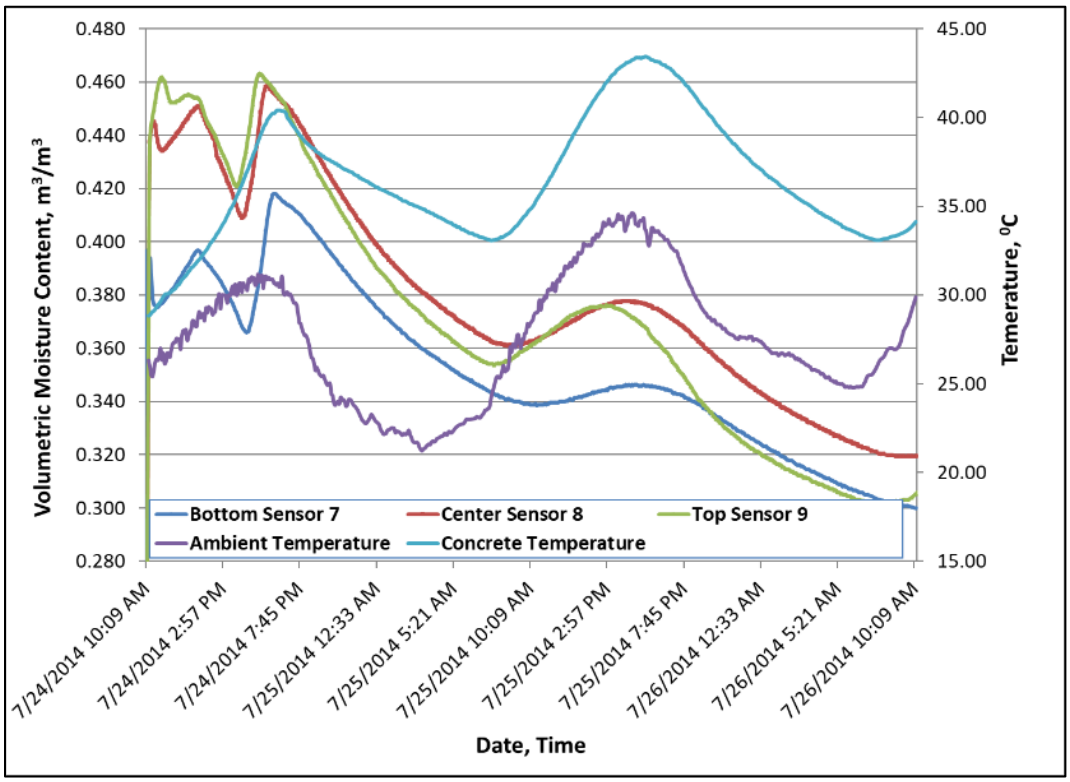

Figure 4.26: Control Section Panel 4 Total Water Content, 48 Hrs.

4.6 Deflections

Section 4.6 presents the Deflection readings for both test sections. The longitudinal references on the graphs indicate the 15 reading points as mapped in Figure 2.7. The depth is a not-to-scale 15-foot traffic lane, with the free edge toward the front of the figures, and the vertical axis is the deflection readings. The deflection readings for each panel are relative to that panel individually; the panels do not use the same benchmark elevation reference. Zero deflection dividers were also placed in the data between each panel to facilitate the graphing.

The initial attempt was to establish a "zero" reading immediately after sawing and continuing the readings through 20–21 days. However, curing compound residue built up on the feet of the Dipstick on the ICC section, resulting in skewed readings and an inaccurate pavement profile. As such, Day 1 was the first reliable reading that was obtained and considered to be the "zero" reading. Figure 4.27 through Figure 4.30 present the deflections of all five panels (Panel 1 on left to Panel 5 on right) for Day 1, Day 3, Day 5, and Day 20 readings from the ICC section. High points, typically at the corners of the adjacent panels can be seen; these high points tended to drop over the 20 days.

Figure 4.31 through Figure 4.34 display the average profiles of all five ICC panels at Day 1, Day 3, Day 5, and Day 20. Looking at the average profiles, it can be observed that the panel profile deflects as the pavement ages. This is a result of the panels warping due to moisture loss. Although a change in deflections can be observed, the deflections do not create a bowl shape as typically expected. Rather the panels tended to have a low area longitudinally near the panel center and free edge. The opposite edge is being influenced by the adjacent panel. The magnitude of all deflections is minimal.

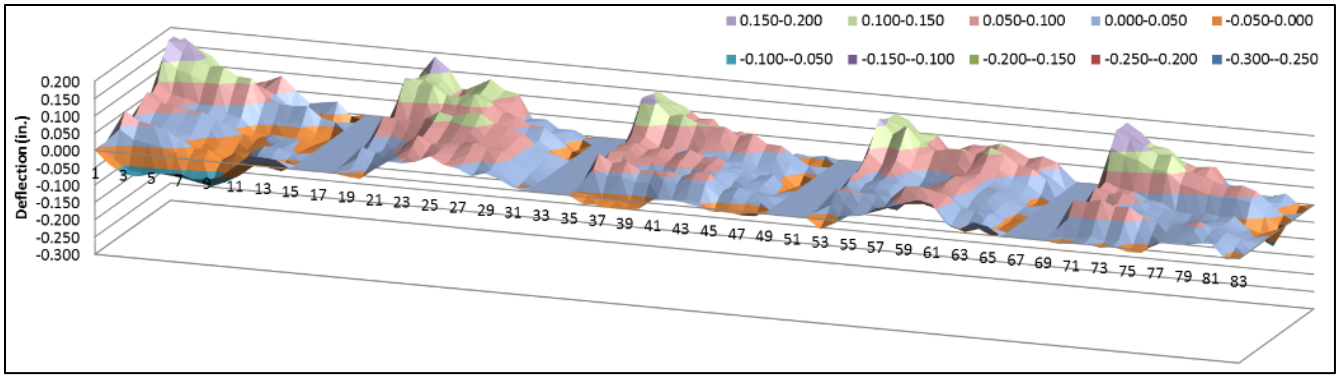

Figure 4.27: ICC Section Deflections Day 1: Morning

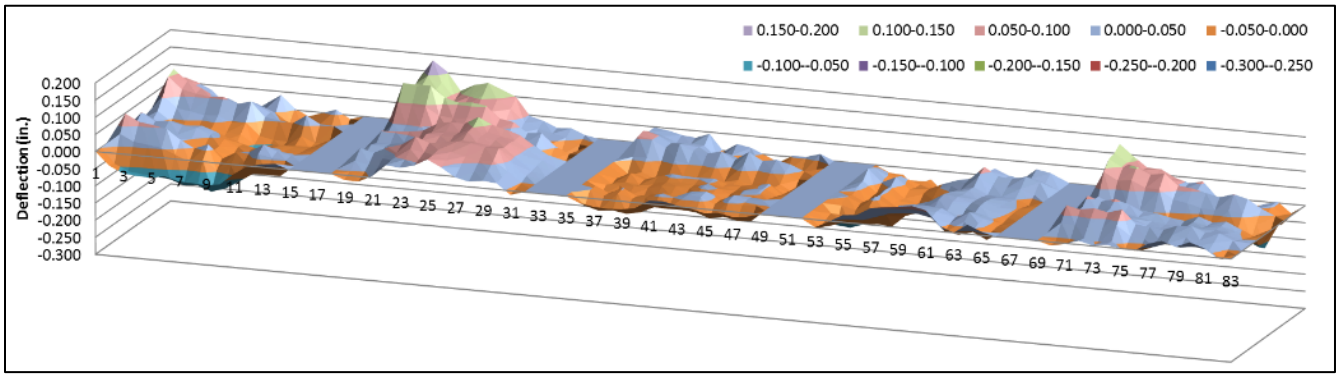

Figure 4.28: ICC Section Deflections Day 3: Morning

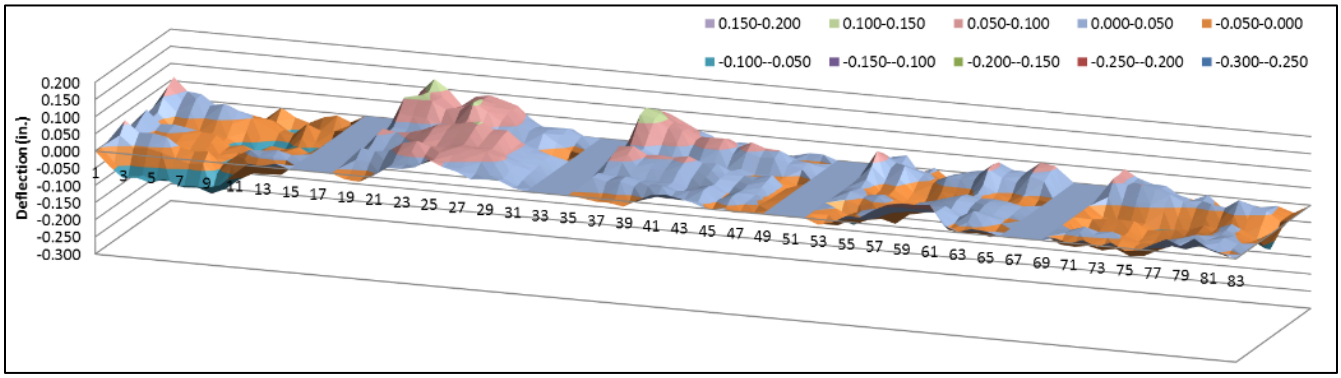

Figure 4.29: ICC Section Deflections Day 5: Morning

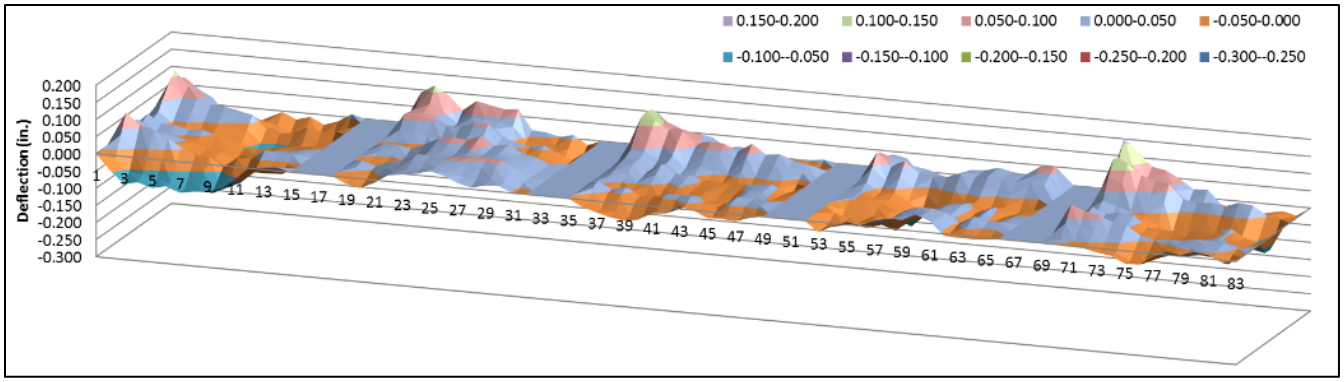

Figure 4.30: ICC Section Deflections Day 20: Morning

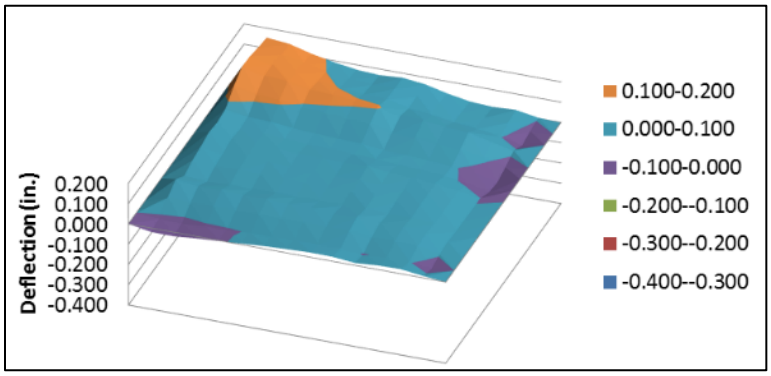

Figure 4.31: ICC Average Panel Profile Day 1: Morning

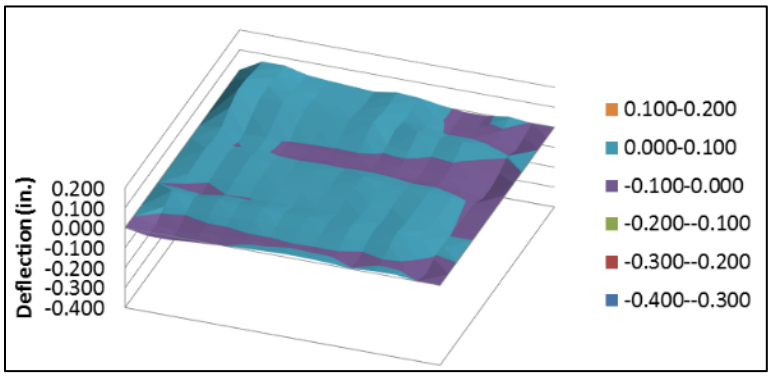

Figure 4.32: ICC Average Panel Profile Day 3: Morning

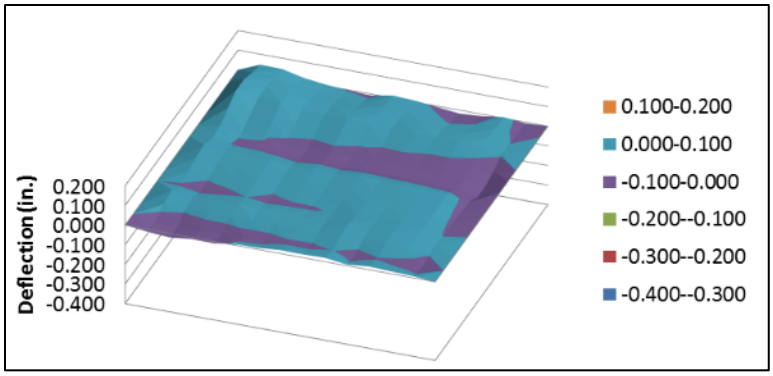

Figure 4.33: ICC Average Panel Profile Day 5: Morning

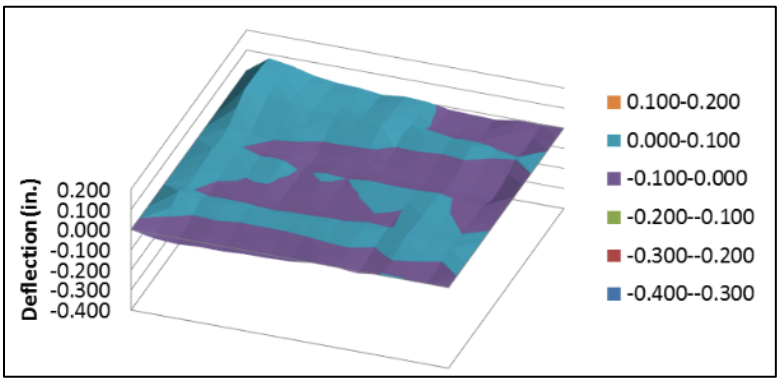

Figure 4.34: ICC Average Panel Profile Day 20: Morning

The intentions were to collect deflection data via Dipstick until Day 20. However, surface grinding was performed on the entire project, as is standard procedure by KDOT for urban projects and deflection data was only collected on the Control section through the morning of Day 7. Figure 4.35 through Figure 4.38 present deflection data for the individual panels of the Control section for Day 1, Day 3, Day 5, and Day 7. The graphs again indicate high points at the corners against the adjacent panels. The deflections are changing during the 7 days but are generally becoming smaller.

Figure 4.39 through Figure 4.42 display the average deflections of the five panels in the Control section. Based on the average panel profiles, the Control section experienced the similar magnitude of deflections as the ICC section. However, the Control panels deflection are more pronounced along the free edge and extend farther into the center of the panel, the ends of the panels tend to be higher than the centers which would result in poor ride quality in comparison to the ICC section. With the significant temperature differences during which the test sections were

placed, the stresses present in the slabs during time of final set are considerably different and influence the slab's response to temperature curling. Therefore, it is difficult to define the effect that the lightweight aggregate had on the pavement deformations observed in the ICC section. Additionally, without the extended data to Day 20 or Day 21, it becomes difficult to evaluate the deflection of the control section due to warping versus deflection due to curling. It is again noted that the magnitude of deflections is minimal.

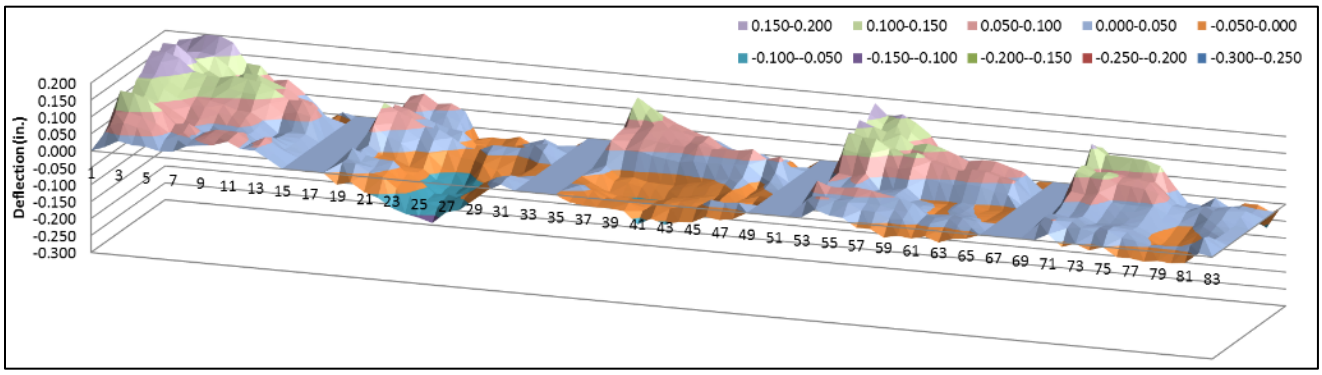

Figure 4.35: Control Section Deflections Day 1: Morning

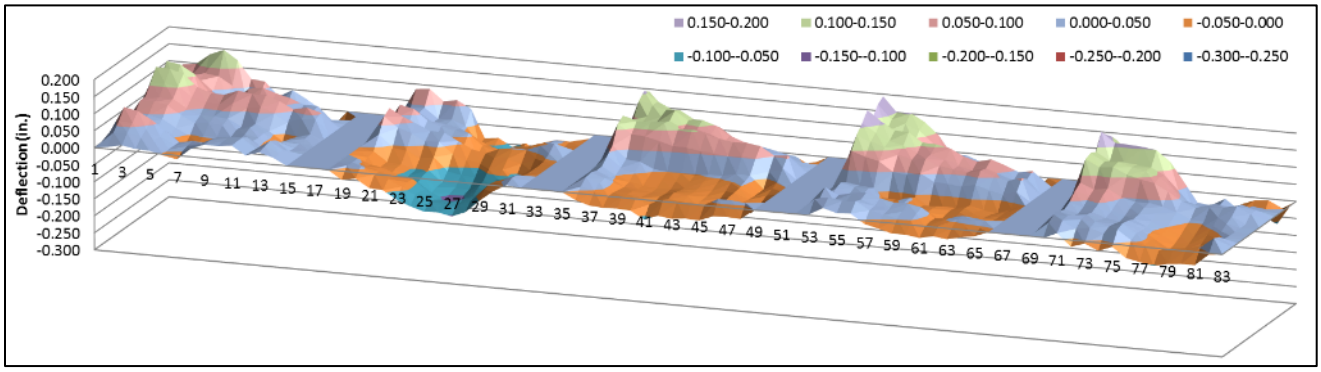

Figure 4.36: Control Section Deflections Day 3: Morning

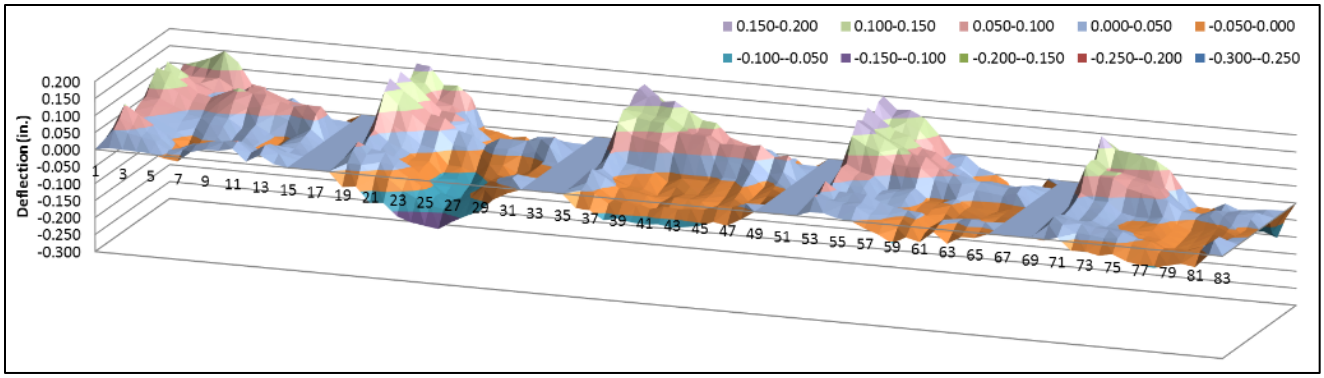

Figure 4.37: Control Section Deflections Day 5: Morning

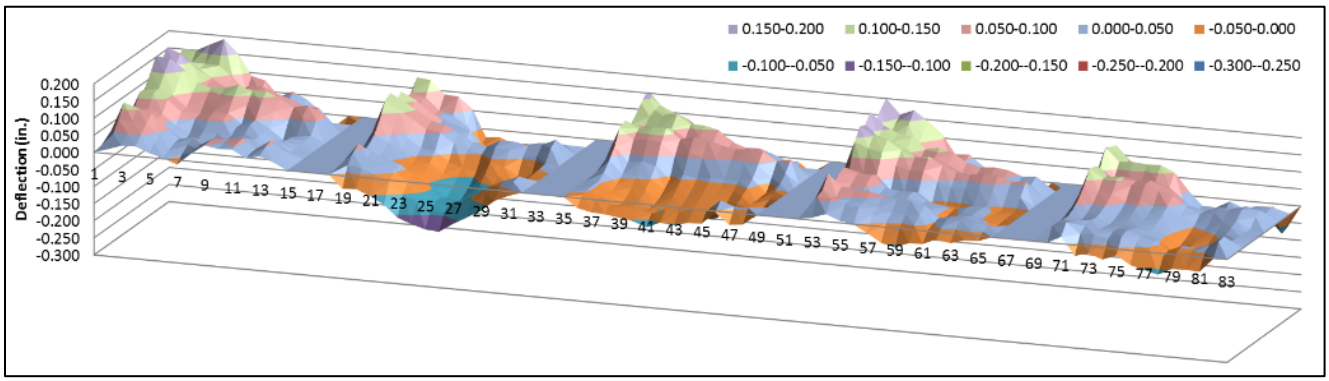

Figure 4.38: Control Section Deflections Day 7: Morning

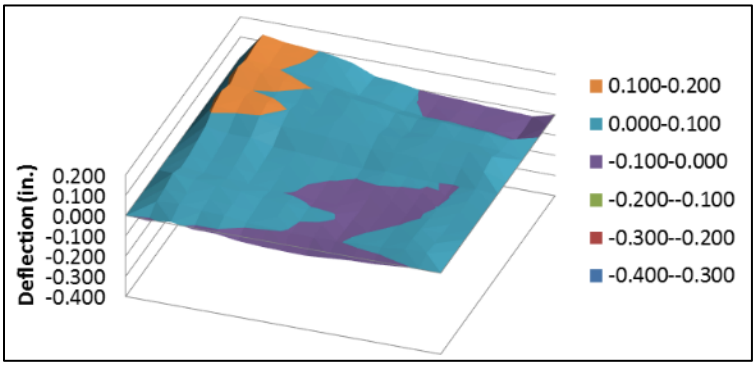

Figure 4.39: Control Average Pavement Profile Day 1: Morning

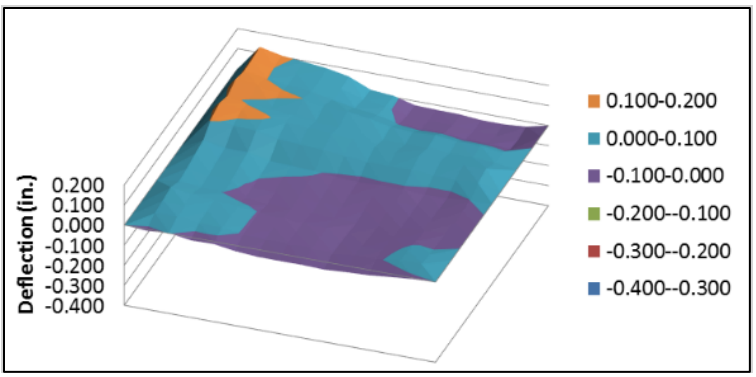

Figure 4.40: Control Average Pavement Profile Day 3: Morning

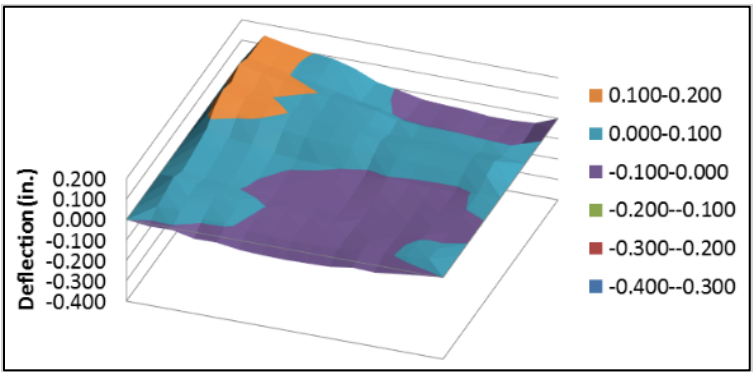

Figure 4.41: Control Average Pavement Profile Day 5: Morning

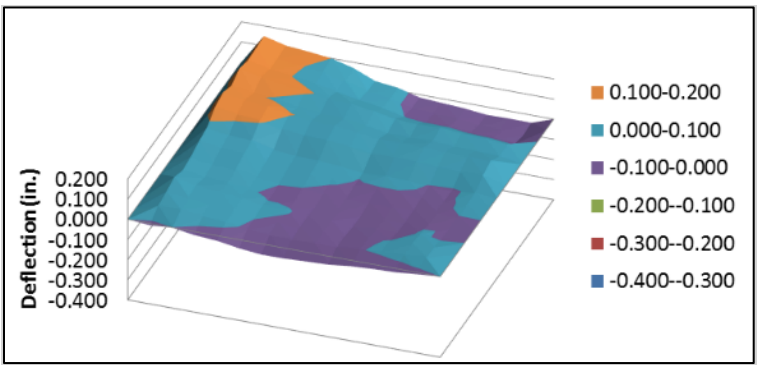

Figure 4.42: Control Average Pavement Profile Day 7: Morning

4.7 HIPERPAV Results

Although data collection techniques using strain gages, moisture sensors, and deflections via Dipstick were very successful in collecting large amounts of reliable data, the differences in placement and curing environments between the ICC section and Control section made it difficult to compare the two sections with certainty. To better evaluate the effects of using internal curing

HIPERPAV III (Transtec and the FHWA) was utilized to evaluate both sections under both curing environments.

Four different strategies were analyzed in HIPERPAV III:

1. Control Concrete Mix and Properties using Control Curing Conditions
2. Control Concrete Mix and Properties using ICC Curing Conditions
3. ICC Concrete Mix and Properties using ICC Curing Conditions
4. ICC Concrete Mix and Properties using Control Curing Conditions

For comparison purposes, Strategy 1 and Strategy 4 were compared to analyze performance of each section using the Control curing conditions. Strategy 2 and Strategy 3 were compared to evaluate the performance of each section using the ICC curing conditions. HIPERPAV III does not have the ability to specifically analyze lightweight aggregate or internal curing therefore, specific physical properties for each mix were input into the program to account for the differences in the mixes.

Figure 4.43 and Figure 4.44 show the critical tensile stresses in the concrete pavement under Control weather conditions and ICC weather conditions, respectively. Using the project weather data, the tensile forces alternate between the top and bottom of the pavement depending on temperature. When the pavement curls in a concave manner, the sides curl upward, but the weight of the panel edges causes tension in the top middle of the panel, and therefore, would cause top-down cracking. Table 4.10 summarizes the critical top of slab tensile stresses and percent reduction indicated in Figure 4.43.

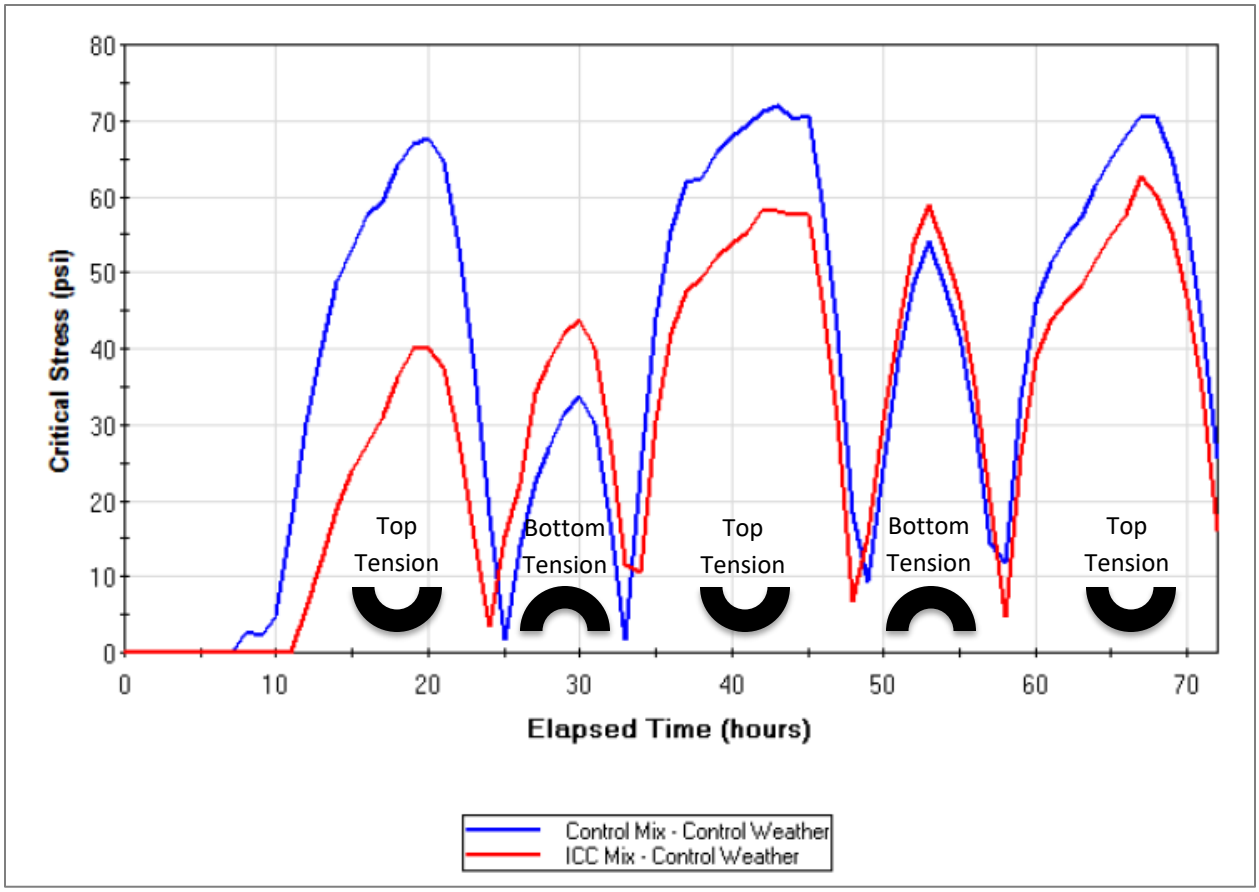

Figure 4.43: Critical Stress of Control and ICC Sections Under Control Weather Conditions (Strategy 1 vs 4)

Table 4.10: Stresses Using Control Weather Conditions

Maximum Tensile Stresses, Control Weather Conditions			
Time, hrs.	Peak (Critical) Stresses, psi		Percent Reduction
	Control	ICC	
20	68	40	41
43	72	58	19
67	71	63	11

Figure 4.44 indicates the maximum tensile stresses in the top of the slab when analyzed using the ICC weather conditions. Table 4.11 summarizes the critical top of slab stresses and corresponding percent reduction in the stresses using lightweight aggregate.

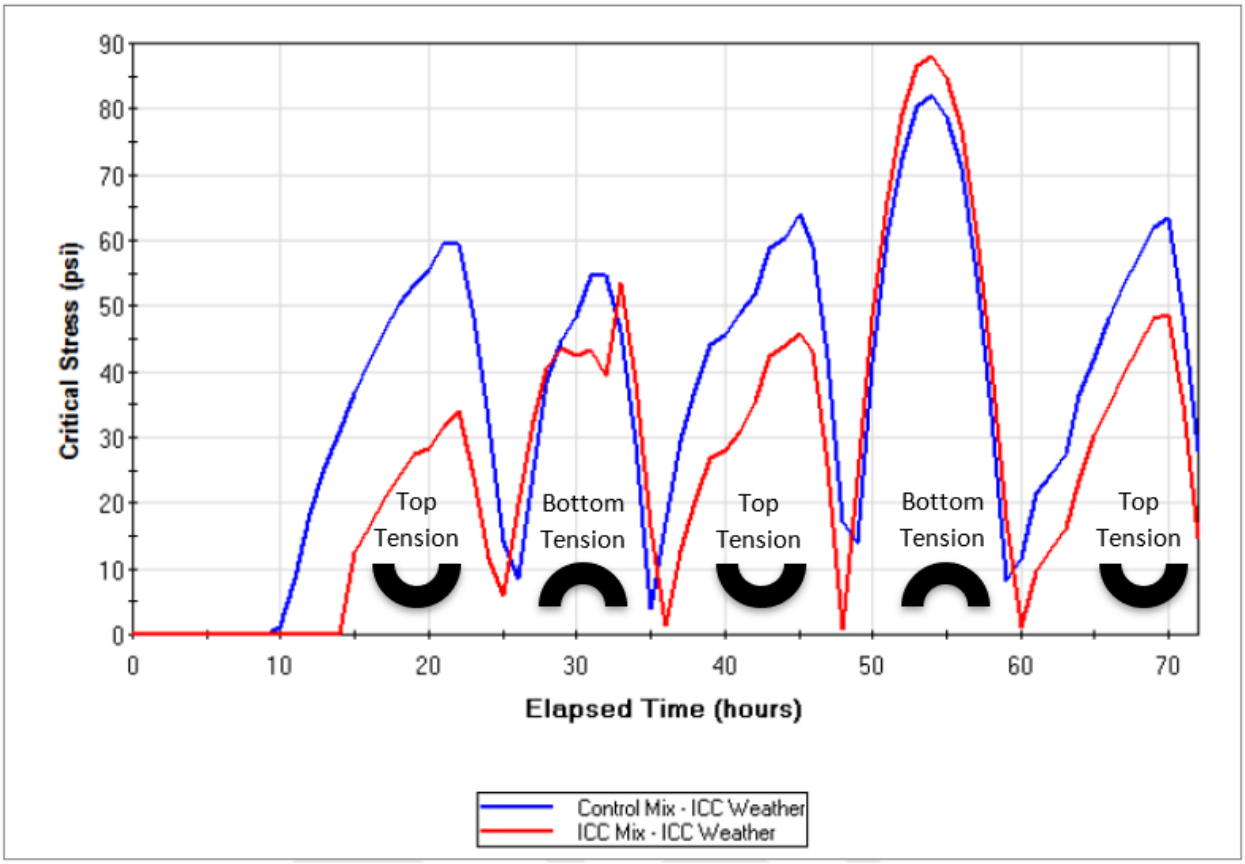

Figure 4.44: Critical Stress of Control and ICC Sections Under ICC Weather Conditions (Strategy 2 vs 3)

Table 4.11: Stresses Using ICC Weather Conditions

Maximum Tensile Stresses, ICC Weather Conditions			
Time, hrs.	Peak (Critical) Stresses, psi		Percent Reduction
	Control	ICC	
22	60	34	43
45	64	46	28
70	63	49	22

The stress to strength ratio over time is shown in Figure 4.45 and Figure 4.46 for the Control weather conditions and ICC weather conditions, respectively. If the stress exceeds the strength resulting in greater than 100% stress to strength ratio, the concrete will crack. Therefore, this ratio is referred to as the cracking risk. Table 4.12 summarizes the reduction in Cracking Risk for the top of the pavement using the ICC mix during Control Weather.

Similarly, in Figure 4.46, the use of ICC mix during ICC weather conditions reduces the cracking risk. The reduction in cracking risk is not as significant as the reduction in critical stress.

This occurs because the ICC mix does not gain strength as fast as the Control mix and ICC weather conditions were much more conducive to placing concrete pavement. This results in a very small reduction in cracking risk for the ICC and Control mixes in both ICC and Control weather conditions. KDOT specifications require reduced paste content in pavement mixes to meet permeability requirements. Therefore, the ICC mix shows minimal improvement in preferred weather conditions.

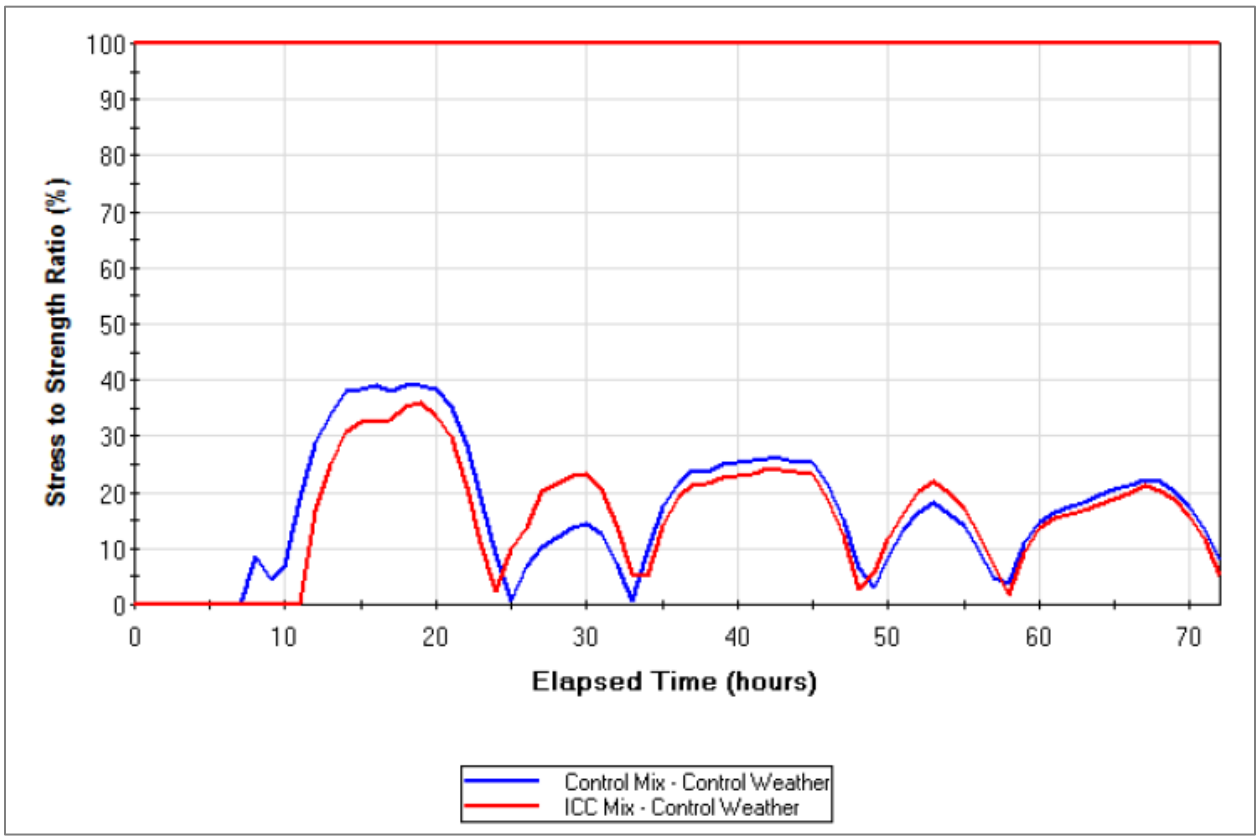

Figure 4.45: Cracking Risk of Control and ICC Sections Under Control Weather Conditions (Strategy 1 vs 4)

Table 4.12: Cracking Risk Reduction Under Control Weather Conditions

Cracking Risk, Control Weather Conditions			
Time, hrs.	Stress/Strength Ratio, %		Risk Reduction %
	Control	ICC	
19	39	36	3
42	26	24	2
67	22	21	1

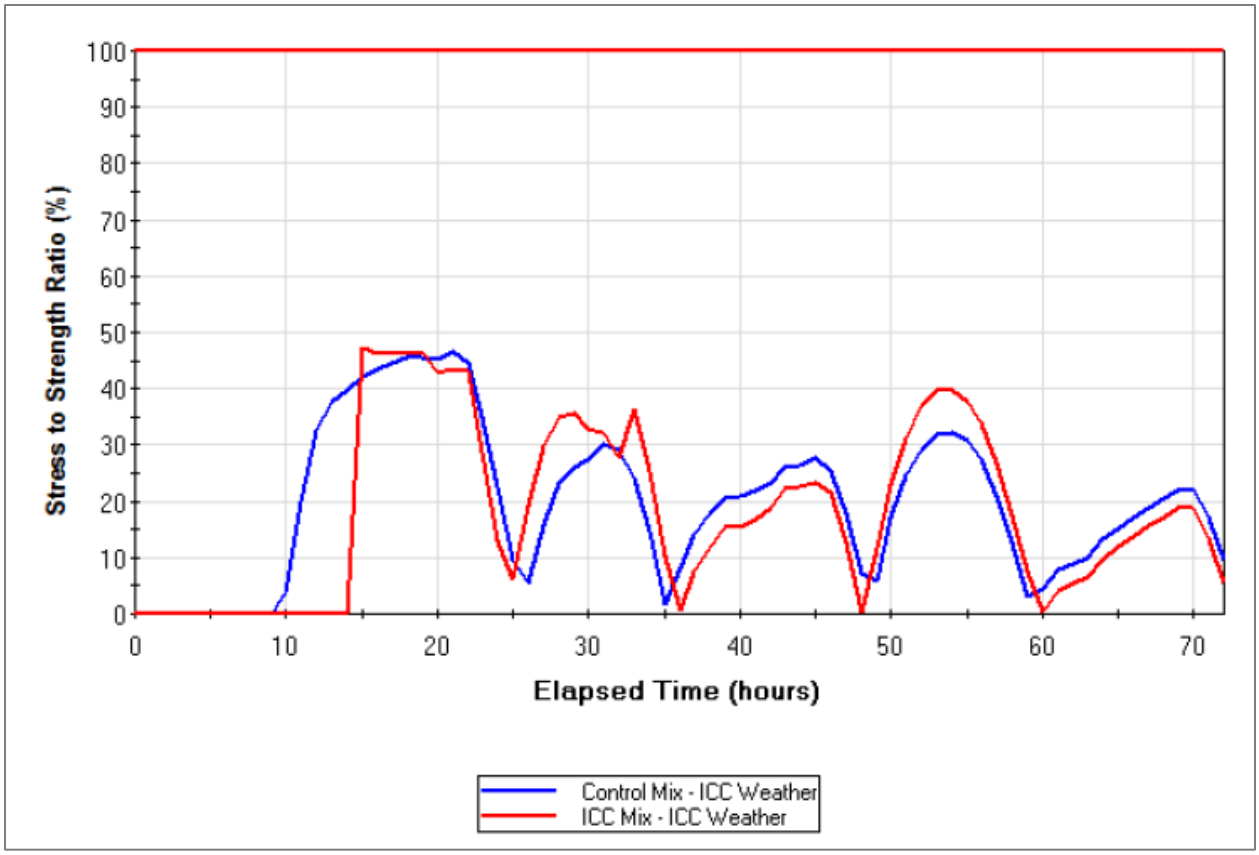

Figure 4.46: Cracking Risk of Control and ICC Sections Under ICC Weather Conditions (Strategy 2 vs 3)

Table 4.13: Cracking Risk Under ICC Weather Conditions

Cracking Risk, ICC Weather Conditions			
Time, hrs.	Stress/Strength Ratio, %		Risk Reduction %
	Control	ICC	
21	47	44	3
45	28	23	5
70	22	19	3

Chapter 5: Summary and Discussion

5.1 Summary and Discussion

The methods used to collect strain and deflection data were highly successful. However, the moisture data collection was an issue as two of the four Decagon data acquisition units failed shortly after placement of the concrete, and a third unit lost one channel.

All methods of data collection including strain, curvature, moisture, deflection, and HIPERPAV III results indicate the use of lightweight aggregate and internally cured concrete reduce the initial strain and undesirable deformations in the concrete.

By analyzing the early strain and moisture data the effect of the significant weather differences can be accounted for, and reasonably accurate analysis can be performed. The significant weather differences between the placement dates have been observed to have impacted the long-term data from the strain gages and moisture sensors. Comparing the early (first 24 to 48 hours) data it can be determined that the use of ICC reduced the early strain and moisture changes that would affect the long-term quality and durability of the concrete.

The plastic and hardened concrete results presented in this report indicate no significant impact of the LWA material. For the majority of the properties tested, comparing the results from the two sections, the values fall within the multiple laboratory precision expected when testing from the same concrete batch. Given that the concretes had different mix designs with different materials and requirements the differences are insignificant.

However, the reduction in unit weight, the slight reduction of elastic modulus, the significant difference in the Coefficient of Thermal expansion response and the slight increase in tensile strength of the ICC indicate a potential improvement in overall durability and potentially increased service life. The more significant differences between the two materials are the early strain response which, when the temperatures are factored out of the analysis, indicate a lower level of cyclic movement and the early Volumetric Moisture Content which again indicated a reduced level of cyclic response of the concrete in the first 24 to 48 hours when the concrete is young and tender and low on tensile strength.

It should also be noted that two of the three permeability tests conducted, the Volume of Permeable Voids and Surface Resistivity would have failed KDOT specifications for both test

sections if testing had been conducted for acceptance/pay. The Rapid Chloride Permeability Test did pass but with higher values than expected given the mix design properties for both sections, the poor results for permeability testing are unclear, potentially due to the inexperience with controlling the increased amount of free water that can occur with the lightweight aggregate. Cores were removed from both sections in October of 2020 and tested for permeability. Rapid Chloride Permeability was extremely low with values of 145 coulombs for the ICC section and 415 coulombs for the Control Section. Volume of Permeable Voids results were slightly lower but still not in the range expected of the ICC, 12.5%, and the Control Section were still failing KDOT's permeability requirement at 13.2%.

5.2 Future Work

General condition surveys are being performed at five-year increments of age for the 20-year design life of the pavement. The first condition survey was performed in October 2020 (6 years after construction), with no significant visual indications of destress observed. Additional surveys will be conducted every five years for the remainder of the 20-year design life, or until a major rehabilitation occurs and the original sections can no longer be surveyed. The surveys consist of a general condition survey noting any cracking, spalling, or other deterioration. If faulting or extensive cracking is noted at any of the surveys, more detailed information will be collected via a fault meter and detailed crack survey respectively. The frequency of the surveys may be altered if extensive deterioration is observed. When the data recording equipment was removed from the project, the strain gages and moisture sensors were terminated in a manner to which they can be read again at any time should KDOT desire to collect additional information.

Additional laboratory work should be done on the early strain and moisture response. This would allow for a more controlled environment to ensure to reduce the effect of temperature. Additional future work should also be performed to determine the viability of using ICC, and the potential reduction in shrinkage and warping, to extend joint spacing for jointed concrete pavements. Initial plans are to extend KDOT's standard 15-ft joint spacing to 18, 21, and 24 feet and evaluate the pavements' ability to resist cracking and excessive warping. This work will be performed when the proper project is available to produce specifications and personnel will be available to do the field installation of instrumentation and perform the testing.

References

AASHTO T 22-17. (2017). *Compressive strength of cylindrical concrete specimens*. Washington, DC: American Association of State Highway and Transportation Officials.

AASHTO T 177-17. (2017). *Flexural strength of concrete (using simple beam with center-point loading)*. Washington, DC: American Association of State Highway and Transportation Officials.

AASHTO TP 95-11. (2011). *Surface resistivity indication of concrete's ability to resist chloride ion penetration*. Washington, DC: American Association of State Highway and Transportation Officials.

Asbahan, R. E., & Vandenbossche, J. M. (2011, August). Effects of temperature and moisture gradients on slab deformations for jointed plain concrete pavements. *Journal of Transportation Engineering, 137*(8). doi:10.1061/(ASCE)TE.1943-5436.0000237

ASTM C31M-18b. (2018). *Standard test method for making and curing concrete test specimens in the field.* West Conshohocken, PA: ASTM International. doi:10.1520/C0031_C0031M-18B, www.astm.org.

ASTM C138M-17a. (2017). *Standard test method for density (unit weight), yield, and air content (gravimetric) of concrete*. West Conshohocken, PA: ASTM International. doi:10.1520/C0138_C0138M-17A, www.astm.org.

ASTM C143M-15a. (2015). *Standard test method for slump of hydraulic-cement concrete*. West Conshohocken, PA: ASTM International. doi:10.1520/C0143_C0143M-15A, www.astm.org.

ASTM C157M-08. (2008). *Standard test method for length change of hardened hydraulic-cement mortar and concrete*. West Conshohocken, PA: ASTM International. doi:10.1520/C0157_C0157M-08, www.astm.org.

ASTM C231M-17a. (2017). *Standard test method for air content of freshly mixed concrete by the pressure method*. West Conshohocken, PA: ASTM International. doi:10.1520/C0231_C0231M-17A, www.astm.org.

ASTM C403M-08. (2008). *Standard test method for time of setting of concrete mixtures by penetration resistance*. West Conshohocken: ASTM International. doi:10.1520/C0403_C0403M-08, www.astm.org.

ASTM C457M-12. (2012). *Standard test method for microscopial determination of parameters of the air-void system in hardened concrete*. West Conshohocken, PA: ASTM International. doi:10.1520/C0457_C0457M-12, www.astm.org.

ASTM C469M-10. (2010). *Standard test method for static modulus of elasticity and Poisson's ratio of concrete in compression*. West Conshohocken, PA: ASTM International. doi:10.1520/C0469_C0469M-10, www.astm.org.

ASTM C496M-11. (2011). *Standard test method for splitting tensile strength of cylindrical concrete specimens*. West Conshohocken, PA: ASTM International. doi:10.1520/C0496_C0496M-11, www.astm.org.

ASTM C642-13. (2013). *Standard test method for density, absorption, and voids in hardened concrete*. West Conshohocken, PA: ASTM International. doi:10.1520/C0642-13, www.astm.org.

ASTM C1064/C1064M-12. (2012). *Standard test method for temperature of freshly mixed hydraulic-cement concrete*. West Conshohocken, PA: ASTM International. doi:10.1520/C1064_C1064M-12, www.astm.org

ASTM C1202-12. (2012). *Standard test method for electrical indication of concrete's ability to resist chloride ion penetration*. West Conshohocken, PA: ASTM International. doi:10.1520/C1202-12, www.astm.org.

Carter, N., Jenkins, A., & Meggers, D. A. (2016). *Curling and warping of concrete pavement: An investigation and proof of concept study* (Report No. FHWA-KS-16-04). Topeka, KS: Kansas Department of Transportation.

Geokon, Inc. (2013). *Instruction manual Model 4200 Series Vibrating Wire Strain Gages*. Lebanon, NH: Geokon, Inc.

KT-71 Kansas Test Method. (2012). Air void analyzer. *Kansas Department of Transportation Construction manual, Part V.* Topeka, KS: Kansas Department of Transportation.

KTMR-22 Kansas Test Method. (2012). *Resistance of concrete to rapid freezing and thawing*. Topeka, KS: Kansas Department of Transportation.

KTMR-23 Kansas Test Method. (1999). *Wetting and drying test of sand and sand-gravel aggregate for concrete*. Topeka, KS: Kansas Department of Transportation.

Appendix A: KT-71 Test Procedure

5.9.71 AIR-VOID ANALYZER (Kansas Test Method KT-71)

1. SCOPE

This method of test covers the determination of characteristics of the air-void system of freshly mixed concrete using a sample of mortar. Spacing factor, specific surface and entrained air content are determined by capturing air bubbles released from a mortar sample.

The sample will only be representative of the depth of the concrete within approximately 2.5 in (60 mm) below the level at which the sampling is begun. This method is applicable to fresh concrete with a minimum slump of 0.4 in (10 mm) and air content between 3.5 and 10% by volume. Only air voids less than 0.1 in (3 mm) in diameter are measured by this method. The test must be performed in sheltered, stable conditions.

2. REFERENCED DOCUMENTS

2.1. Part V**,** 5.9; Sampling and Test Methods Foreword

2.2. KT-18; Air Content of Freshly Mixed Concrete by the Pressure Method

2.3. KT-19; Air Content of Freshly Mixed Concrete by the Volumetric Method

2.4. KT-20; Mass per Cubic Foot (Meter), Yield, and Air Content (Gravimetric) of Freshly Mixed Concrete

2.5. KT-21; Slump of Portland Cement Concrete

2.6. ASTM C 457; Microscopical Determination of Parameters of the Air-Void System in Hardened Concrete

3. APPARATUS

3.1. The balance shall conform to the requirements of **Part V, Section 5.9; Sampling and Test Methods Foreword** for the class of general purpose balance required for the principal sample mass of the sample being tested. The balance shall also have an integral arm from which the dish can be suspended.

3.2. Analysis and data collection apparatus assembly, the sampling equipment and materials is designed and built to function as an integrated system that is demonstrated by the manufacturer to accurately measure and calculate air-void distribution in fresh air-entrained concrete.

3.3. Riser cylinder made of clear plastic with a base and a collar approximately as shown in **Figure 1**. The base shall have an integral heating element capable of maintaining the analysis liquid at 73 ± 4°F (23 ± 2°C) and entry holes for the plastic rod and the sample syringe with gaskets to make a watertight seal.

3.4. Magnetic stirrer capable of maintaining 300 rpm during mixing.

3.5. A cabinet shall house the riser cylinder, magnetic stirrer and balance as shown in **Figure 2**.

3.6. A ferromagnetic steel rod approximately 0.2 in (5mm) in diameter and 2.5 in (62mm) in length.

3.7. A temperature sensor capable of detecting the temperature of the analysis liquid at the bottom of the cylinder. The temperature sensor should be capable of measuring yhr temperature to within 1.0°F (0.5°C) in the range of 59 to 86°F (15 to 30°C) and of transmitting such measurements to the computer through an appropriate interface.

3.8. 20 ml plastic syringes, with the tapered end removed, calibrated and marked for collecting the specified sample volume as shown in **Figure 3**.

3.9. Plastic rod at least 1.5 in (35 mm) longer than the width of the base. The outside diameter of the body of the rod is the same as the syringes used in the test. A 0.04 in (1 mm) length at the end of the rod shall have a reduced diameter that fits tightly within the inside diameter of the syringe as shown in **Figure 3**.

3.10. Clear, shallow dish that is large enough to cover the entire area of the cylinder, retain the rising bubbles and fit within the collar. The dish shall have an opening on the side to allow entrapped air to be removed.

NOTE: An inverted Petri dish with an appropriate slot, as shown in **Figure 3**, can fulfill these requirements.

3.11. A device to suspend the dish from a balance arm by a single wire as shown in **Figure 3**.

3.12. Control System. A computer, software and interface system capable of controlling the test, recording data, and displaying data at least once per minute during the test. It shall also calculate, display and record the air content(s), air-void spacing factor, and specific surface of the air-void system.

3.13. Sampling assembly to hold the syringe and a wire cage and vibrate at approximately 50 Hz with an amplitude that allows the mortar to flow into the wire cage.

NOTE: A drill operating at 3000 rpm with an eccentrically weighted, forked assembly as shown in **Figure 4** can fulfill these requirements. The hammering function of the drill can be used as needed in stiffer concrete mixes.

3.14. A wire cage that is of sufficient size to obtain a sample of fresh concrete mortar, similar to **Figure 4**. The cage wires shall have a clear spacing of 0.24 in (6 mm).
3.15. Rigid, clear plastic plate approximately 10 x 10 x 1/8 in. (250 x 250 x 3 mm) with a center hole of a diameter approximately 1/8 in (3 mm) greater than that of the wire cage.

3.16. A calibrated funnel marked for measuring a specified amount of analysis liquid similar to that shown in **Figure 4**. The funnel is capable of introducing the analysis liquid into the bottom of the water-filled riser cylinder with a minimum of mixing.

3.17. A spatula to trim the mortar sample flush with the end of the syringe.

3.18. A water container with a 2 gallon (4 liter) minimum capacity.

NOTE: A 5 gallon (19 liter) portable insulated drinking water cooler is useful for repeated testing.

3.19. An immersible heating element capable of maintaining the water in the container at approximately 73 ± 4°F (23 ± 2° C).

3.20. Thermometer accurate to ± 1.0°F (± 0.5°C) over the range of 50 to 86°F (10 to 30°C).

3.21. Brush with a handle longer than the riser cylinder is tall and an angled head.

3.22. An insulated “cooler-type” lunchbox is useful.

3.23. Sealable plastic bags, commercially available in pint and quart sizes.

4. MATERIALS

4.1. Analysis Liquid. The analysis liquid shall have physical and chemical properties such that the air-void bubbles remain discrete. The viscosity of the analysis liquid must remain constant over the range of temperatures found in the test and be compatible with the apparatus and the control system. The viscosity of the analysis liquid used shall provide a measurable separation in time between the arrivals of bubbles of different sizes at the top of the water column. The analysis liquid and its viscosity shall be specified by the equipment manufacturer.

NOTE: A commercially-available solution of glycerol in water can fulfill these requirements. A mixture of 4 parts glycerol to 1 part distilled water has been known to work well.

4.2. De-Ionized water from the Materials and Research Chemistry Lab. The water shall be de-aerated and maintained at atmospheric pressure and approximately 73 ± 4°F (23 ± 2°C) for a minimum of 12 hours before use.

NOTE: Properly de-aerated water is crucial to this test. The solubility of air in water increases as pressure increases and temperature decreases. The change in dissolved air content due to temperature occurs slowly; thus, the water must be maintained at constant temperature for a minimum of 12 hours before use. De-aerated water also reabsorbs air when cooled. If the water is not de-aerated correctly or if it is used shortly after reheating, air may be liberated in the riser cylinder. Air bubbles may form in the riser cylinder and on the dish, and may have a considerable effect on the specific surface and spacing factor results.

4.3. Ice as needed in cubes or chips or frozen, re-freezable ice packs or cubes.

5. SAMPLING

5.1. Take samples as soon as possible after the concrete is in the desired state. The sampling location depends on the purpose of the test. Samples can be extracted from concrete in place (pavements, structural members, decks, etc.), from concrete sampling containers such as unit weight buckets, beam molds, or cylinder molds, or from other locations.

5.2. Insert a syringe into the sampling assembly and mount the wire cage onto the sampling assembly. Fully collapse the syringe.

5.3. Place the plastic plate in good contact with the surface of the concrete to be sampled. Begin the vibration of the sampling assembly. Lower the wire cage through the hole in the plastic plate into the concrete. The vibration will cause the mortar fraction of the concrete to flow into the wire cage. Advance the wire cage into the concrete at a rate such that the concrete surface under the plate and the surface of the mortar within the cage remain at approximately the same level at all times. Avoid filling the cage with surface mortar by pressing the plastic plate against the fresh concrete. The pressure is adequate when the air bubbles under the plastic plate do not move towards the hole while sampling.

5.4. Advance the wire cage into the concrete until the end of the syringe plunger is in full contact with the surface of the mortar. While maintaining the vibration, push the syringe cylinder smoothly into the mortar at such a rate that the wire cage remains full of mortar until the syringe is fully extended. Stop the vibration and withdraw the wire cage and syringe from the concrete.

5.5. Remove the wire cage and the syringe from the sampling assembly saving the excess mortar from the wire cage. Pack this excess mortar around the end of the syringe to be used to displace any large air bubbles from the syringe.

5.6. Immediately place the sample in a plastic bag on ice or freezer packs in the insulated box to retard the onset of initial set. Testing must begin before the initial set of the concrete.

5.7. If large air bubbles are present at the base of the syringe, remove the plunger and pack enough excess mortar through the opposite end of the syringe to remove the air bubble. Replace the plunger to contact the mortar. Remove the excess mortar from the outside of the syringe and clean the outside of the syringe with a damp cloth. Advance the plunger to the mark corresponding to the specified sample volume and trim the mortar flush with the end of the syringe cylinder using the spatula. Retract the plunger approximately 0.04 in (1 mm) to allow room for the recessed end of the plastic rod. This step may be performed at any time before **Section 7.9** of this test method, seating the syringe on the plastic rod.

6. PREPARATION OF APPARATUS

6.1. Bring the analysis liquid and at least 0.5 gallon (2 liters) of de-aerated water to a temperature of 73 ± 4°F (23 ± 2°C) without altering other characteristics of the liquids.

NOTE: Using ice in sealed plastic bags, or freezer packs to cool the liquids is acceptable.

6.2. Select a test location protected from any wind, vibration or movement that may affect the balance readings. Place the cabinet on a stable and level surface. Allow the balance to stabilize so that it does not drift more than 0.01 g in four minutes. If the balance has auto-zeroing capability, place a small load on the balance to obtain a non-zero reading in order to observe the variation of the reading.

6.3. Connect the control system.

NOTE: Place the control system so that if the plastic rod is accidentally removed from the base of the riser cylinder the contents of the riser cylinder will not spill onto the control system.

6.4. See **Section 11** of this test method for additional hints on preparation of apparatus.

7. PROCEDURE

7.1. Enter all required data into the control system.

7.2. Place the stirrer rod flat on the bottom of the riser cylinder. Insert the plastic rod through the hole on the wider side of the base of the riser cylinder so that the full diameter of the plastic rod protrudes though the hole on the opposite (narrower) side of the base.

NOTE: Using a light coat of waterproof grease on the rubber o-rings will improve the seal between the plastic rod and the base of the riser cylinder.

NOTE: When testing low-viscosity materials such as self-consolidating concrete, it is permissible to tilt the riser column to seat the syringe on the plastic rod before the liquids are added to the riser column.

7.3. Fill the riser cylinder with de-aerated water to about 0.5 in (15 mm) above the bottom of the top collar. Use the brush to remove all bubbles from the stirrer rod, the plastic rod and the riser cylinder.

NOTE: Rotating the plastic rod can be helpful in assuring that all bubbles are removed.

7.4. Mount the riser cylinder in position on the cabinet. It is permissible to fill the riser cylinder with the water after positioning the riser cylinder on the cabinet.

7.5. Fill the funnel with the manufacture's specified amount of the analysis liquid.

7.6. Insert the analysis liquid into the bottom of the riser cylinder using the funnel to minimize the mixing of the analysis liquid with the de-aerated water. Replace the stopper once the specified amount of analysis liquid has been discharged. Remove the funnel from the riser cylinder and discard any remaining liquid in the funnel.

7.7. Connect the integral heating element of the riser cylinder and the temperature sensor to the control system.

7.8. Insert the dish into the riser cylinder collar. Submerge the dish in the de-aerated water and tilt to allow all entrapped air to escape through the opening. Suspend the dish from the balance arm in such a way that it is approximately centered and does not touch the walls of the riser cylinder collar. Only a single wire of the suspension device may break the surface of the water. Add more de-aerated water if necessary.

7.9. Seat the syringe containing the sample on the reduced end of the plastic rod. Move the syringe and plastic rod together through the riser cylinder base until the junction of the syringe and plastic rod is at the nearest inside edge of the riser cylinder. Leaving the syringe in position, continue withdrawing the plastic rod until the reduced end is flush with the opposite inside edge of the riser cylinder.

NOTE: To make positioning the plastic rod and syringe with respect to the riser cylinder easier, mark the correct position on the plastic rod and note the position of the syringe before starting the test. If moving the plastic rod and syringe is difficult, use a small amount of waterproof grease or analysis fluid on the gaskets and use a twisting motion.

7.10. Remove enough of the air that may have risen during the separation of the syringe and the plastic rod from under the dish so that the dish is neither touching nor close to the wall of the riser cylinder collar.

7.11. When the temperature of the analysis liquid as measured by the temperature sensor is 73 ± 4°F (23 ± 2°C), inject the mortar from the syringe into the riser cylinder. Immediately start the mixing and data collection.

7.12. If any of the recorded temperature readings are outside the range of 73 ± 4°F (23 ± 2°C), discard the test.

7.13. If unusual variations that may be due to vibration or disturbance are noted in the data, discard the test.

7.14. Analyze samples as soon as possible. However, samples may be used whenever they can be completely dispersed in the analysis liquid by the stirring action.

8. REPORT

8.1. The report shall include the following information:

8.2. Project identification

8.3. Test identification number

8.4. Date of test

8.5. Sampling location

8.6. Slump by **KT-21** (if known)

8.7. Air content by **KT-18** or **KT-19** (if known)

8.8. Unit weight by **KT-20** (if known)

8.9. Mortar (material less than 6 mm) volume, percent, as calculated from the mix design

8.10. Paste volume, percent, as calculated from the mix design

8.11. Sample volume, ml

8.12. Test temperature range, °F (°C)

8.13. Air content(s), percent

8.14. Spacing factor, in (mm)

8.15. Specific Surface, in^2/in^3 (mm^2/mm^3)

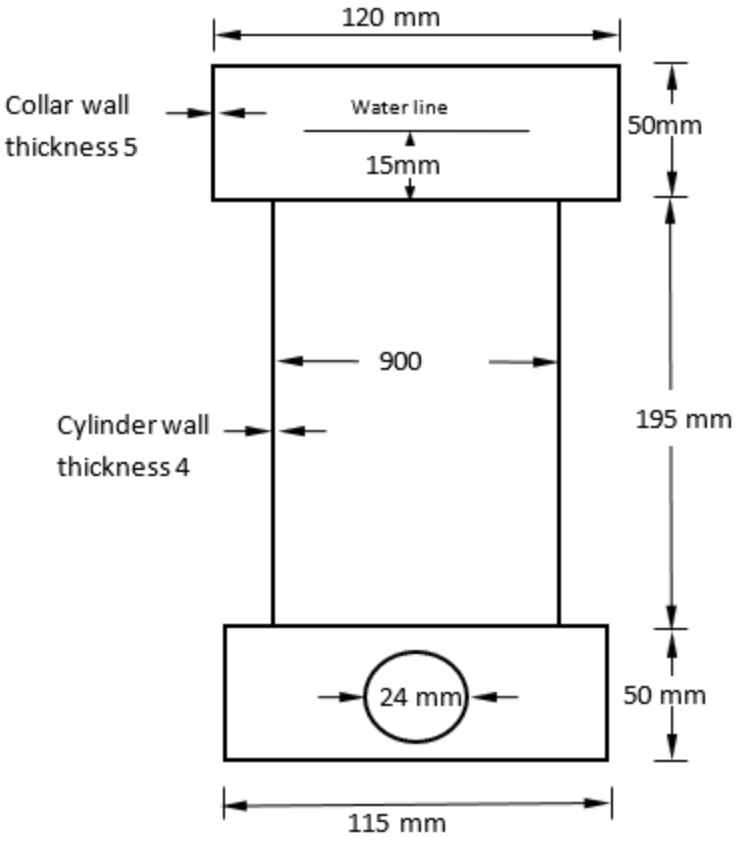

Figure 1
Riser Cylinder

Figure 2
Typical Apparatus with Riser Cylinder, Cabinet, and Computer

Figure 3
Petri dish, 20 ml syringe,
and temperature sensor

Figure 4
Wire cage and funnel

9. VERIFICATION

9.1 To correlate the air-void characteristics (spacing factor, entrained air content or specific surface) as determined by the buoyancy-change method from fresh concrete with those obtained by **ASTM C 457** from hardened concrete, compare a minimum of five pairs of samples. Each pair of samples of the fresh and hardened concrete should be from the same batch of concrete, placed and consolidated uniformly, of comparable depth and located as close together as possible without including any of the area disturbed during sampling the fresh concrete in the hardened sample. Calculate the percent difference of the buoyancy test results from the **ASTM C 457** results for each pair, and then average these percent differences. The

average of the percent differences of the five pairs of should be 20% or less for the results to be considered equivalent. Average percent differences greater than 20% may arise from **ASTM C 457** testing errors such as mistaking fly ash spheres or voids left by sand grains plucked from the polished surface of the specimen during sample preparation for air voids in the concrete paste. Sampling errors, testing errors in the buoyancy change method, admixtures that affect the viscosity or the miscibility of fresh concrete, or other factors may also cause some variation. The buoyancy change method is less likely than **ASTM C 457** to overestimate the quantity and quality of the air voids in any given concrete. In the buoyancy change method, bubbles may coalesce after release into the fluid, and the portion of entrained air associated with the coarse aggregate is excluded from the sample. Thus the buoyancy change method will tend to give a lower specific surface and higher spacing factor than **ASTM C 457**.

10. REPEATABILITY

10.1 Although each buoyancy test requires a unique sample and therefore cannot be duplicated exactly, researchers at the Kansas Department of Transportation have found that pairs of samples obtained within 1.5 feet of each other in the field vary 10% from each other on average.

11. SET UP HINTS

11.1 Several steps can be taken to reduce the amount of time necessary to set up the buoyancy testing equipment Preparing the de-aerated water and the bottle of analysis liquid in an insulated water container at least one day before testing occurs will save time. If the water container will be stored in an area that is cooler than the specified temperature, set the immersible heater to the correct temperature and put it into the covered water container. If the room temperature is slightly higher than the specified temperature, uncovering the container will allow the water to cool approximately 5°F (3°C). If the room temperature is much higher than the specified temperature, a sealed bag of ice or freezer packs placed in the covered water container the night before testing will generally result in the correct water and analysis fluid temperature.

11.2 After the water has been brought to the proper temperature, care should be taken to keep the temperature as constant as possible. Protect the water container from temperature extremes, such as may be encountered in an enclosed vehicle.

11.3 Obtaining a constant balance reading at the beginning of the test may also take a significant amount of time if the equipment is set up in an unstable location. Mobile work trailers that are resting on their tires are generally not stable enough. Any movement by people in the trailer can move the trailer enough to disturb the apparatus and render the test unusable. Generally, only trailers that have been put up on blocks so they are not sitting on their tires are at all acceptable, and only as a last alternative.

11.4 Isolating the test equipment from vibration will reduce the time necessary to obtain a constant balance reading at the beginning of the test. One or two anti-vibration pads may be used under each corner of the cabinet to attenuate shock and vibration.

Appendix B: KTMR-22 Test Procedure

KTMR-22 RESISTANCE OF CONCRETE TO RAPID FREEZING AND THAWING (Kansas Test Method KTMR-22)

KT-MR-22 follows the procedures set forth in ASTM C 666, Test Method for Resistance of Concrete to Rapid Freezing and Thawing (Procedure B), with the following exceptions:

Add 6.1.1

6.1.1 Use the following proportioning of materials, and specific types of materials as stated.

25 %	-19.0 mm + 12.5 mm (-3/4" +1/2") (SSD by toweling)
25 %	- 12.5 mm + 9.5 mm (-1/2" +3/8") (SSD by toweling)
50 %	FA-A (correction made for moisture) Kaw River sand
Y.C.F.	356.9 kg/m^3 (601.60 lbs/yd^3)
w / c	0.4431 to 0.4874 (tap water) (Monarch Cement, Type II)
Air	5 to 7 % (A.E.A. Air Tite by Gifford-Hill)
Slump	38 to 64 mm (1½ to 2½ in)

Total volume approximately 0.017 m^3 (0.6 ft^3) concrete.

Delete 7.4 and Note 5 and add:

7.4 For this test the specimens shall be cured for 90 days as follows:

7.4.1 Place beams in a moisture room for 67 days.

7.4.2 Transfer beams to a room having a relative humidity of approximately 50% and a temperature of approximately 22.8ºC (73ºF), for 21 days.

7.4.3 Place beams in a tempering tank maintained at 21.1ºC (70ºF) for 24 hours.

7.4.4 Place beams in a freezer maintained at 4.4ºC (40ºF) for 24 hours.

Note: Method of determining resonant frequency of the concrete specimen is per ASTM C 215, section 6.2, impact resonance, transverse mode—modified in that the specimen beam is placed on an isolation pad of medium density styrofoam, approximately 50 mm thick, the accelerometer is located on the top surface of the beam approximately 25 mm from one end, and the point of impact is at the opposite end of this top surface approximately 25 mm from the end. The impact and accelerometer locations are marked from the outset of the test for repeatability purposes.

Appendix C: KTMR-23 Test Procedure

KTMR-23 WETTING AND DRYING TEST OF SAND AND SAND-GRAVEL AGGREGATE FOR CONCRETE

a. SCOPE

This test shall be used to determine the acceptability of sand and sand-gravel aggregate to be used in concrete construction, both pavement and structural.

b. REFERENCED DOCUMENTS

b.1. AASHTO T 119; Slump of Hydraulic Cement Concrete

b.2. AASHTO T 126; Making and Curing Concrete Test Specimens in the Laboratory

b.3. AASHTO T 140; Compressive Strength of Concrete Using Portions of Beams Broken in Flexure

b.4. AASHTO T 177; Flexural Strength of Concrete [Using Simple Beam With Center Point Loading]

b.5. AASHTO M 231; Balances Used in the Testing of Materials

c. APPARATUS

c.1. Molds suitable for casting 76.2 X 101.6 X 406.4 mm (3 X 4 X 16 in) beams.

c.2. Rotary concrete mixer as specified in AASHTO T 126.

c.3. A balance of sufficient capacity conforming to requirements of AASHTO M 231.

c.4. Slump cone and rod as specified in AASHTO T 119.

c.5. A drying oven capable of maintaining a temperature of 53.3-54.4ºC (128-130ºF).

c.6. Water bath capable of maintaining a temperature between 15.6-26.7ºC (60-80ºF).

c.7. Length comparator capable of accurately reading beams to the nearest 0.01 mm (0.001 in).

c.8. A testing machine for modulus of rupture determination as specified in AASHTO T 177.

c.9. A 15.9 mm (5/8 in) diameter steel rod having a hemispherical tip the same diameter as the rod.

d. SAMPLE PREPARATION

d.1. Cement: Use Monarch, Type II cement. If not available, then use the cement type and brand designated by the Engineer of Tests.

NOTE a: The requirement for Monarch Type II cement exists because of its alkali level is as close to, but not exceeding, the 0.6% maximum.

d.2. The gradation of the aggregate shall be within the middle 1/3 of the limits specified for MA-1 (**Table 1**) except for the 19 mm (3/4 in) sieve. It shall be further prepared by screening over the 19 mm (3/4 in) sieve and all material retained on the 19 mm (3/4 in) sieve shall be crushed to pass the 19 mm (3/4 in) sieve and incorporated into the mix.

MA-1 Percent Retained - Square Mesh Sieves								
19.0 mm (¾ in.)	12.5 mm (½ in.)	9.5 mm ($^3/_8$ in.)	4.75 mm (No. 4)	2.36 mm (No. 8)	1.18 mm (No. 16)	600 µm (No. 30)	300 µm (No. 50)	150 µm (No.100)
0-5	…	…	20-60	…	…	76-84	90-96	…

Table 1

d.3. Run the specific gravity and absorption tests in accordance with KT-6-94 procedure I & II of the Part V Construction Manual. Run tests on the as-received material.

d.3.a. Using the results from the specific gravity and absorption tests, determine the average specific gravity and absorption in a 40 / 60 mix of dry material. The mix represents 40% being + 4.75 mm (+ 4) material and 60% being - 4.75 mm (- 4) through + 75µm (+ 200) material.

d.3.b. Recombine the material to the following schedule to produce three 18.145 kg (40 lb) batches.

12.5 mm (1/2") - 0.363 kg (0.8 lb)
9.5 mm (3/8") - 2.359 kg (5.2 lb)
4.75 mm (#4) - 4.536 kg (10.0 lb)
2.36 mm (#8) - 2.722 kg (6.0 lb)
1.18 mm (#16) - 1.814 kg (4.0 lb)
600 µm (#30) - 2.722 kg (6.0 lb)
300 µm (#50) - 2.359 kg (5.2 lb)
150 µm (#100) - 0.907 kg (2.0 lb)
75 µm (#200) - 0.363 kg (0.8 lb)

Total -18.145 kg (40.0 lb)

d.3.c. Place the material into galvanized or rust resistant pans, add the amount of water equal to the absorption and mix uniformly. Cover the material with a plastic sheet and let stand for approximately 4 hours in order to reach a saturated surface dry condition.

d.4. Create a concrete mix having a water/cement ratio of 0.51 and having a slump of 50.8 mm (2 in) and 76.2 mm (3 in). Place two 18.145 kg (40 lb) batches of aggregate, design weight of cement and water in the mixer and start mixing. Using the third aggregate batch to bring mix to the desired slump.

d.5. Cast six 76.2 X 101.6 X 406.4 mm (3 X 4 X 16 in) beams as described below, and remove from the molds within 24 ± 8 hours from time of casting. Beams should be protected from loss of moisture during mold removal. Identify each beam for future tracking.

d.5.a. Place the concrete in the molds taking care to ensure each scoop is representative of the mix. Move the scoop around the edge of the mold as the concrete is discharged to minimize segregation and to ensure uniformity of distribution. Further distribute the concrete by use of a tamping rod prior to consolidation. Do not add nonrepresentative concrete to an underfilled mold.

d.5.b. Place the concrete in the mold in two layers of approximately equal volume. Rod each layer 32 times with the rounded end of the rod. Rod the bottom layer throughout its depth, distributing the strokes uniformly over the cross section of the mold. For the upper layer, allow the rod to penetrate about 12.7 mm (1/2 in) into the bottom layer. After each layer is rodded, spade the concrete around the edges of the mold with a trowel or spatula. The molds containing the concrete shall then be tapped lightly on the tabletop to close any remaining voids. Finish the surface with a wood float using the minimum amount of manipulation necessary to produce a plane surface that is essentially level with the top edge of the mold.

d.6. Cure the beams seven days in a moist room maintained at 23 ± 2.2°C (73.4 ± 3°F) and at not less than 95% relative humidity, then 21 days in air at a temperature between 20-27.5°C (68-81.5°F) and 50% relative humidity.

d.7. At 28 days obtain cured (dry) mass and length. Place beams in water bath maintained at 15.6-26.7°C (60-80°F) for a minimum of 1 hour. Obtain mass in water & Saturated surface dry (SSD) to determine the specific gravity as specified in **g.1.** Place beams back in water bath for 48 hours.

NOTE b: Differences in specific gravity between the six beams can be an indication of air entrapment or poor consolidation in specimens.

d.7.a. During the length determination, select the three best fitting beams for 365-day cycling. Best fitting pertains to the ability of the beam to fit in the comparator with pins fully aligned and minimal rocking motion.

d.8. The beams to be tested in flexure at 60 days shall then be cured in the moist room for an additional 30 days.

e. PROCEDURE

e.1. Measure length of beams at the following ages: 30, 60, 120, 180, 240, 300, and 365 days. Make every attempt to choose a time when the 30, 60 and 365 day checks can be guaranteed. Other dates should fall within plus or minus one day. At each age the beams shall be submerged in water maintained between 15.6-26.7°C (60-80°F) for not less than 15.5 $\pm$ 0.5 hours prior to measurement.

e.2. Sixty days after casting, test the three beams cured in the moist room for modulus of rupture as specified in AASHTO T 177. Conduct the test with the 76.2 X 406.4 mm (3 X 16 in) faces perpendicular to the applied load, with the load applied at the center of a 355.6 mm (14 in) span.

e.2.a. Upon completing the modulus of rupture test, break both halves of the beams in accordance to AASHTO T 140 (See **Figure 1**).

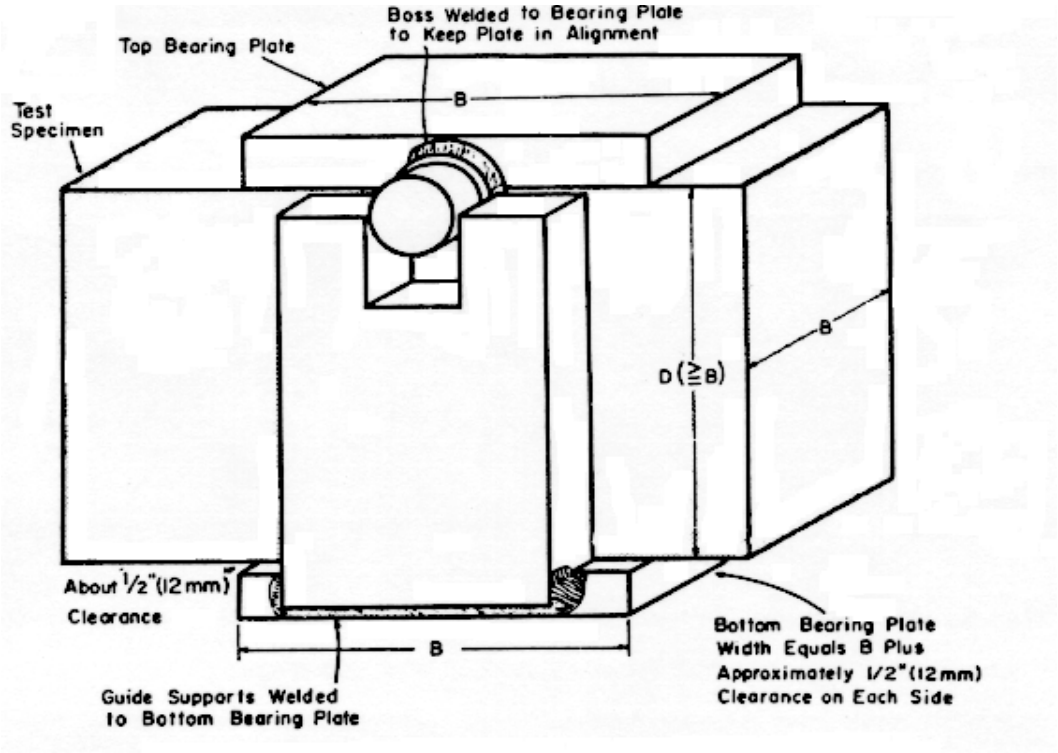

Figure 1

e.3. Beginning 30 days after casting, subject the other three beams to the following wetting and drying test procedure.

e.3.a. Place the beams in the oven maintained at 53-54°C (128-130°F) for eight hours.

e.3.b. Remove the beams from the oven and submerge them in the water bath at 16-27°C (60-80°F) for 15.5 ± 0.5 hours. Procedure (**e.3.a.**) and (**e.3.b.**) constitutes one cycle and shall be completed in 24 hours.

e.3.c. Repeat the cycle each consecutive day throughout the 365-day period except for weekends and holidays when the beams are to remain in the water bath.

e.4. Calculate and record the length change, expressed as percent expansion, at each of the ages stated under (**e.1.**) using the length measured at 30 days as the base as specified in **g.2.**

e.5. The beams shall be tested for modulus of rupture, upon completion of the 365-day test. The test shall be conducted with the 76.2 X 406.4 mm (3 X 16 in) faces perpendicular to the applied load, with the load applied at the center of a 355.6 mm (14 in) span as specified in AASHTO T 177.

e.6. Upon completing the modulus of rupture test, subject each half to a compressive strength test in accordance to AASHTO T 140.

f. REQUIREMENTS FOR ACCEPTABILITY OF THE AGGREGATE

f.1. Each of the two groups of beams tested in flexure at 60 days and 365 days shall have an average modulus of rupture of not less than 3.8 MPa (550 psi).

f.2. Expansion of beams:

f.2.a. At 180 days, the increase in length shall not exceed 0.050%.

f.2.b. At 365 days, the increase in length shall not exceed 0.070%.

g. CALCULATIONS

g.1. Bulk Specific Gravity:

$$G_{sb} = \frac{A}{B - C}$$

Where:

A = Mass of cured beam, g
B = Saturated surface-dry beam, g
C = Mass of beam in water, g

g.2. Percent expansion of beam:

$$\Delta L\% = \frac{100(L_n - L_{30})}{L_{30}}$$

Where:

$\Delta L\%$ = Percent change in length
L_{30} = Length of specimen at 30 days
L_n = Length of specimen at n days (n=60, 120, 180, 240, 300, or 365 days)

h. REPORT

See attached report.

KANSAS DEPARTMENT OF TRANSPORTATION

Sample of Sand Gravel (Wetting Drying)

Laboratory No 96-4776
CMS No. _____
Date reported _____
Date received 10/21/96

Spec. No. 1990 SS, Subsec. 1102 (b) (1.1.3) Qty Unlimited
Property of
Sample from
Submitted by Topeka, KS
Ident. Marks

Project No. Wetting & Drying Co/Dt Type

Contractor

TEST RESULTS

This material was tested in accordance with Article 1117 (t) of the 1990 KDOT Standard Specifications using Type II cement.

MATERIALS:

Aggregate - MA-1

-

Cement - Producer type I/II, Lab. #XX-XXXX

AGGREGATE SIEVE ANALYSIS:

SIEVE ANALYSIS OF MA - 1										
Metric	mm						µm			
	19.0	12.5	9.5	4.75	2.36	1.18	600	300	150	75
English	in.									
	(3/4)	(1/2)	(3/8)	(#4)	(#8)	(#16)	(#30)	(#50)	(#100)	(#200)
% Ret.	0	2	15	40	55	65	80	93	98	100

Agg. Specific Gravity, S.S.D. (Theo. Comb.) ---------- 2.58
% Absorption (Theo. Comb.) ---------- 1.46
-#200 Material (%) ---------- 0.00

Laboratory No XX-XXXX

MIX DESIGN DATA:

Date Made		11/18/96
Cement, kg (lb)	42.64	(94.00)
Water, kg (lb)	21.74	(47.94)
MA-1, kg (lb)	253.14	(558.09)
Slump, mm (in)	57.2	(2.25)

Time of slump after addition of water (min.) ---------- 12:15

Unit Weight:

Theoretical Air Free, kg/m^3 (lb/ft^3)	2380.8	(148.63)
Actual, kg/m^3 (lb/ft^3)	2325.2	(145.16)

Air Content:

Gravimetric, %	2.3
Rollameter, %	3.5

Yield Cement Factor kg (lb)	238.72	(526.29)
Water - Cement Ratio, kgs/kg (lbs/lb)		0.51

TEST DATA:

Specimen	Mod. of Rupture MPa (PSI) Uncorrected		Corrected		Change in Length (%)	Fund, Frequency (%30 day reading)
Note: The corrected modulus of rupture MPa (psi) is for information only.						
A	5.37	(779)	4.90	(710)		
B	5.34	(775)	4.96	(720)		
D	5.57	(808)	5.47	(794)		
Avg. @ 60 days	5.43	(787)	5.11	(741)		
C					0.027	
D					0.027	
E					0.027	
Avg. @ 179 days					0.027	109..31
C	5.10	(740)	5.10	(740)	0.053	
E	4.81	(698)	4.73	(686)	0.040	
F	3.76	(546)	3.63	(526)	0.047	
Avg. @ 365 days	4.56	(661)	4.49	(651)	0.047	108.81

Laboratory No 96-4776

COMPRESSIVE STRENGTH:

		Unit Load		Avg. Unit Load	
Specimen	Age (days)	MPa	(PSI)	MPa	(PSI)
A	60	43.02	(6240)		
A	60	44.54	(6460)		
B	60	42.82	(6210)		
B	60	41.37	(6000)		
D	60	39.85	(5780)		
D	60	43.64	(6330)	42.54	(6170)
C	365	43.44	(6300)		
C	365	42.82	(6210)		
E	365	41.58	(6030)		
E	365	38.75	(5620)		
F	365	40.82	(5920)		
F	365	42.47	(6160)	41.64	(6040)

NOTE: 232 cycles of wetting & drying.

DISPOSITION:

This material meets the requirements of Article 1117(t) of the 1990 KDOT Standard Specifications and is approved for use under the requirements of Sub-Article 1102 (b) (1.1.3) .

Reported by: _____.

XXXX

Title: Engineer of Physical Tests.

Appendix D: FHWA Mobile Technology Center Construction Report

See next page.

United States
Department of Transportation

SUMMARY REPORT

US-54 Expansion

Iola, KS
May 2014

FHWA MCL Project # KS1402

Federal Highway Administration
Office of Asset Management, Pavement and Construction
HIAP-10
1200 New Jersey Avenue, SE
Washington, DC 20590

Table of Contents

US-54 Reconstruction

INTRODUCTION

The project is reconstruction of a five mile section of concrete pavement on US-54. As part of the reconstruction on US-54, Kansas Department of Transportation (KDOT) built two 500′ pavement test sections on US-54 in Iola Kansas. One of the sections utilized internal curing with lightweight aggregate (ICC). The other was a standard pavement section that served as a control which was built with the same mixture as the rest of the project. This report pertains to the MCL participation during the construction of the ICC section of the project. The MCL was invited to the project by Dave Meggers and Andrew Jenkins with KDOT. The MCL sampled concrete from the ICC section as well as from the mixture that was going to be used for the control test section.

Figure 1: A view of the US-54 Reconstruction Section

PURPOSE

The purpose of the ICC section is to evaluate the benefits obtained through internal curing using pre-wetted lightweight aggregate. Plans are to evaluate the benefits obtained with shrinkage properties and therefore a reduction in cracking. The pavements will also be evaluated to determine if there is a significant reduction in permanent panel warping. Permanent panel warping can lead to poor ride quality and possibly structural failure of the pavement if excessive warping occurs. Additional work was also planned to determine any benefits to concrete strength and durability.

Pavement Test Sections

The two test sections were on US-54 between Iola and LaHarpe KS. The pavement design consists of a nine inch concrete pavement with 15 ft. joint spacing. Lane width for the driving lane varied between 12 ft. and 15 ft. depending on the location. Both test sections were chosen so that they had the same lane width. The pavement was on four inches of granular base. Both test sections were on the outside driving lane of the pavement. Two panels in the LWA section and one panel in the control section were instrumented. Deflection measurements were taken for the five panels surrounding the instrumented panels during the initial curing window.

TEST PLAN and MCL's Objective

The MCL visited the US-54 project from April 28 through May 3 2014 and sampled concrete from the ICC test section as well as the control mixture (not from the control test section). The FHWA Mobile Concrete Laboratory's (MCL) field visit to Kansas has two objectives:

1. Perform concrete testing to supplement KDOT's efforts to evaluate concrete pavement utilizing internal curing with light weight aggregate.
2. Demonstrate new concrete testing technologies to KDOT that could help reduce costs associated with testing/construction, increase safety, and increase the performance and durability of concrete pavements.

The following tests were performed by the MCL at the project site:

- Fresh Concrete Properties (slump, air, unit weight, temperature, etc.)
- Strength
- Modulus of Elasticity and Poisson's Ratio
- Maturity
- Coefficient of Thermal Expansion
- AVA (Air Void Analyzer)
- SAM (Super Air Meter)
- Permeability (RCPT and Surface Resistivity)
- MIT Scan T2 (Pavement Thickness)
- MIT Scan 2 (Dowel Alignment)
- Heat Signature (Calorimeter)

MATERIALS

Concrete Mixture Design

The US-54 project mixture was utilized for the ICC section with the exception that a small amount of fine normal weight aggregate was replaced with an equal volume of pre-wetted Light Weight Aggregate (LWA). Based on the LWA properties and the method developed by Expanded Shale Clay and Slate Institute (ESCSI), the amount to be replaced was approximately 12% by weight of the total aggregate to achieve the desired 7 lbs. of internal curing water per 100 lbs of cementitious material in the mixture. The LWA used for the project was supplied by Buildex from their Missouri plant.

Tables 1 and 2 show the sources and proportions of materials used in the control and ICC mixtures respectively. The only difference between the two is the substitution of the LWA for IMA ¼" chips and a slight change in aggregate percentage to account for the LWA needed for ICC (while keeping the amount to a minimum due to cost) while also trying to keep the gradation as optimized as reasonably possible. Appendix A shows the concrete mixture designs for the control and ICC sections.

Table 1: Aggregate Proportions and Sources for the Control Mixture

Control Mixture			
Item	Source	Proportion	Specific Gravity
CPA-4	Nelson	50%	2.56
IMA ¼" Chips	Nelson	10%	2.56
Basic SSG for MA-3	Cornejo & sons	40%	2.61
Cement Type 1/11	Ash Grove	75%	3.51
Fly Ash – Class C	KCPL	25%	2.65
Water	City of Gas, KS		
Design Air		6.5%	
Slump		2"	
Design W/Cm ratio		.40	

Table 2: Aggregate Proportions and Sources for the ICC Mixture

ICC Mixture			
Item	Source	Proportion	Specific Gravity
CPA-4	Nelson	51%	2.56
IMA 3/8 (LWA)	Buildex 3/8	9%	1.71
Basic SSG for MA-3	Cornejo & sons	40%	2.61
Cement Type 1/11	Ash Grove	75%	3.51
Fly Ash – Class C	KCPL	25%	2.65
Water	City of Gas, KS		
Design Air		6.5%	
Slump		2"	
Design W/Cm ratio		.40	

Figures 2 shows the photo of the concrete plant and Figure 3-6 show photos of the aggregates used in the control and the ICC mixture. The percent retained and coarseness factor and the 0.45 power chart for the combined aggregate gradation for the two mixtures are shown in Figure 7, 8 and 9 respectively.

Figure 2: Concrete Batch Plant

Figure 3: Coarse Aggregates

Figure 4: Fine Aggregates

Figure 5: Light Weight Aggregate

Figure 6: Light Weight Aggregate Stockpile

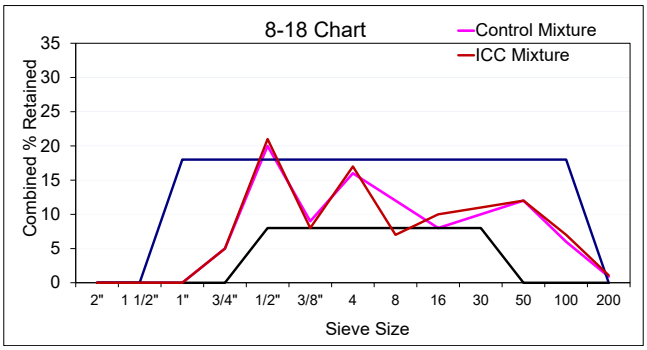

Figure 7: Percent Retained Chart

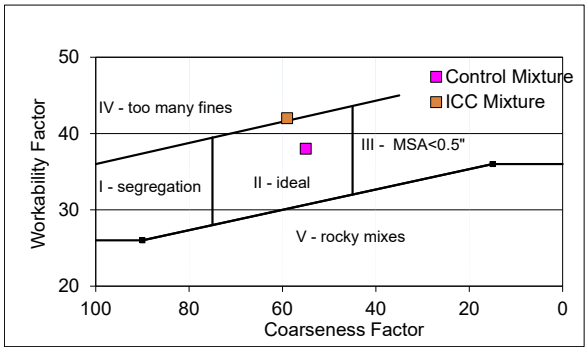

Figure 8: Coarseness Factor Chart

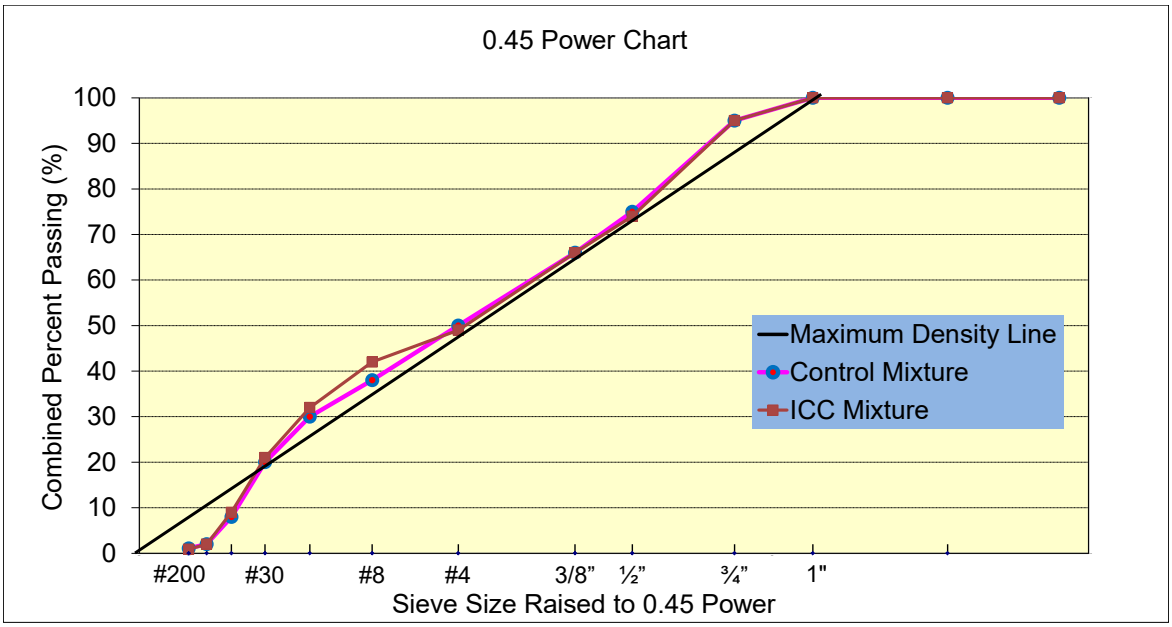

Figure 9: Combined Aggregate Gradation on a 0.45 Power Chart

TIMELINE

The MCL arrived at the contractor's maintenance yard on 4/29 and remained there for the duration of the MCL's visit to this project site. A kick off meeting was held with the KDOT and the contractor staff at the maintenance yard. May 1 was the first day of the project which was paved using the control mixture. The MCL took several samples from the control mixture. The following day, the MCL took several samples from the ICC test section. The test section and the MCL were visited by several folks from KDOT, FHWA, University of Kansas and Kansas State University students on this day. On May 3, the MCL staff performed the MIT Scan 2 and Scan T2 testing and left the project site in the evening.

CONSTRUCTION ACTIVITIES

Figures 10-13 show some of the activities that took place during construction. The paving operation utilized a stringline for controlling the profile. The plant was located 2-3 miles from the paving location. In this project, dowels were placed using baskets and shipping wires for all the baskets were cut prior to the concrete placement. Dowel baskets were preinstalled on the base and concrete was placed using a belt placer. The ICC section was instrumented by the KDOT staff.


Figure 10: Paving Location


Figure 11: Test Cell Instrumentation

Figure 13: Paving Activities

Figure 14: Paving Activities

SAMPLING

All the QA/QC testing and the MCL sampling took place on grade. Figure 14 and 15 show the sampling location. Table 3 shows the various samples that were taken by the MCL staff from the control and the ICC mixtures.

Figure 14: Sampling Location

Figure 15: Sampling Location

Table 3: Text Matrix

	Control Mixture		Internally Cured Concrete Mixture				Control Mixture	
	1-1	**1-2**	**2-1**	**2-2**	**2-3**	**2-4**	**2-5**	**3-1**
Strength Cylinders	X				X			
MOE	X				X			
Microwave WC	X							
SR/RCPT	X			X	X	X	X	x
Calorimeter	X			X	X	X		X
AVA		X	X			X	X	
KDOT AVA			X			X	X	
Super Air Meter (SAM)		X				X	X	
Freeze Thaw						X		
Fresh Properties	X	X		X	X	X	X	
Flexural Strength					X			
CTE	X			X	X	X	X	

In addition to the tests listed in the table above, the following work was performed in the field: 1) Maturity probes were inserted in the pavement for monitoring strength gain 2) MIT Scan T2 targets were placed on the base for measuring pavement thickness and 3) MIT Scan 2 was used to measure the dowel bar alignment at several joints.

SAMPLE CURING and TESTING

Specimens cast from each day of paving were left overnight at the sampling site (after covering them with lids or wet burlap and plastic). The following day, specimens were demolded, and stored in the MCL curing tanks. Depending on testing age requirement, some specimens were tested when the MCL was at the plant site, in transit, and the remaining specimens were tested at the TFHRC (The MCL's station when not on travel).

RESULTS

Fresh Concrete Property Tests

Fresh concrete properties; unit weight (AASHTO T121/ASTM C 138), air content (AASHTO T 152/ASTM C231), slump (AASHTO T119/ASTM C143), and temperature (AASHTO T309/ASTM C1064) were measured for the ten samples and the results are presented in Table 4

Table 4: Fresh Concrete Properties

Serial No.	Sample ID	Date	Time	Slump, inches	Concrete Temp, F	Unit Weight, pcf	Air Content, %
Control	1-1	5/1/14	12:52 p.m.	1.5	63.6	145.7	5.1
Control	1-2	5/1/14	1:51 p.m.	1.75	60	Did not run	5.7
LWA	2-1	5/2/14	-	-	-	-	-
LWA	2-2	5/2/14	8:30 – 9:00	2.25	59.5	133.5	missing
LWA	2-3	5/2/14	9:39 a.m.	2.25	57	136.9	5.8
LWA	2-4	5/2/14	9:45 a.m.	2	58	136.1	6.5
Control	2-5	5/2/14	11:50 a.m.	1.5	61	145	5.3
Specification Requirement				**0-3" max**	**90,F**		**5 to 8%**

The unit weight of fresh concrete is a good indicator of batch-to-batch uniformity and can also be used to check weights and proportioning equipment. A variability of more than 3 pcf is typically considered significant. The green line shown in Figure 16 is the mixture design unit weight. Upper and lower limits shown in Figure 16 are three pcf above and below the average value. The blue data points in Figure 16 represent the control mixture while the pink data points represent the ICC mixture. As expected, unit weight was lower for the ICC mixture compared to the control mixture. The unit weight for the control mixture was higher than the mixture design target. However, the unit weights within a given mixture (control and ICC) were consistent.

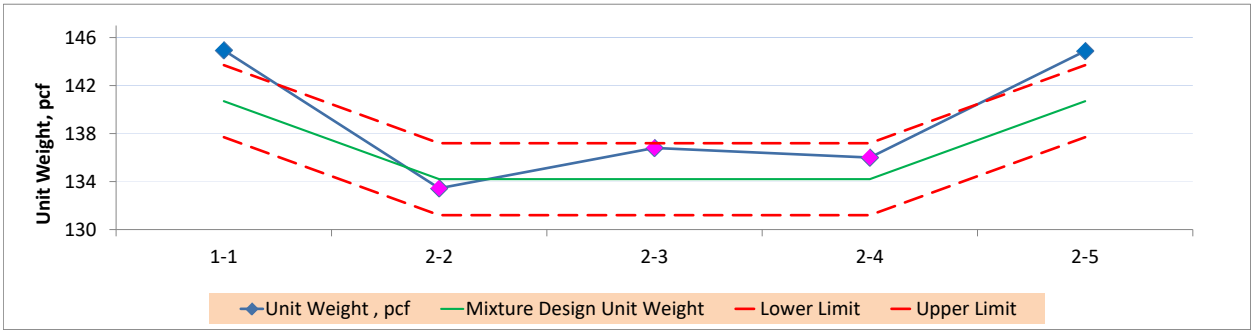

Figure 16: Control Chart – Unit Weight

Figure 17 shows air content results for the control and the ICC mixtures. The upper and lower limits are the specification limits of 5% and 8% respectively. The air content for both the mixtures changed only from 5.1% to 6.3% (blue data markers represent control mixture and pink data markers represent ICC mixture).

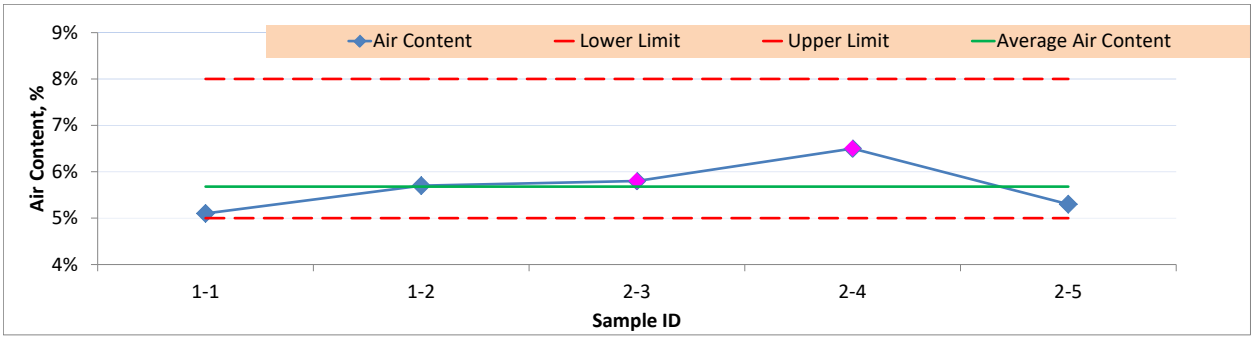

Figure 17: Control Chart - Air Content

Figure 18 shows the control chart for slump for the control and the ICC mixtures. Slump measurements for the ICC mixture were slightly higher than the control mixture (blue data markers).

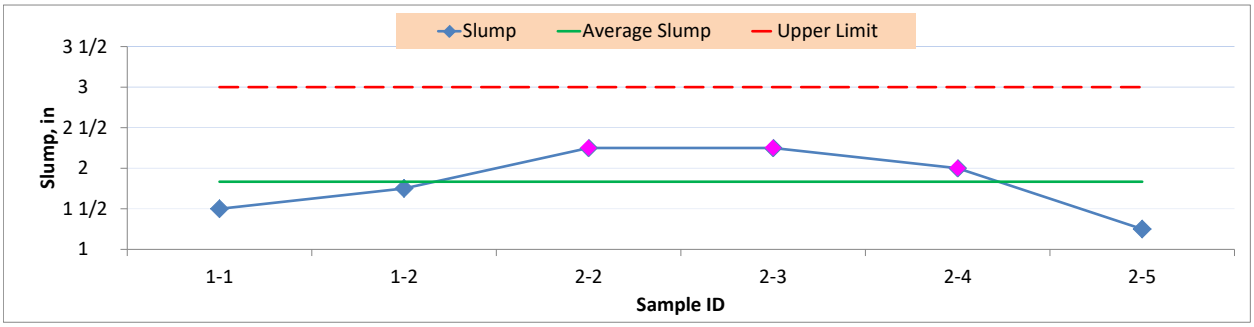

Figure 18: Control Chart – Slump

Figure 19 shows the concrete temperatures for all the samples. The concrete temperature stayed consistent (ranged between 57°F and 63.6°F).

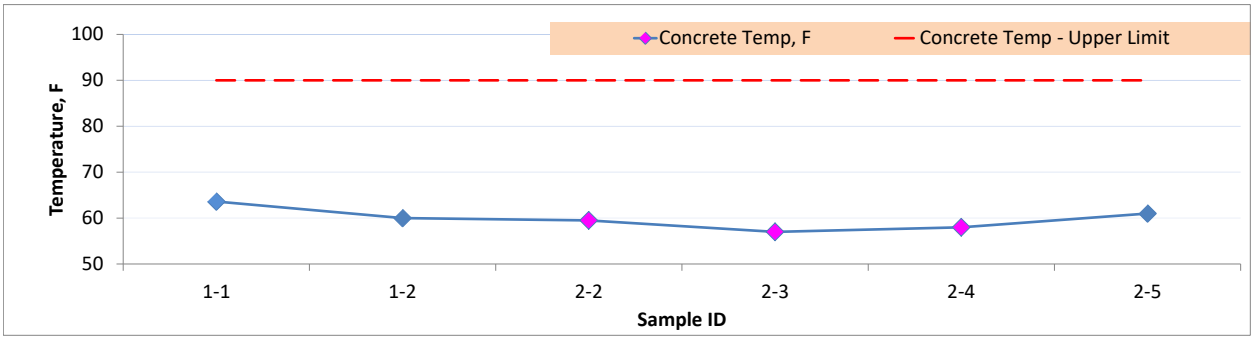

Figure 19: Control Chart – Temperature

Compressive Strengths

Cylinders were cast for compressive strength from the control and the ICC mixture and were tested at 7, 28 and 56 days according to the ASTM C 39. Table 5 and Figure 20 show the average compressive strength results (three cylinders were tested at each age). From the two samples taken by the MCL, the control section had higher compressive strength than ICC mixture at all

ages. Both the mixtures met the 28 day strength requirement in only 7 days. It appears that there is a potential opportunity to optimize the mixture designs by reducing the cement content.

Table 5: Compressive Strength Test Data

	Compressive Strength, psi	
	1-1	2-3
	Control Mixture	ICC Mixture
Cast Date	5/1/2014	5/2/2014
7 Day	4852	4137
28 Day	7317	6051
56 Day	8175	6982

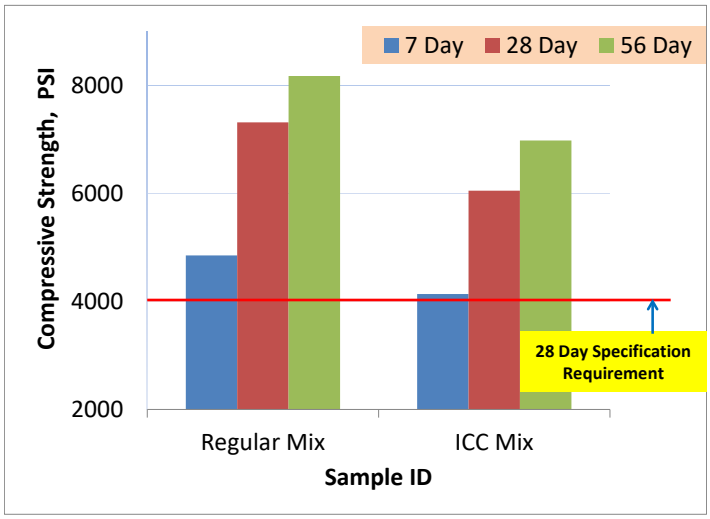

Figure 20: Compressive Strength versus Age

Flexural Strengths

Three standard size beams (6″x6″x21″) and 3 small beams (4″x4″x14) were cast from the ICC mixture sample (2-3) on 5/2/14 and were tested for flexural strength (using third point loading) at 28 days by TFHRC. The average of these results is reported in Table 6. The FHWA TFHRC is currently conducting a study to determine if smaller size beams could be used in lieu of standard size beams for measuring flexural strength in the field. The MCL cast these beams as part of this study.

Table 6: Average Flexural Strength at 28 days for the ICC Mixture

			4″x4″x10″ Beams		6″x6″x21″ Beams	
Mixture	Sample ID	Age, Days	Flexural Strength, psi	Coefficient of Variation, %	Flexural Strength, psi	Coefficient of Variation, %
ICC Mixture	2-3	28	735	4.7	660	2.9

Modulus of Elasticity and Poisson's Ratio

Table 7 shows the modulus of elasticity and poisson's ratio for the control and ICC mixture samples. The MOE and Poisson's ratio values of the control mixture were significantly higher than the ICC mixture. Typically, a lower modulus of elasticity reduces the long term stresses in concrete and results in better performance.

Table 7: Modulus of Elasticity and Poisson's Ratio

		Control Mixture	ICC Mixture
	Sample ID	1-1	2-3
MOE, psi	1	5,149,858	4,124,433
	2	5,237,257	4,092,004
	3	5,120,827	4,068,166
Poisson's Ratio	1	0.26	0.23
	2	0.27	0.23
	3	0.26	0.22

Coefficient of Thermal Expansion

Coefficient of Thermal Expansion (CTE) is a level 1 material input for the AASHTO Pavement ME Design software. The coefficient of thermal expansion is a parameter that quantifies the extent with which a material changes length in response to changes in temperature. The CTE is the length change per unit length per unit temperature – microstrain/^{0}C for example. CTE has a large impact on the performance of concrete pavements because a uniform temperature change will affect the opening/closing of joints and a temperature gradient through the thickness of the slab will produce curling of the slab. Accurate measurements of CTE will allow for better estimates of slab movement and stress development due to temperature changes.

With the recent release of the AASHTO Pavement ME Design pavement design software, there will be a greater emphasis on using CTE of concrete for pavement design since several research studies have shown CTE to have a significant impact on pavement design. The MCL cast 4x8″ cylinders from some control and ICC mixture samples to measure CTE. Table 8 shows the MCL CTE data and the testing age. Based on the data shown in Table 8, it appears that there was statistically no significant difference in CTE between the two mixtures.

Table 8: Coefficient of Thermal Expansion per AASHTO T 336

Sample ID	Mixture	Test Date	Age, Days	T 336 – CTE, Microstrain/^{0}C	T 336 – CTE, Microstrain/^{0}F
KS 1-1	Control	6/12/2014	42	7.2	4.0
KS 2-2	ICC	6/12/2014	41	7.6	4.2
KS 2-3	ICC	6/13/2014	42	7.4	4.1
KS 2-4	ICC	6/13/2014	42	7.5	4.2
KS 2-5	Control	6/15/2014	48	7.5	4.2

Note: A Titanium specimen with a CTE of 4.94 microstrain/ºF was used as the calibration specimen for CTE testing. For use in MEPDG (current versions of the AASHTO Pavement ME Design as of the date of this report), the CTE values shown in Table 8 should be increased by 0.83 microstrain/ºF (for example, 4.2 +0.83=5.03 microstrain/ºF) in order to account for LTTP CTE values used to calibrate the models in the current version of the AASHTO Pavement ME Design software.

Maturity

The maturity method (ASTM C1074: Standard Practice for Estimating Concrete Strength by the Maturity Method) is a technique used to estimate the strength of concrete based upon the temperature-time history recorded by a maturity meter. The method is based on the assumption that samples of a given concrete mixture attain equal strengths if they attain equal values of maturity. The main advantage of maturity testing is the ability to estimate the in-place concrete strength, non-destructively. Both time and cost can be significantly reduced, especially for fast track projects. The ability to open a pavement to construction traffic when acceptable strength is reached: results in shortened project time, decreased cost, and increased safety, without sacrificing long term pavement performance.

KDOT specification for this project requires that the concrete pavement shall not be opened to traffic until the beams cast from the paving mixture reach 450 psi flexural strength or the pavement is at least 4 days old.

MCL staff cast a number of beams from the control mixture on 5/1/14 to develop a maturity curve in the laboratory. Figure 21 shows photos of a maturity data logger that was instrumented in one of the maturity beams and beams being cast for developing the maturity curve. To develop the maturity curve, beams cast from the same batch of concrete were tested for flexural strength at multiple ages and the corresponding maturity number is noted from the beam with the data logger. Figure 22 shows the maturity curve developed for this mixture.

Figure 21 (a): Maturity Logger Figure 21(b): Beams for the Maturity Curve

Based on Figure 22, the maturity number that corresponds to 450 psi flexural strength was 1850 °Chrs. So for the concrete mixture produced on 5/1/14, when the maturity of the paving mixture reaches 1850 °Chrs, for any subsequent concrete placement, its flexural strength is approximately 450 psi (as long as the mixture stays relatively consistent).

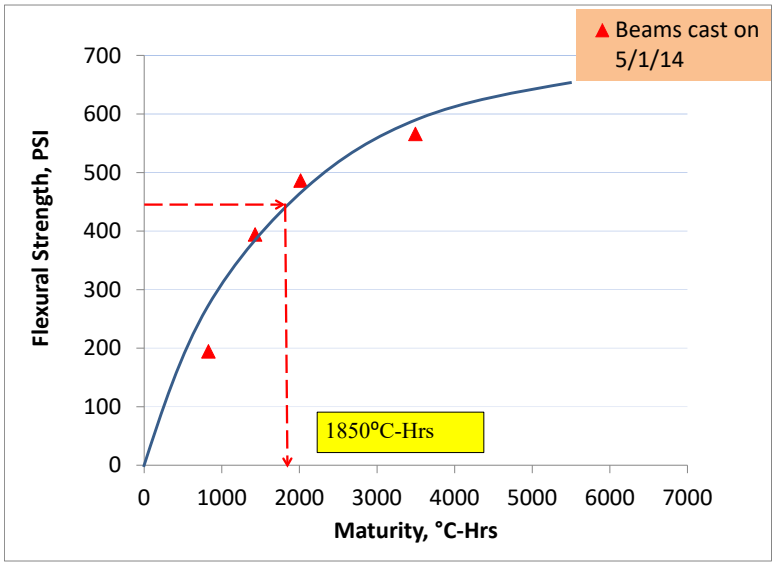

Figure 22: Maturity Curve from cylinders cast on 5/1/14

A data logger was placed in a pavement section on 5/1/14 to measure the maturity of the pavement. Figures 23 and 24 shows the MCL staff in the process of placing a data logger in the pavement and downloading data respectively (photos from a different project).

Figure 23: Maturity meter Instrumented in the Pavement

Figure 24: MCL staff downloading data from maturity sensor

Figure 25 shows the maturity of the pavement from data loggers instrumented in the field on 5/1. From this figure, it can be seen that, for the specific site conditions on 5/1 the pavement reached a 1850 °Chrs maturity value (equivalent to a flexural strength of 450psi) in 56 hours.

So using the concept of maturity, the pavement can be opened to construction traffic 40hrs in advance of the current requirement (4 days minimum and flexural strength of 450 psi from cylinders). This is because the strength gain of the pavement is faster than the cylinders due to the greater mass of concrete (higher heat of hydration) and greater exposure to the environment (The environment could increase or decrease the strength gain compared to lab cured specimens depending on the temperature and moisture conditions). The maturity method measures the actual in place pavement strength development under actual field conditions. Test specimens cured at standard conditions represent the concrete strength under laboratory conditions which are different than what the pavement experiences.

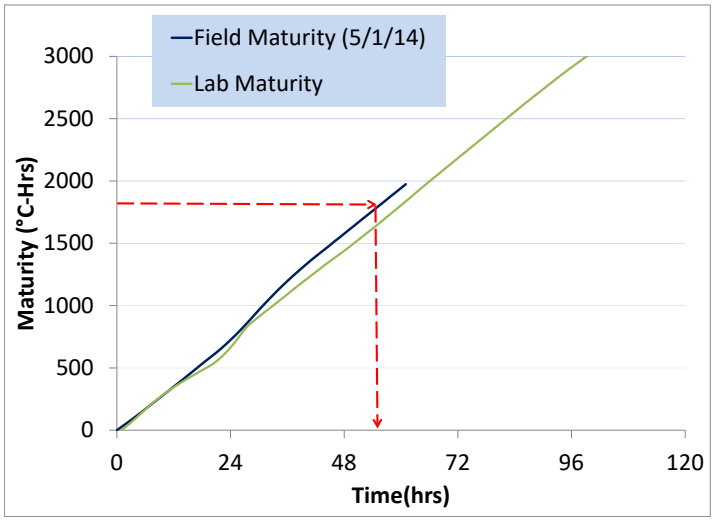

Figure 25: Maturity of the Pavement

So the concept of maturity can be used to open pavements for construction traffic sooner, which in turn can help reduce costs, speed up the construction operations and also helps in safety

related issues. Figures 22 and 25 are shown for illustration purposes. Maturity meters currently available in the market automate the process shown in these figures. They are very easy to use and relatively inexpensive. By using the maturity concept to open pavements to traffic sooner, KDOT and contractor can benefit significantly in terms of time and money savings.

Air Void Analyzer (AVA)

The presence of closely spaced air voids in concrete is recognized as the primary factor in improving the freeze-thaw durability of concrete. Normal tests performed on fresh content provide information on the total air content of the sample, but do not give any indication of the quality of the air void system. Petrographic methods are normally used to determine the spacing and specific surface of hardened samples, but the petrographic analysis process takes many days and therefore is of little value in controlling concrete during construction. The MCL is equipped with an efficient, real-time method of determining the distribution of air voids in fresh concrete. The Air Void Analyzer (AVA) releases air from a fresh concrete sample and measures the quantity of air rising in a water column. From this information, the air void parameters, such as spacing factor (SF) and specific surface (SS), can be calculated. A provisional test method was adopted by AASHTO in 2008 entitled AASHTO TP 75-08 "Air-Void Characteristics of Freshly Mixed Concrete By Buoyancy change". This provisional test method is based on the Air Void Analyzer.

For the purpose of AVA testing in this project, cylinders were cast from the sampled concrete and an AVA sample was taken from each cylinder. Figure 26 shows an AVA sample being taken from a cylindrical mold. Figure 27 shows a picture of the AVA. Overall, four AVA tests were run by the MCL at this project, three from the control mixture and one from the ICC mixture. Due to the relatively short paving window for the ICC section, only one AVA test was performed from the ICC mixture.

Figure 26: AVA sample being taken from a standard beam mold

Figure 27 : The Air Void Analyzer (AVA)

The AVA test results from the four samples are shown in Table 9. According to the Materials and Construction Optimization (MCO) project *(2),* for adequate protection of concrete in freeze-thaw environment, SF values less than 0.01" are desirable, although values smaller than 0.015" are commonly considered as acceptable. Generally, SS greater than 600 in-1 are desirable for adequate freeze-thaw durability. From the data in Table 9, it can be seen that the SFs of all the AVA tests from this project were significantly lower than 0.015 in. The SSs of two of the four AVA tests was higher than 600 in-1. Based on this information, it can be said that the air void distribution for the concrete sampled at the plant is fair based on AASHTO TP 75-08 criteria.

Table 9: Spacing Factor and Specific Surface Results

Date	Sample ID	Spacing Factor, in	Specific Surface, 1/in
5/1/14	001	.005	1103
5/2/14	002 ICC	.010	448
5/2/14	003	.011	785
5/2/14	004	.011	530
Recommended Limits		**<.015**	**>600**

Comparison with Kansas DOT AVA

The KDOT materials division staff also used their AVA on this project. On three of the four samples tested by the MCL, the KDOT staff also took a companion AVA sample. In other words, two 6"x12" cylinders were cast from each sample and the MCL and the KDOT staff took their AVA samples from the respective 6"x12" cylinders. Table 10 shows the MCL and KDOT AVA data for the same samples. Overall, it appears that the MCL AVA numbers (both Specific Surface and Spacing Factor) indicate slightly better freeze thaw resistance than KDOT AVA numbers for the same samples.

Table 10: Comparison between the MCL and KDOT AVA results

		Specific Surface, 1/in		**Spacing Factor, in**	
Mixture	Sample ID	MCL	KDOT	MCL	KDOT
ICC	002 LWA	448	399	0.010	0.013
Control	003	785	599	0.011	0.011
Control	004	530	399	0.011	0.015

SUPER AIR METER (SAM)

The Super Air Meter or SAM is a modified ASTM C231 Type B Pressure Meter. The meter can function in two ways. First, it provides all the same information as a Type B meter, under the same analytical conditions as a conventional pressure meter. After completing the conventional testing the meter is then able to move into a second mode of operation that places the concrete under a series of higher pressures. By understanding how the concrete responds to the series of high pressures, the meter can assess properties of the air-void system beyond the air content. The result is a measurement that has been shown to correlate well with the spacing factor

measurement from ASTM C457 and freeze-thaw performance data such as ASTM C666. Figure 28 shows a photo of the SAM. The current version of the meter uses a digital pressure gage and a restraint cage.

To run the test concrete is placed and consolidated similar to running a typical ASTM C231 test. However with this test, **the test is run multiple times without releasing the pressure in the bottom bowl**. The test takes just over 10 minutes to run and provides immediate information about the air void quality in the fresh concrete. This is especially useful to evaluate a concrete mixture before and after a paver, or a pump and for investigation of concrete mixtures with a number of admixtures.

Figure 28: The SAM meter

The SAM number is a value calculated from the pressure curves produced in the test based on a spacing factor of 0.008". The FHWA is currently evaluating the SAM by using it in several field projects across the country.

In this project, SAM tests were conducted on two control samples (currently SAM tests are not performed on ICC mixtures). These results are presented in Table 11 and Figure 28. According to the current criteria, "SAM Number" smaller than 0.20 is considered to have a good Air Void System. Based on the results shown in Table 11 both the control samples have low SAM number. However, the SAM number for one of the samples was slightly higher than the 0.2 criteria and so is classified as not having a Good air void system and the other sample is classified as having a Good air void system due to the smaller SAM number (0.13). It should be mentioned that the SAM classification of "Good" and "Not Good" air void system is based on SF of 0.008" and not 0.015"

Table 11: The SAM Test Results

		Control Mixture			Control Mixture	
		Sample 1-2			Sample 2-5	
		1:51 p.m.			11:50 a.m.	
		Step I	Step II		Step I	Step II
Air Pot Pressure Level,	**14.5**	7.17	7.27		7.75	7.83
	30	18.26	18.44		19.36	19.54
	45	31.07	31.29		32.6	32.73
ASTM C 457 air content			5.24			4.47
Improved air content (%)			5.72			4.86
SAM Number			0.22			0.13
Classification of Air Void System		**Not A Good Air Void System**			**GOOD Air Void System**	

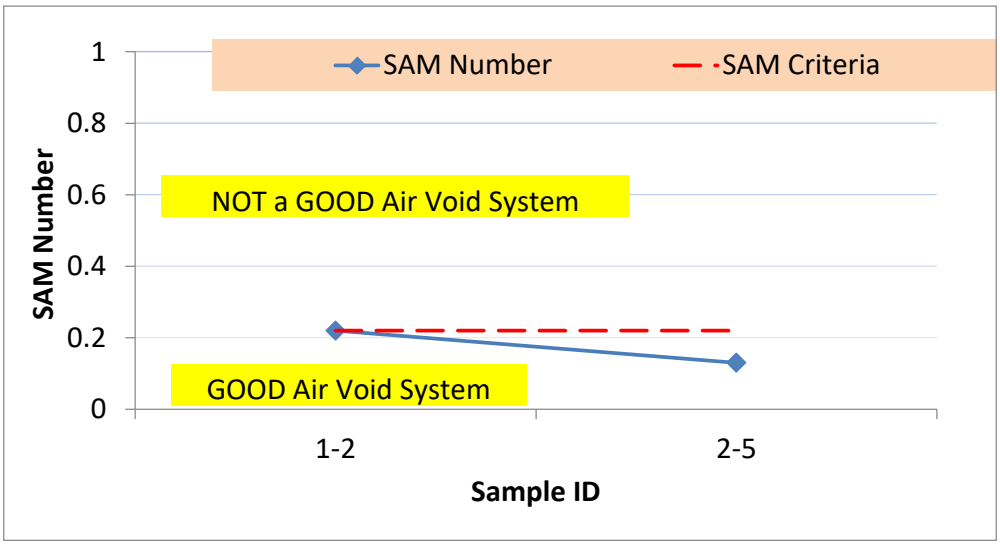

Figure 29: SAM Results

The SAM is a state of the art technology for measuring the air void system of fresh concrete. As mentioned previously, the MCL is currently evaluating the SAM by using it in several field projects and correlating SAM data with Freeze-Thaw and Hardened Air Content Test (ASTM C 457) tests. The SAM has the potential to revolutionize the way air is tested in concrete. Some of the advantages of SAM are its ease of use, economical, rapid results, and field implementable.

Permeability

Surface Resistivity Meter (SR Meter)

Checking concrete for its permeability is a very important agency activity both during mixture design phase as well as during construction of highways and bridges. The Surface Resistivity Test can be used to evaluate the electrical resistivity of water-saturated concrete to provide a rapid indication of the concrete's resistance to chloride ion penetration. Measurements from this test have shown good correlations with other electrical indication tests, such as the Rapid Chloride Permeability Test (RCPT) (AASHTO T 277 /ASTM C 1202). This technology has the potential to save significant costs associated with testing time for both agencies as well as contractors. The primary advantage of this test is that it is rapid (less than five minutes) and does not require any sample preparation unlike the RCPT test method. Figures 30 and 31 show pictures of the RCPT and SR meter respectively.

Table 12 shows the chloride ion penetration classification based on the readings from the RCPT and SR meter tests *(2)*. The MCL cast one 4"x8" specimen from some samples for SR meter testing. Since this is a relatively new test method, the intent of the MCL was to observe the change in SR meter readings between samples at the same age (to observe consistency between samples) and show the correlation between SR meter and RCPT readings on the same set of specimens.

Table 12: Chloride Ion Penetration Classification

Chloride Ion Penetration	AASHTO T277	Surface Resistivity Test
	RCP Test Charges Passed (Columbs)	4 in. X 8 in. Cylinder (KOhm-cm)
High	> 4,000	< 12
Moderate	2000-4000	12 - 21
Low	1000-2000	21 - 37
Very Low	100-1000	37 - 254
Negligible	<100	> 254

Figure 30: Rapid Chloride Permeability Test

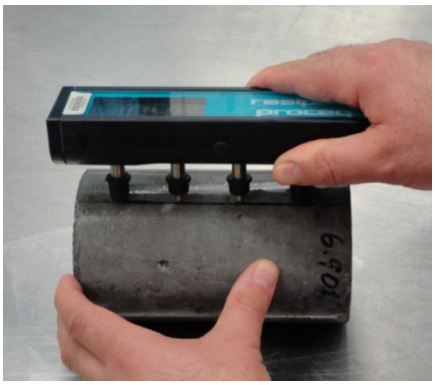

Figure 31: Surface Resisitivity Meter in Operation

SR Meter Readings between Samples

Figure 32 shows SR meter readings for all the samples at 7, 28, and 56 days respectively. Figure 32 shows that all the samples had a high level of permeability (based on SR meter classification) at 7 days, and at 28 days. However, all of them fell in the moderate permeability category at 56 days. Interestingly there was not a significant difference in SR meter readings between the Control and ICC mixtures.

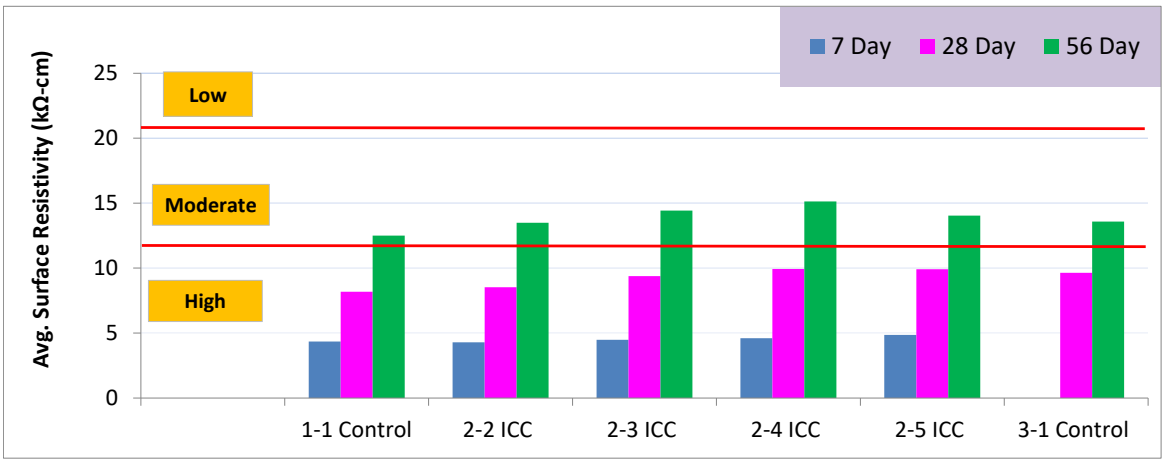

Figure 32: 7, 28 and 56 Day Test Results for SR Meter

SR Meter versus RCPT Readings

In order to show the correlation between RCPT and SR, specimens shown in Figure 32 were also tested for RCPT. These specimens were tested for SR immediately prior to RCPT testing. After the SR meter testing, 2″ slices were obtained from each 4x8″ cylinder and was tested for RCPT. All these test results are presented in Table 13. It can be seen from Table 13 that both the RCPT and SR tests classify the concrete in the same permeability category.

Table 13: RCPT and SR Meter Results at 56 Days

ID	Date	Age, Days	Adjusted charge passed	Permeability class	Surface Resistivity	SR Meter Classification
1-1	5/1/2014	60	2582	Moderate	13.0	Moderate
2-2	5/2/2014	59	3330	Moderate	13.7	Moderate
2-3	5/2/2014	59	2344	Moderate	15.3	Moderate
2-4	5/2/2014	59	2130	Moderate	16.0	Moderate
2-5	5/2/2014	59	2139	Moderate	14.7	Moderate
3-1	5/3/2014	58	2256	Moderate	14.6	Moderate

Based on several published research studies *(2, 3, 4),* the SR meter results correlate extremely well with RCPT results. However, the major advantage of the SR meter is it takes less than 5 minutes to take readings. RCPT test (including the sample preparation) takes more than 2 days to perform. States such as Florida and Louisiana *(3)* have already realized the significant cost savings associated with the SR meter test and have started implementing it in their specifications. AASHTO recently published a provisional test method for this test: Surface Resistivity Indication of Concrete's Ability to Resist Chloride Ions Penetration (AASHTO TP 95).

MIT SCAN 2

MIT Scan-2 is a state-of-the-art, nondestructive testing device for measuring the position of dowel bars embedded in concrete. The operating principle behind the device is pulse-induction. The equipment emits a weak, pulsating magnetic signal and detects the transient magnetic response signal induced in metal bars. The response signals are measured with high precision using special receivers in the testing device. The detected signals are recorded at a relatively high sampling rate to assure large quantities of data for mathematical evaluation. The basis of the solution technique employed in the MIT Scan-2 is magnetic tomography. In magnetic tomography the response of the dowel bars to external magnetic fields is measured in both space and time. The signals contain information on the distribution of electrical conductivity and magnetic properties, which permit the determination of horizontal misalignment, vertical misalignment, side shift and depth of the dowel bar from the top of the pavement. Figure 33 show the various dowel bar positions that can be measured by MIT Scan 2 device.

In the US 54 project, dowels were placed using dowel baskets and the shipping wires of the baskets were cut prior to concrete placement. The MCL staff scanned 13 consecutive joints over two lanes (Lane 1 and Lane 2) at the US 54 project, in order to demonstrate the MIT Scan 2. Lane 1 was 15′ with 15 dowels and Lane 2 was 12′ with 12 dowels. Figure 34 shows dowel bars

placed in baskets in front of the paver and Figure 35 shows Warren Ebberts with Kansas DOT observing the scanning operation as a joint was being scanned.

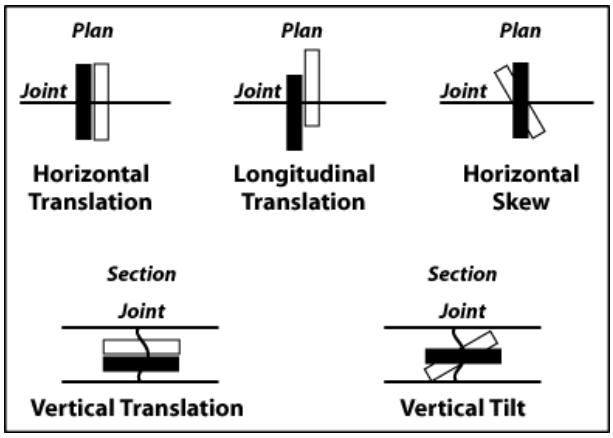

Figure 33: Various Misalignments that can be measured using the MIT Scan 2.

Figure 34: Dowels placed using Dowel Baskets

Figure 35: MIT Scan 2 in Operation

The numerical values of horizontal and vertical misalignment, sideshift and depth of the dowels bars are presented in Tables 14-17. Figure 36 to 39 show the graphical output (magnetic signal intensity plots) of the MIT Scan 2 of four random joints. The signal intensity plots for the remaining joints also showed similar alignment of dowel bars. The horizontal red images in each figure represent a dowel bar. In some of the figures, there is an overlap of the individual dowel bar images. This is due to the influence of additional metal from the tie bars that are close to these dowels. Due to this reason, data generated for dowels 14 through 17 at each joint (two dowel on either side of the tie bars) was excluded (shaded cells in Tables 14-17).

From Tables 14-17 and Figures 36-39, it can be seen that there was very little horizontal and vertical misalignment. Except for Joint 4 in Table 16, there was very little sideshift at all the joints scanned. The average depth of dowel bars at each position ranged from 5.6 to 7.0 inches. Overall, the MIT Scan 2 testing showed that all the dowels are well alignment without any major issues.

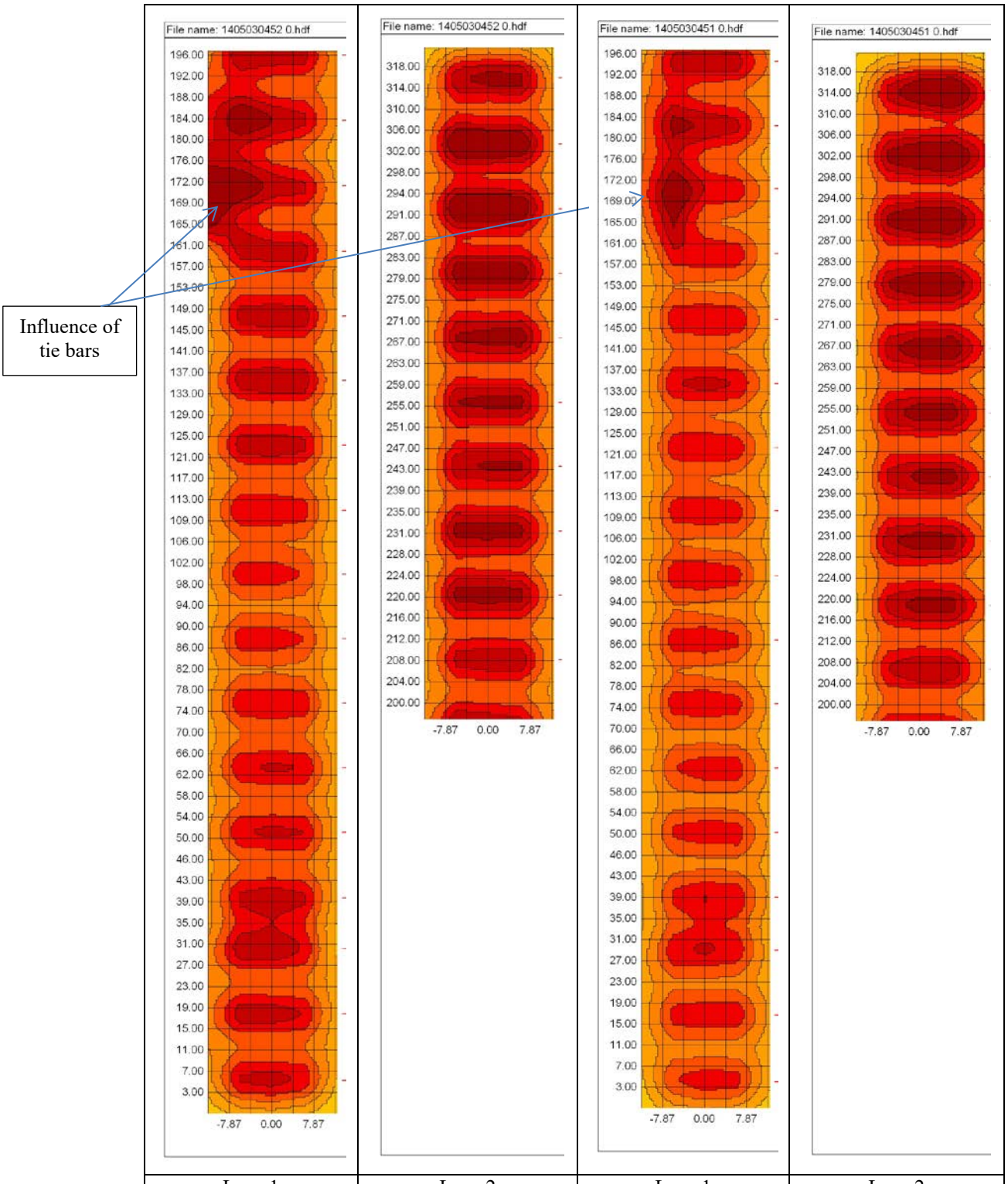

Lane 1	Lane 2	Lane 1	Lane 2

Figure 36: Magnetic Signal Intensity Plot for a Random Joint 1

Figure 37: Magnetic Signal Intensity Plot for a Random Joint 2

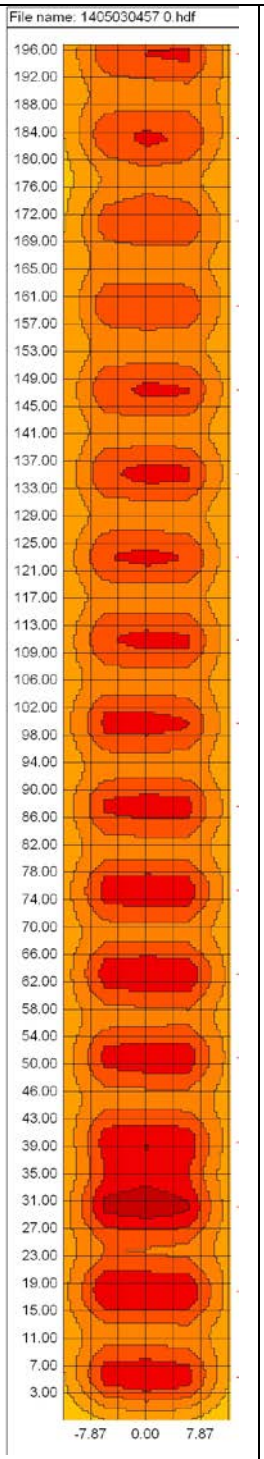

Lane 1

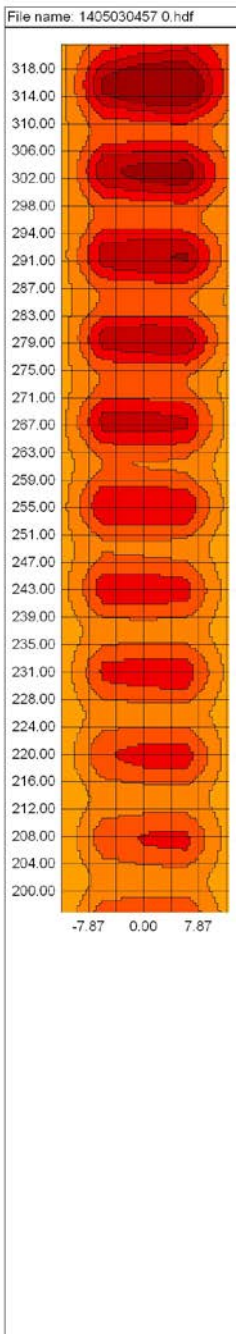

Lane 2

Figure 38: Magnetic Signal Intensity Plot for a Random Joint 3

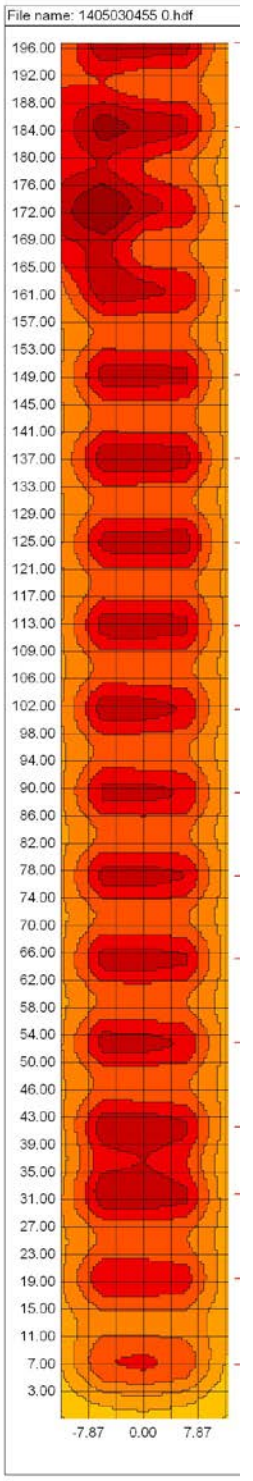

Lane 1

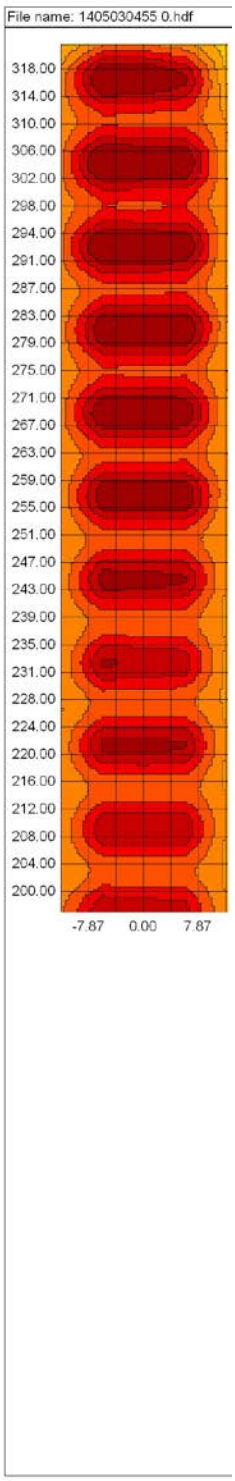

Lane 2

Figure 40: Magnetic Signal Intensity Plot for a Random Joint 4

Table 14: Horizontal Misalignment of Dowel Bars

Horizontal Misalignment, in																											
Jt.	**1**	**2**	**3**	**4**	**5**	**6**	**7**	**8**	**9**	**10**	**11**	**12**	**13**	**14**	**15**	**16**	**17**	**18**	**19**	**20**	**21**	**22**	**23**	**24**	**25**	**26**	**27**
1	0.4	0.9	0.4	0.4	0.3	0.2	0.2	0.1	0.1	0.2	0.1	0.0	0.7	##	1.1	-3.8	-0.6	0.2	0.3	0.3	0.2	0.1	0.2	0.2	0.1	0.2	0.0
2	0.8	0.4	-0.1	0.5	-0.1	-0.1	0.0	-0.2	-0.1	-0.1	-0.1	0.0	0.0	1.0	2.9	-1.7	-0.7	-0.1	0.0	0.0	0.0	-0.2	-0.2	-0.2	-0.2	-0.1	0.0
3	0.2	0.0	-0.1	0.5	0.4	0.4	0.5	0.4	0.3	0.4	0.4	0.4	0.9	##	-0.1	-3.8	-0.8	0.0	0.0	-0.2	-0.1	-0.2	-0.1	-0.2	-0.2	-0.1	0.1
4	1.0	-0.2	-1.0	1.0	0.2	-0.1	0.0	-0.2	0.0	0.0	0.0	0.0	0.8	##	-0.7	-2.2	-1.5	0.0	0.0	-0.1	-0.1	-0.2	0.0	-0.1	0.1	0.0	-0.3
5	-0.3	-0.4	-0.5	-0.1	0.0	-0.1	-0.1	-0.3	-0.3	-0.3	-0.1	0.0	-0.1	0.0	0.1	0.5	0.2	0.1	0.1	0.0	0.1	0.1	0.0	0.1	-0.1	0.1	0.3
6	1.1	0.6	0.2	0.5	0.3	0.1	0.2	0.0	0.0	-0.1	0.1	0.1	0.2	0.9	0.7	0.3	0.0	0.1	0.1	-0.1	-0.1	0.0	0.1	-0.1	0.0	0.0	0.3
7	0.2	0.0	-0.2	0.5	0.4	0.4	0.4	0.3	0.2	0.4	0.4	0.2	0.5	3.6	0.1	0.1	-0.1	0.2	0.2	0.1	0.1	0.0	0.1	0.1	0.2	0.1	-0.1
8	-0.3	0.0	0.3	0.2	0.3	0.3	0.2	0.1	0.1	0.3	0.3	0.3	0.4	1.6	-0.4	0.0	0.2	0.3	0.2	0.2	0.2	0.1	0.0	0.0	0.1	0.1	-0.1
9	1.0	1.1	1.3	0.1	0.1	0.0	-0.1	-0.1	-0.1	-0.1	-0.2	0.0	0.1	0.3	0.6	0.4	0.5	0.6	0.5	0.4	0.5	0.6	0.5	0.4	0.5	0.5	0.3
10	0.0	0.2	0.5	0.2	0.3	0.2	0.1	0.2	0.0	0.1	0.1	0.0	0.3	1.8	0.4	-0.3	-0.1	0.0	0.0	-0.1	-0.1	0.0	-0.1	-0.2	-0.1	0.0	0.2
11	0.1	0.3	0.3	0.4	0.3	0.2	0.2	0.1	0.1	0.2	0.2	0.1	0.1	0.2	0.2	0.6	0.4	0.2	0.1	0.1	0.1	0.1	0.2	0.0	0.1	0.1	-0.2
12	0.3	0.4	0.3	0.5	0.2	0.4	0.2	0.2	0.3	0.3	0.3	0.2	0.3	0.3	0.2	0.5	0.5	0.4	0.4	0.3	0.4	0.4	0.4	0.4	0.5	0.6	0.0
13	0.0	0.4	0.8	0.0	0.1	0.0	0.1	-0.2	-0.2	-0.2	-0.2	-0.1	-0.2	0.3	-1.0	-0.3	0.1	0.1	0.0	-0.1	0.0	-0.1	0.0	-0.2	-0.2	-0.3	-1.3

Table 15: Vertical Misalignment of Dowel Bars

Vertical Misalignment, in																											
Jt.	**1**	**2**	**3**	**4**	**5**	**6**	**7**	**8**	**9**	**10**	**11**	**12**	**13**	**14**	**15**	**16**	**17**	**18**	**19**	**20**	**21**	**22**	**23**	**24**	**25**	**26**	**27**
1	0.1	0.0	0.0	0.0	0.0	0.0	0.0	0.0	0.0	0.0	0.0	0.0	0.0	##	0.2	0.0	-0.1	0.0	0.0	0.0	0.0	0.0	0.0	0.0	0.0	0.0	0.0
2	0.0	0.0	0.0	0.0	0.0	0.0	0.0	0.0	0.0	0.0	0.0	0.0	0.0	0.0	0.0	0.0	-0.1	0.0	0.0	0.0	0.0	0.0	0.0	0.1	0.1	0.0	0.0
3	0.1	0.0	0.0	0.0	0.0	0.0	0.0	0.0	0.0	0.0	0.0	0.0	0.0	##	0.2	0.0	0.0	0.0	0.0	0.0	0.0	0.0	0.0	0.0	0.1	0.0	0.0
4	0.1	0.1	0.0	0.0	0.1	0.1	0.1	0.1	0.1	0.1	0.1	0.1	0.1	##	0.2	0.1	0.1	0.1	0.1	0.1	0.1	0.1	0.0	0.0	0.1	0.1	0.1
5	0.0	0.0	0.0	0.0	0.0	0.0	0.0	0.0	0.0	0.0	0.0	0.0	0.0	0.0	0.0	0.0	0.0	0.0	0.0	0.0	0.0	0.0	0.0	0.0	0.0	0.0	0.0
6	0.0	0.0	0.0	0.0	0.0	0.1	0.1	0.1	0.0	0.1	0.0	0.0	0.0	0.0	0.0	0.0	0.0	0.0	0.1	0.1	0.0	0.0	0.0	0.0	0.0	0.0	0.0
7	0.0	0.0	0.0	0.0	0.0	0.0	0.0	0.1	0.1	0.1	0.1	0.1	0.0	0.1	0.1	0.1	0.1	0.1	0.1	0.1	0.0	0.1	0.0	0.0	0.0	0.0	0.0
8	0.0	0.0	0.0	0.0	0.0	0.0	0.0	0.0	0.0	0.0	0.0	0.0	0.0	-0.1	0.0	0.0	0.0	0.0	0.0	0.0	0.0	0.0	0.0	0.0	0.0	0.0	0.0
9	0.0	0.0	0.0	0.0	0.0	0.0	0.0	0.0	0.0	0.0	0.0	0.0	0.0	0.0	-0.1	-0.1	0.0	0.0	0.0	0.0	0.1	0.1	0.0	0.1	0.0	0.0	0.1
10	0.0	0.0	0.0	0.0	0.0	0.0	0.0	0.0	0.0	0.0	0.0	0.0	0.0	0.0	0.1	0.0	0.0	0.0	0.0	0.0	0.0	0.0	0.0	0.0	0.0	0.0	0.0
11	0.0	0.0	0.0	0.0	0.0	0.0	0.0	0.0	0.0	0.0	0.0	0.0	0.0	0.1	0.0	0.0	0.0	0.0	0.0	0.0	0.0	0.0	0.0	0.0	0.0	0.0	0.0
12	0.0	0.0	0.0	0.0	0.0	0.0	0.0	0.0	0.0	0.0	0.0	0.0	0.0	0.0	0.0	0.0	0.0	0.0	0.0	0.0	0.0	0.0	0.0	0.0	0.0	0.0	0.0
13	0.0	0.0	0.0	0.0	0.0	0.0	0.0	0.0	0.0	0.0	0.0	0.0	0.0	-0.1	-0.2	-0.1	-0.1	0.0	0.0	0.0	0.0	0.0	0.0	0.0	0.0	0.0	0.1

Table 16: Side Shift of Dowel Bars

	Side Shift, in																									
Jt.	**1**	**2**	**3**	**4**	**5**	**6**	**7**	**8**	**9**	**10**	**11**	**12**	**13**	**14**	**15**	**16**	**17**	**18**	**19**	**20**	**21**	**22**	**23**	**24**	**25**	**26**	**27**
1	0.2	-0.1	0.0	0.5	0.0	0.3	0.2	0.5	0.5	0.8	0.9	0.8	0.5	##	0.0	-1.2	-1.5	0.3	0.4	0.5	0.5	0.7	0.7	0.7	0.6	0.7	0.4
2	1.3	1.2	1.0	1.3	0.9	1.0	0.8	0.8	0.7	0.9	0.8	0.8	0.7	-0.7	-1.7	-1.7	-1.2	0.4	0.3	0.3	0.4	0.3	0.3	0.4	0.2	0.1	-0.3
3	0.7	0.2	-0.2	0.5	0.1	0.4	0.3	0.4	0.4	0.7	0.8	0.8	0.8	##	-0.3	-0.9	0.0	1.1	0.9	0.8	0.8	0.6	0.5	0.3	0.2	0.1	-0.2
4	2.7	2.3	2.1	2.4	2.2	2.2	2.1	2.0	1.6	1.9	1.8	1.9	1.5	##	-0.5	0.7	1.8	2.1	2.0	1.9	1.8	1.8	1.4	1.4	1.4	1.3	1.6
5	0.6	0.2	-0.2	0.8	0.2	0.2	0.0	-0.2	-0.1	-0.2	-0.2	-0.1	0.0	0.1	0.0	0.8	0.2	0.2	0.0	0.0	-0.2	0.0	0.0	0.0	-0.1	0.0	-0.3
6	0.6	0.7	0.7	0.8	0.5	0.7	0.6	0.5	0.5	0.3	0.2	0.0	-0.1	-0.4	-0.7	-0.7	-0.3	0.3	0.3	0.3	0.1	0.2	0.1	0.0	-0.2	-0.1	-0.3
7	0.4	0.3	0.0	0.9	0.5	0.7	0.7	0.8	0.9	0.9	0.9	1.1	1.1	0.6	0.0	1.0	1.6	1.7	1.9	1.6	1.9	1.8	1.9	1.7	1.7	1.8	1.6
8	-0.4	-0.8	-1.1	-0.3	-0.4	-0.3	-0.3	-0.2	-0.3	-0.3	-0.3	-0.1	0.0	-1.1	-1.8	-0.9	0.0	0.1	0.5	0.5	0.6	0.5	0.5	0.5	0.4	0.6	0.3
9	-0.3	-0.2	-0.1	-0.3	-0.4	-0.5	-0.4	-0.3	-0.4	-0.4	-0.6	-0.6	-0.8	-1.1	-2.2	-1.9	-0.7	0.0	0.2	0.1	0.4	0.2	0.5	0.7	0.8	0.9	1.1
10	-0.1	-0.3	-0.3	0.0	-0.2	-0.2	-0.2	-0.2	-0.1	-0.2	-0.3	-0.3	-0.3	-0.6	-0.8	-1.4	-0.8	-0.2	-0.2	0.0	-0.1	-0.1	-0.3	-0.3	-0.4	-0.3	-0.6
11	0.0	-0.1	-0.1	0.0	0.1	0.0	0.2	0.1	0.2	0.2	0.3	0.4	0.3	0.3	0.3	0.6	0.5	0.4	0.5	0.5	0.4	0.4	0.4	0.4	0.4	0.5	0.4
12	0.1	0.0	0.0	0.2	0.1	0.1	0.1	0.1	0.0	0.1	0.1	0.2	0.4	0.7	1.0	0.8	0.3	0.1	0.1	0.2	0.2	0.1	0.2	0.5	0.7	1.1	1.7
13	-0.6	-0.5	-0.4	-0.3	-0.4	-0.5	-0.4	-0.5	-0.3	-0.5	-0.5	-0.8	-0.9	-1.8	-3.5	-1.9	-0.9	-0.8	-0.8	-0.9	-1.0	-0.9	-1.1	-1.0	-1.2	-1.3	2.1

Table 17: Depth (Vertical Translation) of Dowel Bars

	Depth, in																									
Jt.	**1**	**2**	**3**	**4**	**5**	**6**	**7**	**8**	**9**	**10**	**11**	**12**	**13**	**14**	**15**	**16**	**17**	**18**	**19**	**20**	**21**	**22**	**23**	**24**	**25**	**26**	**27**
1	8.0	7.8	7.7	7.7	7.6	7.5	7.4	7.4	7.4	7.3	7.1	7.0	7.0	7.1	7.0	6.8	7.0	6.7	6.5	6.4	6.5	6.3	6.0	5.9	5.8	5.6	5.3
2	7.9	7.8	7.6	7.7	7.6	7.5	7.4	7.5	7.5	7.3	7.3	7.1	7.0	7.0	6.8	6.8	6.8	6.6	6.5	6.3	6.0	5.8	5.8	5.9	5.8	5.8	5.8
3	8.2	7.9	7.6	7.7	7.7	7.6	7.5	7.4	7.3	7.2	7.0	6.9	6.8	6.7	6.4	6.4	6.4	6.1	6.0	5.9	5.8	5.6	5.5	5.5	5.4	5.4	5.5
4	8.1	7.8	7.6	7.8	7.8	7.6	7.5	7.5	7.6	7.4	7.2	7.0	6.9	6.6	6.3	6.4	6.4	6.1	5.9	5.9	5.9	5.8	5.9	5.8	5.7	5.7	5.5
5	7.8	7.7	7.5	7.7	7.6	7.5	7.4	7.3	7.3	7.1	7.0	6.8	6.7	6.8	6.6	6.4	6.3	6.1	5.9	5.8	5.8	5.9	5.8	5.7	5.7	5.6	5.5
6	6.8	6.8	6.7	6.9	6.8	6.6	6.6	6.6	6.7	6.6	6.6	6.5	6.5	6.6	6.7	6.4	6.2	5.8	5.6	5.6	6.0	5.7	5.7	5.6	5.7	5.7	5.8
7	6.4	6.5	6.4	6.4	6.5	6.5	6.5	6.5	6.4	6.5	6.4	6.2	6.4	6.4	6.4	6.1	6.1	6.0	5.9	5.8	5.9	5.8	5.7	5.7	5.6	5.6	5.5
8	6.2	6.3	6.3	6.3	6.4	6.4	6.5	6.7	6.7	6.5	6.2	6.2	6.2	6.3	6.3	6.1	6.3	6.2	6.0	5.9	6.1	6.0	6.0	5.8	5.7	5.7	5.9
9	6.7	6.5	6.4	6.5	6.5	6.5	6.6	6.6	6.4	6.3	6.3	6.2	6.4	6.4	6.4	6.5	6.4	6.2	6.0	5.9	5.8	5.8	5.8	5.9	5.7	5.8	5.8
10	6.6	6.5	6.2	6.2	6.3	6.2	6.3	6.3	6.3	6.2	6.2	6.2	6.3	6.3	6.3	6.2	6.2	6.1	5.9	6.1	5.9	5.7	5.7	5.7	5.6	5.6	5.6
11	6.6	6.4	6.2	6.3	6.3	6.2	6.2	6.2	6.2	6.1	6.1	6.2	6.5	6.8	6.6	6.6	6.6	6.5	6.3	6.2	6.1	6.0	5.9	5.9	5.8	5.9	5.7
12	6.2	6.2	6.1	6.3	6.3	6.2	6.3	6.4	6.5	6.5	6.5	6.5	6.5	6.7	6.6	6.5	6.6	6.6	6.4	6.3	6.3	6.2	6.0	5.9	5.8	5.7	5.4
13	6.2	6.3	6.2	6.2	6.3	6.3	6.3	6.4	6.5	6.5	6.5	6.5	6.6	6.6	6.7	6.6	6.6	6.6	6.5	6.4	6.4	6.3	6.2	6.1	6.0	5.9	5.2

MIT Scan 2 is a very effective tool specifically designed to non-destructively identify the presence and alignment of dowel bars at a joint. The advantage with MIT Scan 2 is it can be used as soon as the pavement can be walked upon to check the presence and alignment of dowel bars and allows the contractor to take corrective action immediately. Coring is not typically resorted to unless dowel bar placement issues are suspected. Even in those cases, coring is not a good method to check the presence and alignment of dowel bars, since coring can be performed at only a limited number of joints. In addition, multiple cores have to be taken at each joint since taking one or two cores will not reveal the overall picture of dowel bar alignment at a joint. The major benefit of MIT Scan 2 is that it is nondestructive, results can be seen in a graphical display or a tabular format immediately in the field for quality control and it is not too complicated to operate.

MIT Scan T2

MIT Scan T2 (T2) is a nondestructive testing device for measuring pavement thickness. The operating principle behind the device is pulse-induction. A metal target must be pre-placed on the top of the base. The equipment emits a weak, pulsating magnetic signal. The T2 device detects the plate and pulse induction is utilized to determine the thickness of the concrete pavement.

At the ICC section, prior to the concrete placement, the MCL staff placed eight T2 targets on the base. To prevent the targets from being displaced during the paving process, they were nailed down to the base. The approximate locations of the targets were marked. After the pavement was constructed, the MCL staff in the presence of the KDOT staff identified the exact locations of the targets and pavement thicknesses were measured using the T2. Figure 40 shows one of the T2 targets on the base at the ICC section. Figure 41 shows KDOT staff using T2 to measure pavement thickness. Table 18 shows the pavement thickness measurements data using the T2.

Figure 40: Metal Target placed on top of the base

Figure 41: KDOT staff measuring Pavement Thickness using the MIT Scan T2

Overall, all the eight measurements made using the T2 were higher than the design thickness of 9". The average of the eight measurements was 9.5".

Table 18: Pavement Depth Measurements using MIT Scan T2 and Core Measurements

S. No	Paving Day	Location Number	Target at Slab (12' or 15')	Scan T2 Measurements, Inches	Scan T2 Thickness, inches
1	5/2/2014	1	12	246	9.7
2	5/2/2014	2	15	237	9.3
3	5/2/2014	3	12	245	9.6
4	5/2/2014	4	15	236	9.3
5	5/2/2014	5	12	250	9.8
6	5/2/2014	6	15	231	9.1
7	5/2/2014	7	12	248	9.8
8	5/2/2014	8	15	230	9.1
				Average, in	**9.5**
				Design Thickness, in	**9**
				Minimum Thickness, in	**9.1**

Even though cores were not taken to verify the Scan T2 measurements in Table 18, there is published research which shows that the MIT Scan T2 works well and is accurate over a wide range of concrete pavement thicknesses and base conditions (*6*) and can be used in lieu of taking cores for measuring pavement thickness. MIT Scan T2 offers several benefits such as cost savings (in general, it is at least four times cheaper than taking cores in the long run), faster measurements (can take measurements as soon as the pavement can be walked upon), larger number of locations (more robust statistical analysis) and finally, it eliminates the need to cut cores on new pavements and thereby reducing the need to patch the core holes. Iowa DOT has realized the benefit of using the T2 and has started using it as part of their specifications (http://www.iowadot.gov/specifications/dev_specs/DS-09063.pdf).

Heat Signature (Calorimeter)

The hydration of cementitious materials results in a number of exothermic chemical reactions. These reactions can be monitored by measuring the total heat liberated over time. The heat generated during early hydration reactions of cementitious materials can be measured using a calorimeter. F-Cal® is a commercially available Semi-Adiabatic calorimeter that can be used in the field to monitor the hydration reactions. Figure 42 shows a picture of a commercially available calorimeter.

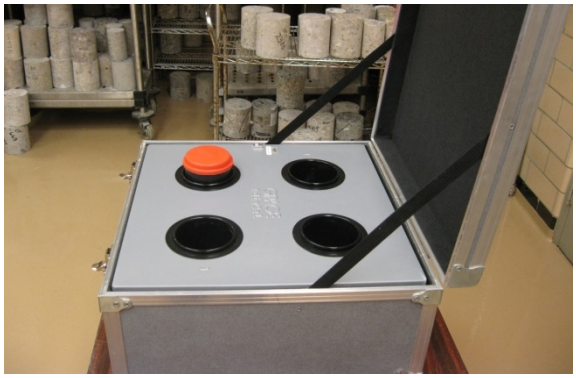

Figure 42: F-Cal® Calorimeter

The amount of heat liberated by cement hydration greatly depends on the chemical and physical properties of the cementitious materials and admixtures used in the concrete mixture. Concrete mixture proportions and curing conditions also play important roles, and deviations in the quantities or characteristics of the concrete materials can be detected by monitoring the heat of hydration. Variations in the chemistry and dosage of Portland cement and supplementary cementitious materials (SCMs), along with interactions between them and chemical admixtures, may be flagged by the heat signature. Typically, significant changes in the heat signature may indicate that the source materials have changed, there was a problem with batching or there is an incompatibility issue.

Results

During this project, 4" x 8" concrete specimens were cast from the ICC and control samples and transferred to a calorimeter immediately (three ICC and one control samples were taken). The calorimeter insulates the concrete cylinder mold from the influence of outside temperatures and uses temperature sensors to record the heat generated by the concrete. Figure 43 shows the results from the calorimeter for various field samples. The x-axis in the figures represents time and y-axis represents the change in concrete temperature. Heat signature curves are usually interpreted empirically by comparing with each other visually. The area underneath the heat signature curve is indicative of the strength gain.

The overall shape of the heat signature curves for all the samples is the same. However, the control curve (red in Figure 43) has slightly higher heat of hydration which suggests that it has slightly higher strength which is consistent with the compressive strength results. The peak heat of hydration of all the four curves was between 12-15 hrs and data shows that for the ICC samples, the time to reach and magnitude of peak heat of hydration is a function of the initial concrete temperature.

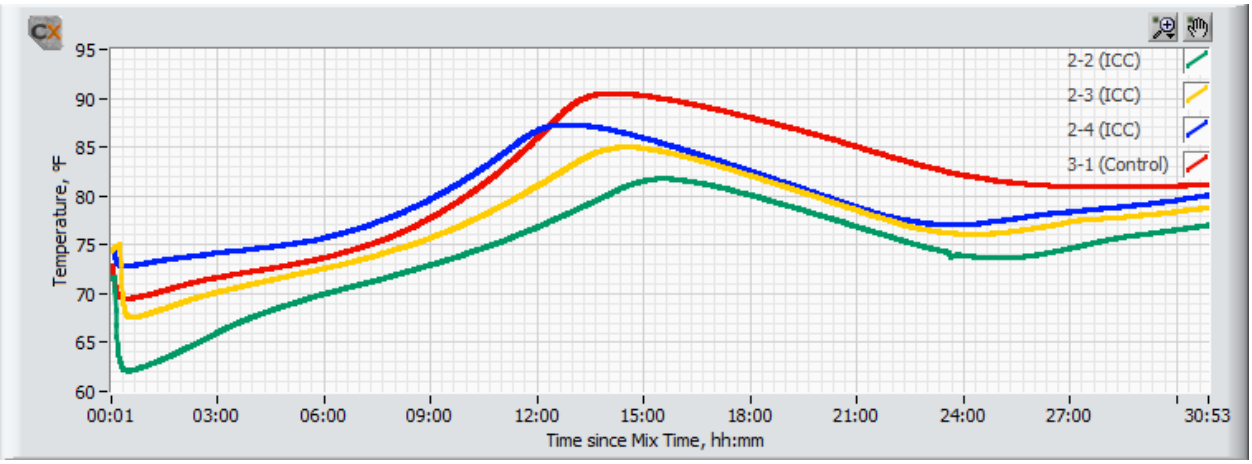

Figure 43: Heat Signature Curves

Measuring heat signature using a semi-adiabatic calorimeter is a very easy and relatively inexpensive test to perform. The test requires a standard cylinder to be cast from a concrete sample and put in the calorimeter. The initial temperature of the concrete and time of placing the cylinder mold in the apparatus is noted. For such a simple test, the heat signature data can

be used for a variety of purposes such as identifying changes in source and quantities of cementitious materials as well as detect any incompatibilities during production. The semi-adiabatic device that was used by the MCL in this project is designed to be used in a laboratory as well as field setting.

CONCLUSIONS

Based upon results from the test program conducted by FHWA's Mobile Concrete Laboratory at this project, the following conclusions can be drawn:

1. The average unit weight of the control and the ICC paving mixture samples taken by the MCL were 144.9 pcf and 135.4 pcf respectively. The unit weights within a given mixture (control and ICC) were consistent. The air content of the control and the ICC mixtures ranged between 5.1 to 6.5%

2. The average compressive strength of cylinders cast from the control mixture was higher than that of the ICC mixture at 7, 28 and 56 days. The average 28 compressive strengths of the control and ICC mixture were 7317 psi and 6051 psi respectively. Both the mixtures met the 28 day strength specification requirement in only 7 days. It appears that there is a potential opportunity to optimize the mixture designs by reducing the cement content.

3. The 28 day flexural strength for this ICC mixture was 660 psi.

4. The average modulus of elasticity and poisons ratio of cylinders cast from the control mixture was higher than that of the ICC mixture at 28 days. The average modulus of elasticity of the control and ICC mixture were 5,169,000 psi and 4,094,000psi respectively.

5. There was no significant difference in CTE between the control and ICC mixtures. The average CTE of the control and ICC mixtures were 4.1 microstrain/F and 4.2 microstrain/F.

6. Implementing the use of maturity can enable the contractor and Kansas DOT to realize significant time savings associated with measuring the in-place pavement strength. For the specific conditions encountered during our field visit, time savings of 2 days is possible. Construction schedules may be significantly accelerated by allowing construction traffic on the pavements much earlier.

7. The AVA data indicate that the air void distribution for the control and ICC concrete used in this project was fair for resistance against Freeze-Thaw damage. AVA data from the MCL and Kansas DOT on same samples compare well.

8. The Super Air Meter (SAM) testing indicated that the control mixture had good air void distribution to resist Freeze-Thaw damage.

9. The SR Meter results indicate that there was no difference in permeability characteristics between the control and the ICC paving mixture at all the three ages tested. The permeability category for the control and the ICC paving mixture was in the moderate category at 56 days. SR data correlated well with the Rapid Chloride Permeability data for both the control and the ICC mixture.

   In addition to significant savings in testing time as well as cost compared to the RCPT test method, the SR meter test also offers many other benefits such as the ability to test a standard size concrete cylinder or core, which can be later used for strength testing thereby reducing the number of specimens to be cast.

10. The MIT Scan 2 is a very powerful non-destructive tool to measure the three dimensional alignment of dowel bars. In this project, all of the 13 joints that were scanned were aligned well and did not have any alignment issues.

11. The MIT Scan T2 is a great tool to non-destructively evaluate the pavement thickness. The average MIT Scan T2 measured thickness at 8 locations was 9.5" (design thickness was 9"). Thickness measurements using Scan T2 offers many benefits such as cost savings (in general, it is at least four times cheaper than taking cores), measured sooner (can take measurements as soon as the pavement can be walked upon), larger number of locations (more robust statistical analysis) and finally, it eliminates the need to cut cores on new pavements and thereby reducing the need to patch the core holes.

TESTING PERSONNEL
The following MCL personnel performed testing at the project:

Nicolai Morari-Fresh Concrete Properties, SR meter testing, CTE, SAM, RCPT, Bulk Resistivity, Strength Testing, SAM
Jon Anderson: AVA, Microwave Water Content, and MIT Scan T2, MIT Scan 2
Jagan Gudimettla- calorimetry, MIT Scan 2, MIT Scan T2

Casting, transporting, instrumenting maturity meters, was performed by all the MCL personnel

ACKNOWLEDGEMENTS
Assistance provided by the following individuals is greatly appreciated:

Kansas DOT: Andrew Jenkins, Dave Meggers, Nicole Carter, Jennifer Distlehorst, Warren Ebberts, Mitchel Hoag.

FHWA Division Office: Tom Deddens, Eric Deitcher

Contractor: Shane Griggs (Koss Construction Company), Daron Brown (Buildex)

ACPA: Todd LaTorella

REFERENCES

1. Integrated Materials and Construction Practices for Concrete Pavement: A State-of-the-Practice Manual, A State of the Practice Manual, National Concrete Pavement Technology Center, October 2007. (http://www.cptechcenter.org/publications/imcp/)

2. Kessler, Powers, Vivas, Paredes, Virmani, "Surface Resistivity as an Indicator of Concrete Chloride Penetration Resistance", 2008 Concrete Bridge Conference.

3. Rupnow, Icenogle, "Evaluation of Surface Resistivity Measurements as an Alternative to the Rapid Chloride Permeability Test for Quality Assurance and Acceptance", Louisiana Transportation Research Center Project Report, July 2011.

4. Eric William Ryan, Master's thesis, "Comparison of Two Methods for the Assessment of Chloride Ion Penetration in Concrete: A Field Study", University of Tennessee, Knoxville, 2011.

5. Wang, Ge, Grove, Ruiz, Rasmussen, Developing a Simple and Rapid Test for Monitoring the Heat Evaluation of Concrete Mixtures for Both Laboratory and Field Applications, National Concrete Pavement Technology Center Report, January 2006.

APPENDIX A – Concrete Mixture Design

KANSAS DOT
CONCRETE MIX DESIGN

PRINT ALL PAGES

Project Number	54-1 KA 2202-01	Spec Max W/C	0.44	* Design Air	6.5%
Contract Number	513036414	* Design W/C	0.4	Slump	2
Concrete Class	PCCP	Spec Min CF	532		
Aggregate Designation	MA-3	* Design CF	540	(includes all cementitious)	

Fields above with an asterisk are required for batch calculcations.

	Material Type or Name	Producer		Official Quality	Amount in Mix*	Specific Gravity
		Name	ID Number			
Aggregate No. 1	CPA-4	Nelson	800101		50.0%	2.56
Aggregate No. 2	IMA 1/4" chips	Nelson	800101		10.0%	2.56
Aggregate No. 3	Basic SSG for MA-3	Cornejo & Sons	819304		40.0%	2.61
Aggregate No. 4						
Cement	Type I/II	Ash Grove	3001		75.0%	3.15
Other Cementitious No. 1	Fly Ash/Conc/Class C	KCPL	18901		25.0%	2.65
Other Cementitious No. 2						
Water		City of Gas, Kansas				
Air Entraining Admixture	Air Entrainment	Euclid	1201		13.5	
Admixture No. 1	Type A Water Reducer	Euclid	1201		5	
Admixture No. 2						
Admixture No. 3						

* Amount in Mix column: Use whole number percentages (i.e. 40 or 15) for aggregates and cementitious materials; assume oz/cy for admixtures.

Mix Design Used Previously? no KDOT Mix Design Number 4P131K2A-D (if known) Date Last Used currently

Please include the following information along with this completed form:
- Materials Certifications
- Compressive Strength Results (KT-76)
- Permeability Test Results (KT-73, KT-79, or AASHTO T-277)
- Reactivity Test Results (ASTM C 1567, if SCMs are used)
- Air Void Analyzer Results (KT-71, only for PCCP)

NOTE: Please make sure that when this form is submitted to the construction or district office, ensure that all three (3) pages are included.

Printed on 5/14/2014 KDOT Form Number 694

KANSAS DOT
CONCRETE MIX DESIGN

PRINT ALL PAGES

Project Number	54-1 KA 2202-01	Spec Max W/C	0.44	* Design Air	6.5%
Contract Number	513036414	* Design W/C	0.4	Slump	2
Concrete Class	PCCP	Spec Min CF	532		
Aggregate Designation	MA-3	* Design CF	540	(includes all cementitious)	

Fields above with an asterisk are required for batch calculcations.

	Material Type or Name	Producer		Official Quality	Amount in Mix*	Specific Gravity
		Name	ID Number			
Aggregate No. 1	CPA-4	Nelson	800101		51.0%	2.56
Aggregate No. 2	IMA 3/8 X 0 (lt wt aggr.)	Buildex 3/8 X 0	816302		9.0%	1.71
Aggregate No. 3	Basic SSG for MA-3	Cornejo & Sons	819304		40.0%	2.61
Aggregate No. 4						
Cement	Type I/II	Ash Grove	3001		75.0%	3.15
Other Cementitious No. 1	Fly Ash/Conc/Class C	KCPL	18901		25.0%	2.65
Other Cementitious No. 2						
Water		City of Gas, Kansas				
Air Entraining Admixture	Air Entrainment	Euclid	1201		13.5	
Admixture No. 1	Type A Water Reducer	Euclid	1201		5	
Admixture No. 2						
Admixture No. 3						

* Amount in Mix column: Use whole number percentages (i.e. 40 or 15) for aggregates and cementitious materials; assume oz/cy for admixtures.

Mix Design Used Previously? no KDOT Mix Design Number 4P141K1A-D (if known) Date Last Used

Please include the following information along with this completed form:
- Materials Certifications
- Compressive Strength Results (KT-76)
- Permeability Test Results (KT-73, KT-79, or AASHTO T-277)
- Reactivity Test Results (ASTM C 1567, if SCMs are used)
- Air Void Analyzer Results (KT-71, only for PCCP)

NOTE: Please make sure that when this form is submitted to the construction or district office, ensure that all three (3) pages are included.

Printed on 5/22/2014

KDOT Form Number 694

Appendix E: Strain Evaluation, Calculations and Equations

When evaluating the strain, the first step is to determine the time of set in each panel. This step is required to calculate the actual strain based on the raw strain data gathered from the strain gages. In order to determine the time of final set (also defined as the time of zero stress), raw strain is plotted against temperature for each strain gage (Figure E.1 represents a typical plot based on one gage from Panel 4 of the ICC section). The point at which strain begins to vary linearly with temperature is defined as the point of zero stress. Figure E.2 and Figure E.3 illustrate zoomed-in views of the data from Figure E.1 to better illustrate the point at which time of zero stress occurs. This analysis was performed on all of the strain gages in both test sections and the time of zero stress, or time of final set, was determined as the average for the ICC and Control test sections. Table E.1 presents the time of placement, time of zero stress, age at zero stress, and ambient temperature at the time of zero stress. It should be noted that due to the significantly different temperatures at time of placement, time of zero stress occurs significantly earlier for the control section. The significance of this difference is the stress profile cast into the section. The stresses present in the panel at time of zero stress are permanently cast into the section. In the ICC section, the top surface of the panel was much cooler than the bottom, resulting in temperature related shrinkage at the top (relative to the bottom) to be permanently cast into the panels. Given the high temperatures during placement of the control section, the opposite occurred; a permanent expansion of the top surface (again relative to the bottom) was developed. While either scenario is neither detrimental nor beneficial by itself, is makes comparing the two test sections difficult.

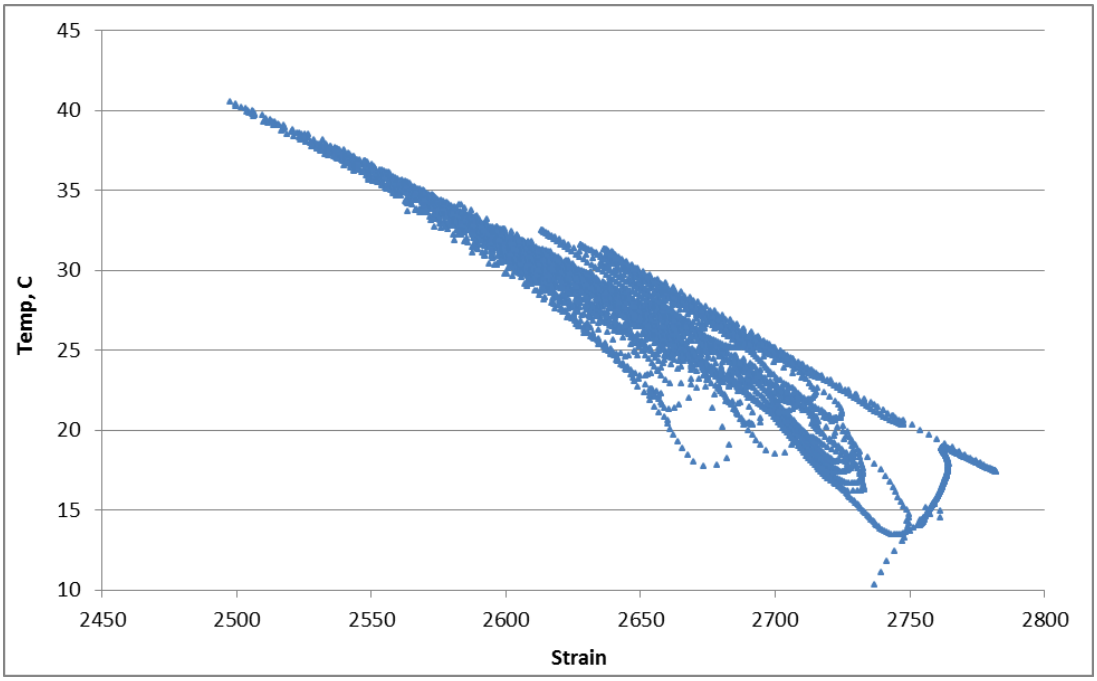

Figure E.1: ICC Section Panel 4 Bottom Sensor Strain vs. Temperature

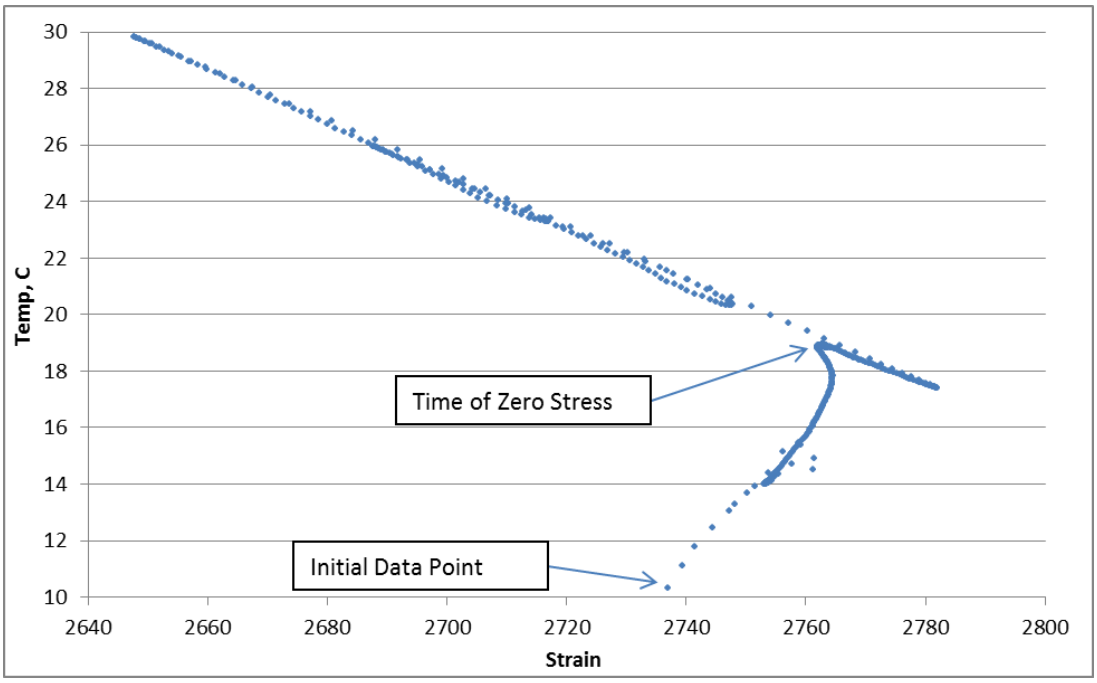

Figure E.2: ICC Section Panel 4 Bottom Sensor Strain vs. Temp. (First 500 Readings)

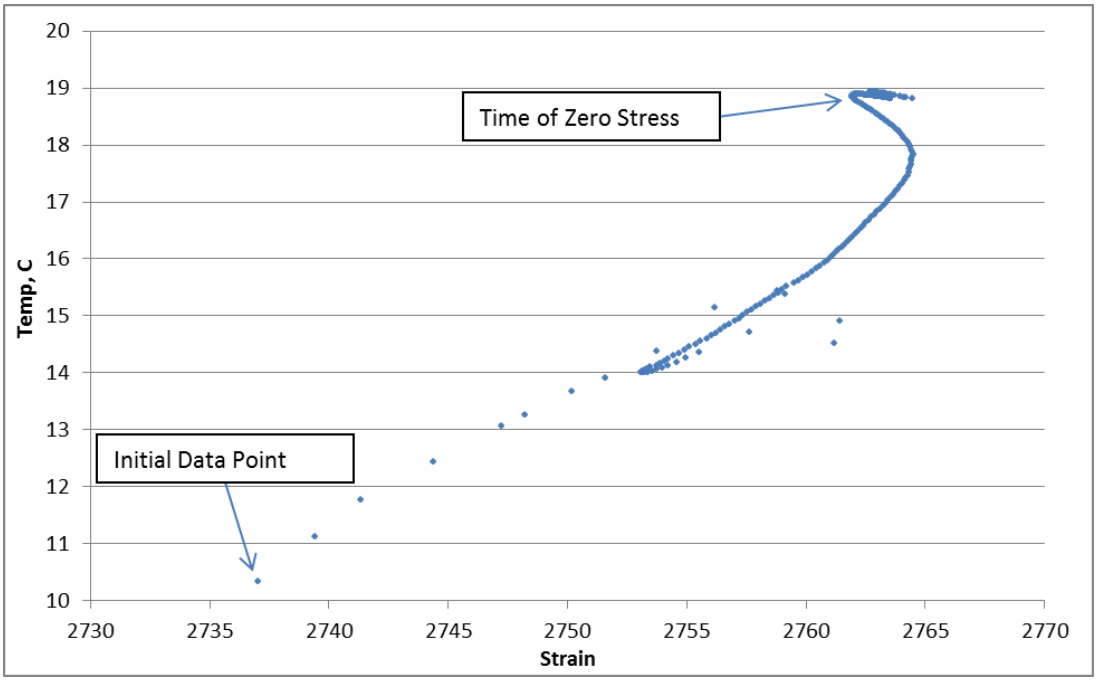

Figure E.3: ICC Section Panel 4 Bottom Sensor Strain vs. Temp. (First 250 Readings)

Table E.1: Time of Zero Stress

Section	Time of Placement	Time of Zero Stress	Age at Zero Stress, h:m	Temp. at Time of Zero Stress, C
ICC Section	9:39 AM 5/2/14	3:10 AM 5/3/2014	17:32	8.5
Control Section	10:30 AM 7/24/14	7:15 PM 2/24/14	8:45	30.5

E.1 Strain Gage Data and Calculations

1. Strain Gage Data Recorded:
    a. Date/Time
    b. Raw Strain Reading (με)
    c. Raw Temperature Reading (°C)
2. Calculate Actual Stain ($\mu\varepsilon_{actual}$):

$$\mu\varepsilon_{actual} = (R_1 - R_0)B + (T_1 - T_0)C_1$$

$\mu\varepsilon_{actual} = actual\ strain\ experienced\ by\ concrete$
$R_1 = raw\ strain\ measured\ at\ each\ reading\ (\mu\varepsilon)$
$R_0 = raw\ strain\ reading\ at\ time\ of\ final\ set\ (\mu\varepsilon)$
$B = nominal\ batch\ factor\ \ as\ determined\ by\ the\ manufacturer\ as\ 0.97$
$T_1 = temperature\ measured\ at\ each\ reading\ (℃)$
$T_0 = temperature\ measured\ at\ the\ time\ of\ final\ set\ (℃)$
$C_1 = coeffiecient\ of\ thermal\ expansion\ of\ steel\ wire\ in\ gage = +12.2\ \mu\varepsilon/℃$

(Geokon, Inc., 2013)

3. Calculate Strain due to Temperature:

$$\mu\varepsilon_{temp} = (T_1 - T_0)C_1$$

$\mu\varepsilon_{temp} = strain\ due\ to\ temperature$
$T_1 = temperature\ measured\ at\ each\ reading\ (℃)$
$T_0 = temperature\ measured\ at\ the\ time\ of\ zero\ stress\ (℃)$
$C_1 = coeffiecient\ of\ thermal\ expansion\ of\ steel\ wire\ in\ gage = +12.2\ \mu\varepsilon/℃$

(Geokon, Inc., 2013)

1. Curvature (ρ):

$$\rho = -\frac{\varepsilon_t - \varepsilon_b}{D(1 + \varepsilon_t + \varepsilon_b)}$$

$\rho = Slab\ Curvature\ (^1/_{in.})$
$\varepsilon_t = Strain\ at\ top\ of\ slab$
$\varepsilon_b = Strain\ at\ bottom\ of\ slab$
$D = Distance\ between\ the\ top\ strain\ and\ bottom\ strain\ (5\ in.)$

(Rania and Vandenbossche, 2011)

2. Coefficient of Thermal Expansion (C_T):

$$C_T = \frac{\Delta\varepsilon_{actual} \times L_0}{\Delta T \times L_0}$$

$\Delta\varepsilon_{actual} = change\ between\ consecutive\ actual\ strain\ readings\ (\mu\varepsilon)$
$L_0 = initial\ strain\ gage\ wire\ length = 6\ in\ (0.1524\ m)$
$\Delta T = change\ between\ consecutive\ temperature\ readings\ (℃)$

(Geokon, Inc., 2013)

AD ASTRA PER ASPERA

Kansas

Department of Transportation